Review

Strategies To Improve the Performance of Hydrogen Storage Systems by Liquefaction Methods: A Comprehensive Review

Bahram Ghorbani, Sohrab Zendehboudi,* Noori M. Cata Saady, Xili Duan, and Talib M. Albayati

Read Online

ACCESS | Metrics & More | Article Recommendations

ABSTRACT: The main challenges of liquid hydrogen (H_2) storage as one of the most promising techniques for large-scale transport and long-term storage include its high specific energy consumption (SEC), low exergy efficiency, high total expenses, and boil-off gas losses. This article reviews different approaches to improving H_2 liquefaction methods, including the implementation of absorption cooling cycles (ACCs), ejector cooling units, liquid nitrogen/liquid natural gas (LNG)/liquid air cold energy recovery, cascade liquefaction processes, mixed refrigerant systems, integration with other structures, optimization algorithms, combined with renewable energy sources, and the pinch strategy. This review discusses the economic, safety, and environmental aspects of various improvement techniques for H_2 liquefaction systems in more detail. Standards and codes for H_2 liquefaction technologies are presented, and the current status and future potentials of H_2 liquefaction processes are investigated. The cost-efficient H_2 liquefaction systems are those with higher production rates (>100 tonne/day), higher efficiency (>40%), lower SEC (<6 kWh/kgLH$_2$), and lower investment costs (1−2 \$/kgLH$_2$). Increasing the stages in the conversion of ortho- to para-H_2 lowers the SEC and increases the investment costs. Moreover, using low-temperature waste heat from various industries and renewable energy in the ACC for precooling is significantly more efficient than electricity generation in power generation cycles to be utilized in H_2 liquefaction cycles. In addition, the substitution of LNG cold recovery for the precooling cycle is associated with the lower SEC and cost compared to its combination with the precooling cycle.
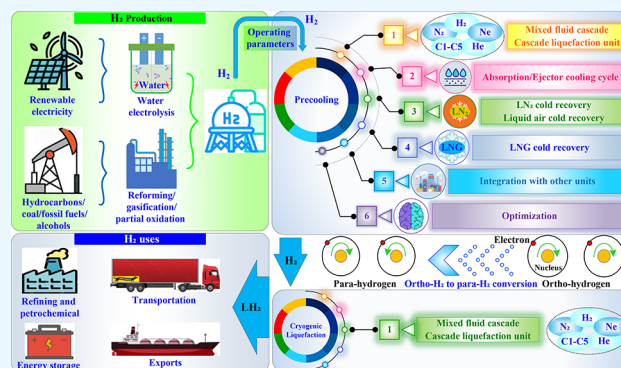
1. INTRODUCTION

The worldwide ever-increasing growth in energy demand, the exploitation of underground resources, and the emission of greenhouse gases have triggered energy experts to move toward the utilization of clean fuels.[1−3] Renewable energy sources such as algal biofuels are alternatives to fossil and nuclear fuels.[4] Energy storage plays a fundamental role in using renewable energies to counteract intermittent fluctuations in production and improve reliability and stability.[5,6] Common systems for energy storage include electrochemical (fuel cells/batteries), mechanical (flywheels/compressed air), electrical (superconducting magnetic/supercapacitors), chemical (hydrogen cycle), and thermal (sensible heat/phase change) systems.[7−11] Hydrogen (H_2) energy storage is the main option for longer periods with higher storage capacity.[12,13] In 2021, H_2 demand reached 94 million tonnes, equivalent to about 2.5% of global final energy consumption. This demand grew by 3.3% compared to the pre-Coronavirus pandemic (91 million tonnes before 2019).[14] Based on the International Conference on Climate Change (IPCC) statement, greenhouse gas (GHG) emissions can increase the mean global temperature from 1.1 to 6.4 °C by the end of the century.[15−18] Global warming of more than 2 °C will

lead to serious consequences, including weather change, polar ice melting, and lowering of the pH of ocean water.[19] Based on the Paris Agreement, many countries have committed to seriously reducing carbon dioxide (CO_2) emissions, reducing temperatures below 2 °C, and reaching net-zero carbon emissions by 2050.[20−22] Moreover, global net GHG emissions should be reduced by nearly 24% by 2030 on most pathways to limit global warming to below 2 °C.[23] The Paris Agreement signatories are interested in increasing the use of H_2 as a clean fuel alongside other energy carriers.[24] H_2 demand to reach net-zero carbon goals is estimated at 200[14] and 530[25] million tonnes for 2030 and 2050, respectively.

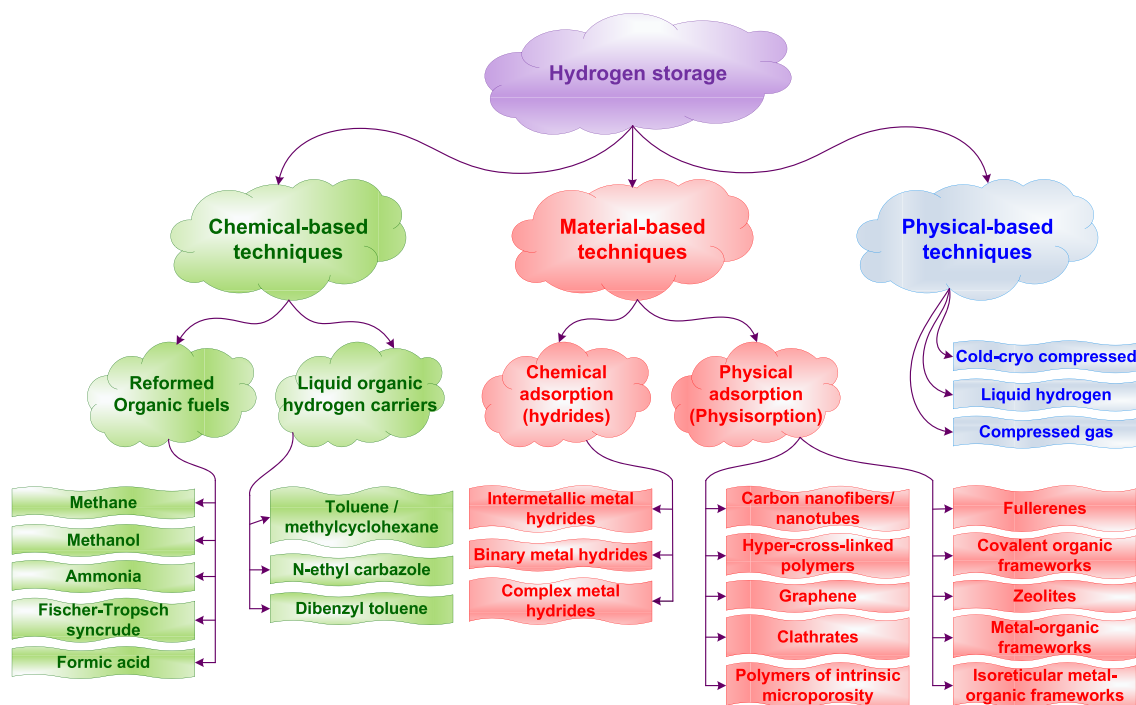**1.1. Hydrogen Storage Importance.** Storage and distribution of H_2 on a large scale is the main challenge due to

Figure 1. Different methods of H_2 storage based on physical, material, and chemical categorization.

its low energy density in the gas form.[26] H_2 storage can be categorized into physical-based (compressed gas/liquid/two phase), material-based (physical/chemical adsorption), and chemical-based methods (reformed organic fuels/liquid organic H_2 carriers (LOHCs)).[27−32] Figure 1 illustrates various methods of H_2 storage based on physical, material, and chemical categorization. Standard H_2 storage tanks are used at an operating pressure of 350−700 bar and have not yet reached the storage gravimetric/volumetric target of 6.5 wt % or 0.050 kgH_2/L for the desired driving range (the Department of Energy (DOE) targets for on-board H_2 storage).[33−38] The main challenges for liquid H_2 (LH_2) storage include its high specific energy consumption (SEC), low exergy efficiency, and inevitable boil-off gas (IBOG) losses.[39,40] The densities of liquid H_2 and high-pressure gas, are, respectively 70.8 and under 40 kg/m^3.[41] For instance, the densities of H_2 at 35 and 70 bar are around 23 and 38 kg/m^3, respectively.[42] H_2 low-temperature compression (cryo-compressed) reduces the problems caused by the volume and pressure required by compression methods and the IBOG losses due to liquefaction; it is a promising strategy for H_2 storage, but it has not yet been commercialized.[43,44]

A small amount of H_2 adsorbed in porous activated carbon materials, zeolites, organometallic−organic, and covalent frameworks at low temperatures is the main challenge for H_2 storage based on physical adsorption. Most of the studies about this method are on a laboratory scale that did not meet the DOE technical requirements.[30,45−47] Metal hydrides have special problems, such as high adsorption/desorption temperatures, low reversibility, mass density limitations, slow kinetics, and the energy required, and most research investigations are conducted at a laboratory scale.[48,49] The main challenge in material-based techniques is the development of progressive materials for efficient H_2 storage.[50] Chemical H_2 storage based on ammonia (NH_3) and methanol (CH_3OH) is compatible with liquid H_2 infrastructure. However, their dehydrogenation requires a lot of

energy and capital compared to the LOHCs.[51−55] Environmentally friendly fuels for storing H_2 include chemical-based fuels such as methanol, ammonia, and formic acid. Nowadays, they are not cost effective in pure H_2 production due to the high SEC at high temperatures for dehydrogenation and purification.[53] The dehydrogenation temperatures of CH_3OH, LOHCs, and NH_3 were reported to be up to 420, 50−250, and 650 °C, respectively.[53,56] The transportation and storage of H_2 are very important because it is the most promising energy carrier for large-scale adoption and longer period. For these purposes, liquid H_2 has been widely considered. Therefore, it is important to identify the most promising H_2 liquefaction processes for storage purposes.[57]

1.2. Recent Studies in Hydrogen Liquefaction Systems. Many studies have been conducted in recent years to examine H_2 liquefaction cycles, techniques of lowering the SEC, and the utilization of appropriate materials for ortho- to para-H_2 conversion. Asadnia et al.[58] reviewed H_2 liquefaction of different cycles and concluded that the SEC reduction of H_2 liquefaction would remain in the range of 5−8 $kWh/kgLH_2$ in the near future. Also, utilizing isentropic expansion processes instead of isenthalpic, cascade refrigeration cycles (CRCs), mixed refrigerant cycles (MRCs), and integrating renewable energy systems are the four principal growing techniques in H_2 liquefaction. Ghafri et al.[59] suggested reducing the cost of H_2 liquefaction to 1−2 $/kgLH_2$ and the SEC to 6−8 $kWh/kgLH_2$ to be economical in the near future. The capacity of liquefaction systems should be increased to about 100 tonne per day (TPD) or more to achieve these objectives. Currently, the size of the largest H_2 liquefaction system is 32 TPD. The SEC and H_2 liquefaction price in the current commercial liquefaction plants are 15−11.9 $kWh/kgLH_2$ and 3−2.5 $/kgLH_2$, respectively. Wijayanta et al.[60] investigated H_2 storage in the form of liquid, methylcyclohexane (C_7H_{14}), and NH_3 in Japan. The results indicated that liquid H_2 is associated with the high SEC, high IBOG losses, and low exergy efficiency. C_7H_{14} has a high SEC in
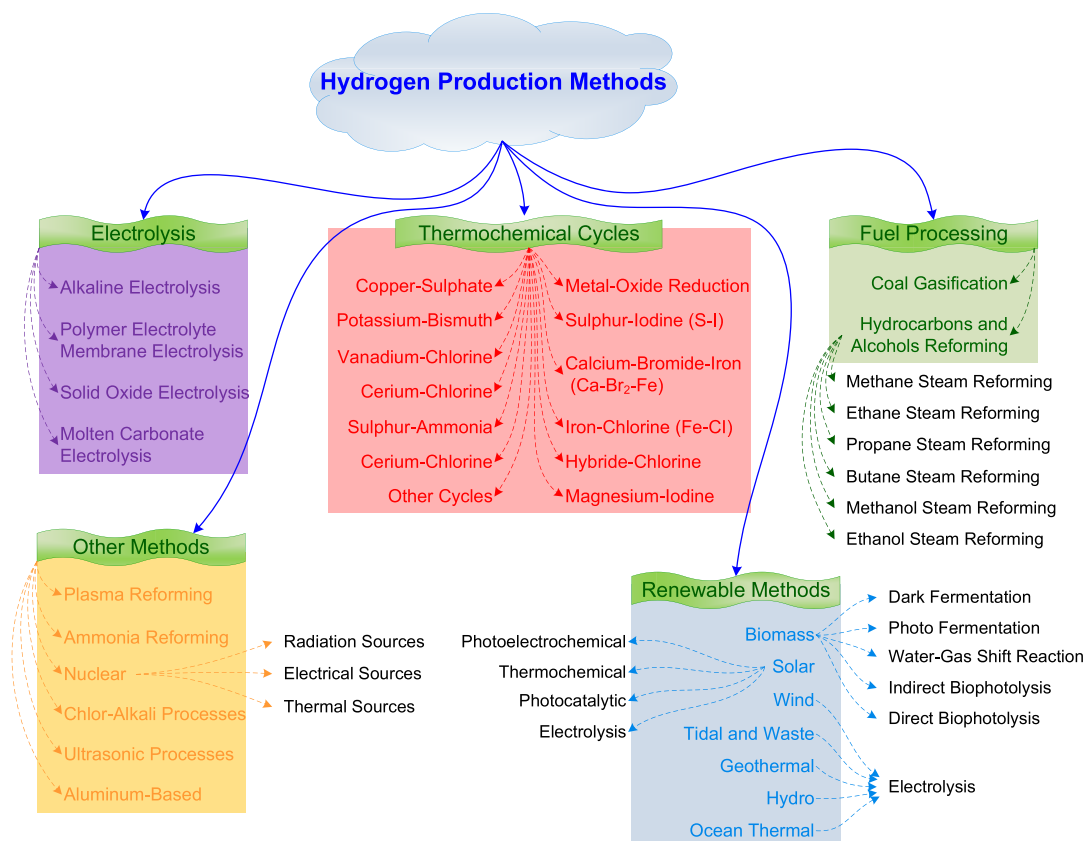
Figure 2. Various techniques of hydrogen production. Modified from ref 105.

dehydrogenation and purification. Also, NH_3 faces a high energy request in decomposition (544−586 kJ/mol).[61] Besides, liquid H_2 in fuel cell systems is a promising option for achieving net-zero emissions goals by 2050 compared to C_7H_{14} and ammonia. Krasae-in et al.[62] investigated large-scale H_2 liquefaction plants until 2008 and reported their exergy efficiency to be between 20% and 30%. The results of the review of H_2 liquefaction conceptual plans until 2008 revealed that the exergy efficiency was 40−50%. In 2010, SINTEF Energy Research and Norwegian University of Science and Technology (NTNU) suggested a novel MRC plant with an exergy efficiency of over 50%. The H_2 liquefaction system has precooling and cryogenic parts. The precooling section is critical in optimization because it has higher freedom degrees than the cryogenic section.[63] The use of multicomponent refrigerants as well as different operating pressures lead to an increase in the degree of freedom of precooling cycles compared to cryogenic processes. Yin et al.[64] reviewed different methods for the precooling in the H_2 liquefaction cycle including LN_2 cold recovery, helium, Joule−Brayton (J−B), MRCs, and the LNG regasification precooled cycles. The SEC and exergy efficiency in the conceptual liquefaction plants were reported to be 5−8 kWh/kgLH_2 and 40−60%, respectively. There are various H_2 liquefaction structures containing the Linde−Hampson (L−H) unit, Linde dual-pressure system, L−H process with precooled, Claude process, Claude process with LN_2 or helium precooled, Kapitza cycle, Collins process, and reverse Brayton cooling system.[65−67] The main advantage of the Claude system (as an improved L−H process) compared to the L−H process is the presence of an expansion device that partially powers the system. Also, the Claude cycle compared to the L−H process uses more heat exchangers to liquefy H_2 and has a greater efficiency.[68,69]

Due to the high SEC and low energy yield in corresponding industries, several research efforts regarding conceptual modeling of H_2 liquefaction systems based on the L−H cycle, Claude process, and reverse Brayton system have been conducted lately. Several strategies have been utilized to decrease the SEC in H_2 liquefaction systems. These techniques include using absorption and ejector cooling cycles,[70−75] LN_2 regasification,[64,76−79] LNG/LAC energy recovery,[62,80−86] cascade liquefaction process,[71,87,88] multicomponent refrigerant cycle,[88−93] integration with other integrated structures,[94,95] optimization algorithms,[93,96] combined with renewable energy sources,[97−99] and the pinch approach.[100,101] Yilmaz et al.[97] developed seven H_2 production and liquefaction cycles according to geothermal energy, the absorption cooling cycle (ACC) to precooling, and the L−H process for liquefaction. The price of H_2 liquefaction was calculated to be 0.98−2.62 $/kg$LH_2$. Yilmaz et al.[72] concluded that utilizing the ACC reduces the cost and the SEC by 32.4% and 49.95%, respectively. Ebrahimi et al.[101] modeled a H_2 production and liquefaction process employing an electrothermochemical unit, solar collectors, and an MRC. Pinch analysis was performed to decrease the SEC in the hybrid structure. The SEC in the integrated structure was lowered by evaluating the network of heat exchangers and the composite curves. A reduction in pinch point increases the complexity and investment cost of heat exchangers. Cardella et al.[93,102] assessed the economics of increasing the capacity by two suggested liquefaction cycles. The proposed structure included a dual H_2−neon (Ne) process and a high-pressure Claude unit. The results revealed that by increasing the factory capacity from 5 to 100 TPD, the SEC could be decreased to more than 6 kWh/kgLH_2. Moreover, increasing the capacity of H_2 liquefaction systems increases

capital investment and system complexity. Lee et al.[69] developed a H_2 and CO_2 liquefaction system using the steam methane reforming (SMR) cycle and LNG regasification for precooling and improved Claude cycle. A comprehensive analysis indicated that the SEC of the offered structure decreased by approximately 47.4% (from 11.7 to 6.15 $kWh/kgLH_2$). Also, the levelized cost of liquid H_2 (LCOH) decreased from 6.08 $/kgLH_2$ for the reference system to 3 $/kgLH_2$ for the hybrid process, representing a remarkable savings of 51% in the cost of liquid H_2 production. Taghavi et al.[85] revealed that using the LAC recovery system for the precooling in the H_2 liquefaction cycle leads to a reduction of the SEC, coefficient of performance (COP), and exergy efficiency of 6.916%, 22.04%, and 25.65%, respectively. The economic analysis for this modified system has not been investigated.

1.3. Directions and Aims of the Current Study. The SEC reduction in H_2 liquefaction procedures is critical to meeting DOE targets. Recommendation of several strategies for lowering the SEC of H_2 liquefaction cycles may make it a viable option for large-scale H_2 storage in the near future. Nonetheless, it can be noticed that in most research works on H_2 liquefaction systems, more emphasis has been placed on lowering the SEC while capital/operating costs, complexity levels, and relative emissions have been overlooked. Also, the improvement rate of efficiency (energy and exergy) in some techniques for decreasing the SEC is low compared to the reduction in total expenses and an increase in system complexities. To the best of our knowledge, no comprehensive review studies have been conducted to improve the performance of hydrogen liquefaction systems considering energy consumption, energy/exergy efficiency, capital/operating costs, capacity, complexity levels, and relative emissions. This review aims to fill in the knowledge gaps in this research area. This review summarizes several H_2 liquefaction processes and technologies. It discusses in detail the technologies for improving H_2 liquefaction performance using the ACC, ejector cooling cycle, LN_2/LNG/LAC energy recovery, a cascade liquefaction process, MRCs, integration with other hybrid structures, optimization algorithms, combined with renewable energy sources, waste heat from industries (i.e., chemical plants, furnaces, and incinerators), and the pinch approach. This review discusses the economic, safety, and environmental aspects of different techniques for H_2 liquefaction systems. Standards and codes for various storage technologies of H_2 liquefaction are provided. Finally, the current status and future opportunities for H_2 liquefaction processes are investigated.

2. PHYSICAL AND CHEMICAL CHARACTERISTICS OF HYDROGEN

As element number one on the periodic table, hydrogen is the simplest, the most plenteous, and the lightest substance in the universe.[103] However, H_2 is naturally bonded with other elements (carbon and oxygen) and cannot be uncovered in its free state.[104] The share of principal feedstock for H_2 production includes natural gas (49%), crude oil (29%), coal (18%), and electrolysis (4%).[105,106] Figure 2 illustrates different techniques of H_2 production. Nowadays, reforming (hydrocarbons/alcohols), gasification processes (coal/fossil fuels), and partial oxidation (fossil fuel) have the most significant shares in H_2 production techniques.[105,107−109] The principal challenges for the techniques are the high SEC and CO_2 emissions to the surroundings.[105,110] Water electrochemical processes are yet under expansion and can be integrated with carbon-free sources

(tidal/solar/wind/geothermal) to provide an eco-friendly system.[111] Electrothermochemical systems such as copper−chlorine,[112−115] magnesium−chlorine,[116−119] iron−chlorine,[120,121] zinc−sulfur−iodine,[122−125] and vanadium−chlorine[126,127] and bio-H_2 via biological methods[105] can be promising processes for H_2 production in the future.

Its isotopes, including deuterium (D or 2H) and tritium (T or 3H), are radioactive, produced by the bombardment of H_2 with neutrons.[128] Table 1 presents some of the main physical

Table 1. Physical Properties of Hydrogen

properties	value	units
molecular weight[134]	2.016	g/mol
lower heating value[135]	119.9	MJ/kg
higher heating value[135]	141.6	MJ/kg
viscosity, 25 °C[136]	0.000892	cP
boiling temperature, 1 atm[137]	−253	°C
melting temperature[137]	−259.1	°C
critical temperature[138]	−240.1	°C
critical pressure[138]	1.29	MPa
density of gaseous H_2, 0 °C[136]	0.0898	kg/m³
density of liquid H_2, −253 °C[136]	70.85	kg/m³
density of solid H_2, −259 °C[136]	858	kg/m³
critical density[136]	31.2	kg/m³
heat capacity of gaseous H_2, 0 °C[134]	14.3	kJ/kg °C
heat capacity of liquid H_2, −256 °C[134]	8.1	kJ/kg °C
heat capacity of solid H_2, −259.8 °C[134]	2.63	kJ/kg °C
heat of vaporization, −253 °C[139]	0.447	MJ/kg
heat of fusion, −259 °C[139]	0.058	MJ/kg
thermal conductivity, 25 °C[139]	0.018	W/cm K
ionization energy[139]	13.59	eV
flame emissivity[140]	17−25	%
liquid to gas expansion ratio at atmospheric condition[139]	1:848	
flame temperature in air[141]	2045	°C
adiabatic flame temperature[139]	2107	°C
research octane number[142]	>130	
thermal conductivity, 20 °C and 1 atm[139]	0.1825	
specific gravity of gas H_2, 20 °C and 1 atm[139]	0.0696	
specific gravity of liquid H_2, −253 °C and 1 atm[139]	0.0710	
latent heat of vaporization[139]	0.461	MJ/kg

properties of H_2. The molecule of H_2 is extremely small and light (120 pm van der Waals radius, and molar mass of 1.00794 g/mol), and its diffusion rate (0.61 cm^2/s) is comparatively high.[129] Compared to gasoline or diesel fuels, its gravimetric energy content and lower heating value are nearly three times higher but lower in energy density per volume, which means it requires roughly four times more space than gasoline to provide equal energy.[130] This odorless and colorless energy source produces just water vapor and a significant quantity of heat without emitting GHGs, making this nontoxic gas a promising green fuel.[131] Moreover, the research octane number of H_2, which relates to its antiknock characteristics, is comparatively higher than that of current fossil fuels.[132] Besides, the H_2 flash point is −231 °C, the lowest among conventional fuels.[133]

The H_2 density in the gaseous state is lower than that of liquid H_2. Therefore, H_2 transportation in the gaseous state requires large storage tanks with high pressure, which is not justified due to the tank's resistance.[143] However, special liquid H_2 storage tanks can solve the problem of transporting H_2, especially over long distances.[144] Also, H_2 liquefaction structures can be utilized

for peak shaving within high energy demand in various industries.[145] Notwithstanding the numerous advantages of liquefaction storage systems, it should be highlighted that these technologies face numerous challenges, such as a lack of efficiency, a high economic expense, and a lack of creative technological advancement.[146]

H_2 molecules consist of two protons and two electrons. If the two electrons' rotations are antiparallel, they drive the molecule into a bonded state. Therefore, there are two groups of H_2 molecules based on antiparallel ($I = 0$) and parallel ($I = 1$) nuclear spins.[13,147,148] The number of states for the H_2 molecule is determined from the relationship of the nucleus spin states ($2I + 1$), in which I is the quantum number of the nucleus spin and is equal to 1/2. Given that the numbers are $\alpha = +\frac{1}{2}$ and $\beta = -\frac{1}{2}$, the nuclear spin quantum number is equal to $I = \left(\frac{1}{2} + \frac{1}{2}\right) = 1$ for ortho-H_2, and the molecular form has three states. In para-H_2, the nuclear spin quantum number is $I = \left(\frac{1}{2} - \frac{1}{2}\right) = 0$ and thus has only one state.[101,149] Therefore, the number of ortho states is 3 times that of para-H_2 at environment temperature (i.e., 75% ortho−25% para).[69,150] Figure 3 illustrates the graphical
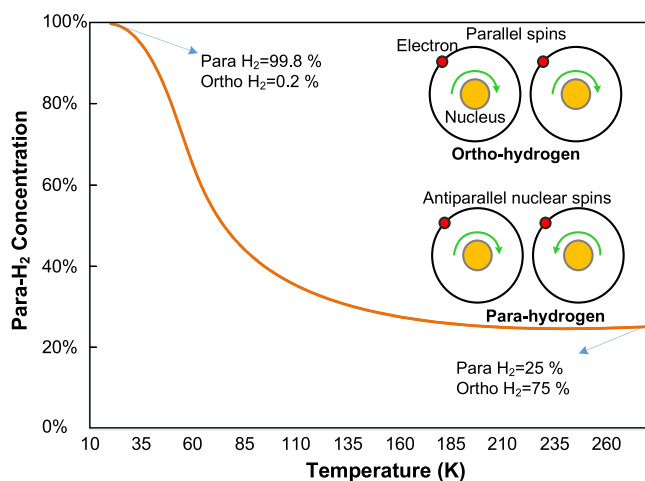

Figure 3. Graphical layout of the parallel and antiparallel nuclear spins in ortho- and para-H_2. Modified from refs 59, 139, 154, and 155.

layout of the parallel and antiparallel spins in ortho- and para-H_2. It is also not possible to produce pure ortho-H_2. These two states of the H_2 molecule are the same in terms of chemical properties, but they differ in physical properties. The boiling and melting point for para-H_2 are 0.1 K lower than those of normal H_2.[151] By decreasing the temperature to the normal boiling point of H_2 (21.2 K), approximately 99.9% para-H_2 can be produced. In its natural state, ortho-H_2 tends to cool slowly and over a long time frame, causing the reserved liquid H_2 to evaporate and become waste. The ortho- to para-H_2 conversion appears with a transition from the ortho triplet state to a para singlet state, which in the normal state of this transition is very slow, and more time is spent in this process.[101,152,153]

The mutation and conversion rates can be enhanced by using proper catalysts of sodium oxide, iron(III), nickel, chromium, manganese, all metals with paramagnetic properties, rhodium phosphine complex, potassium triphenyl complex, and ruthenium.[156] The ortho-H_2 with a higher energy grade than para-H_2 is an excited condition. Also, para-H_2 with a lower energy surface is easily formed at a lower temperature.[157] The ortho- to para-H_2 conversion is exothermic and temperature associated. As a result, when storing liquid H_2, some of the H_2 is wasted, which is called boil-off gas.[158,159] Thus, the ortho- to para-H_2 conversion is essential for LH_2 production in distant transport and to decrease IBOG losses. By storing normal H_2 inside a tank, the conversion enthalpy is released in the tank and causes the liquid H_2 losses.[101,152] The reactions occurring in the conversion reactors are listed as[75]

$$\text{hydrogen} \rightarrow \text{para-hydrogen} + \text{heat} \tag{1}$$
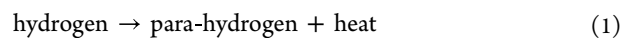
The conversion rate is dependent on the reaction temperature as in eq 2

$$\text{conversion} = C_0 + C_1 \times T + C_2 \times T^2 \tag{2}$$

The conversion coefficients can be defined using experimental information.[160] The volume rate constant for the first-order reaction, $k_v\left(\frac{\text{mol}}{\text{cm}^3 \text{s}}\right)$, is obtained from eq 3[161,162]

$$k_v = \frac{n}{V} \times \ln\left(\frac{1 - \frac{C_0}{C_{eq}}}{1 - \frac{C}{C_{eq}}}\right) \tag{3}$$

where n, V, and C_0 are the feed molar flow rate (mol/s), the catalyst volume (cm^3), and the initial concentration, respectively, and the parameters C and C_{eq} are the achieved and equilibrium concentrations, respectively. Three various reactors, including adiabatic and isothermal converters and continuous conversion, are employed to perform the ortho- to para-H_2
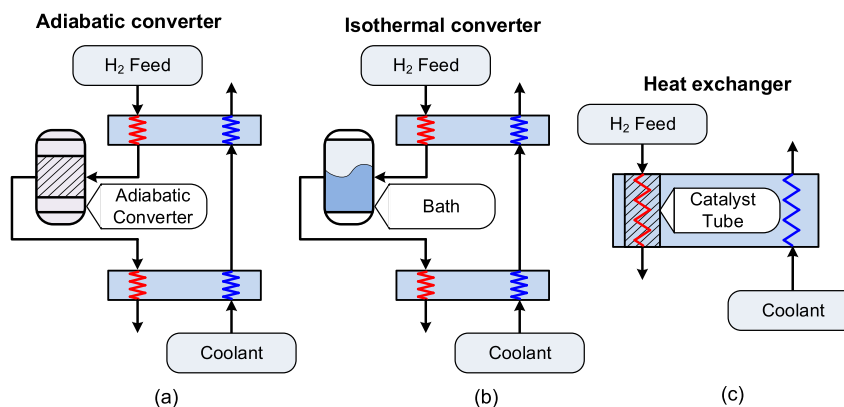

Figure 4. Reactors involved in the ortho- to para-H_2 conversion. Modified from ref 69.

conversion. Adiabatic converters are easy to accomplish, but they increase the flow temperature after the exchangers and require numerous beds, which causes an increase in temperature and cost and a reduction in thermal efficiency. Isothermal converters are used to eliminate the flow temperature increase in adiabatic reactors, but this method increases the equipment required in the liquefaction procedure, which increases operational and capital costs.[69] The operating principle of each converter is presented in Figure 4. Continuous conversion has the highest efficiency and the lowest energy consumption compared to isothermal and adiabatic methods.[163] Table 2 lists

Table 2. Information on Ortho- to Para-H$_2$ for Various Systems[a]

refs	year	ortho- to para-H$_2$ type	conversion stages
Baker et al.[76]	1978	isothermal	2
Quack[165]	2002	adiabatic	continuous
Staat[166]	2008	isothermal	3
Valenti et al.[167]	2008	adiabatic	continuous
Berstad et al.[168]	2010	isothermal	continuous
Krasae-In et al.[89]	2010	adiabatic–isothermal	5
Krasae-In[91]	2014	adiabatic–isothermal	6
Yuksel et al.[169]	2017	isothermal	3
Cardella et al.[93]	2017	adiabatic	4
Asadnia et al.[92]	2017	adiabatic	5
Sadaghiani et al.[170]	2017	isothermal	2
Sadaghiani et al.[171]	2017	adiabatic	4
Hammad et al.[172]	2018	adiabatic	3
Chang et al.[173]	2018	adiabatic–isothermal	2
Aasadnia et al.[71]	2018	adiabatic	5
Yang et al.[84]	2019	adiabatic–isothermal	4
Ghorbani et al.[74]	2019	isothermal	2
Ansarinasab et al.[88]	2019	isothermal	2
Yin et al.[95]	2020	adiabatic–isothermal	4
Nouri et al.[174]	2020	adiabatic	2
Ebrahimi et al.[100]	2020	adiabatic	2
Chang et al.[83]	2020	adiabatic–isothermal	2
Taghavi et al.[85]	2021	adiabatic	2
Ghorbani et al.[175]	2021	adiabatic	3
Ebrahimi et al.[101]	2021	adiabatic	4
Ghorbani et al.[146]	2021	adiabatic	2
Bi et al.[176]	2022	adiabatic	2
Khatami Jouybari et al.[177]	2022	adiabatic	2
Faramarzi et al.[152]	2022	adiabatic	5
Zhang et al.[178]	2022	isothermal	2
Ghorbani et al.[179]	2023	adiabatic	2

[a]Modified from ref 164.

information on ortho- to para-H$_2$ liquefaction various systems (modified from ref 164). The SEC of the H$_2$ liquefaction cycle is decreased by increasing the stages of ortho- to para-H$_2$ conversion. The slope of reducing the SEC by increasing the ortho- to para-H$_2$ conversion stages from the first to the second reactor is done rapidly, and from the second reactor onward, it is done slowly.[164]

3. DESCRIPTION OF LIQUID HYDROGEN TECHNOLOGIES

The classic H$_2$ liquefaction process is divided into four parts: compression at ambient temperature, precooling from environ-

ment temperature to 80 K, cryogenic refrigeration from 80 to 30 K, and liquefaction due to pressure reduction to ambient pressure. The H$_2$ temperature in the liquefaction system should be decreased to boiling temperature (20 K). Figure 5 depicts a schematic of the H$_2$ liquefaction cycle according to various temperatures in a Claude simple process. Temperature can be reduced by passing the gas through the Joule–Thomson (J–T) valve, through expanders, and using an external auxiliary fluid.[58] In the J–T system, the pressure of a gas decreases under constant enthalpy. The temperature difference of the exhaust gas from the throttling valve depends on the J–T coefficient. This coefficient ($\mu_{JT} = (\delta T/\delta P)_h$) represents temperature changes to gas pressure changes in a constant enthalpy process. If the initial gas temperature is lower than the maximum inversion temperature ($\mu_{JT} = 0$) then the temperature decreases as a result of the choking process. For all gases (except helium, H$_2$, and Ne), the peak inversion temperature is higher than the environment.[180,181] Therefore, to decrease the H$_2$ temperature using the J–T process, it is necessary to first cool its temperature to less than the H$_2$ inversion temperature (205 K). As a result, H$_2$ gas cannot be liquefied at ambient temperature only by using the J–T process, and a precooling process is necessary.[182] Figure 6 shows the J–T diagram of several different gases and their inversion point. In the H$_2$ liquefaction process, any fluid whose triple-point temperature is lower than the H$_2$ maximum inversion temperature can be utilized as a precooler. These fluids can be fluorine, oxygen, air, methane, argon, and nitrogen; the first four are unsuitable due to the explosion risk, and argon is expensive compared to nitrogen.

The selection of the appropriate precooling refrigerant and the optimal configuration of the precooling section provide promising guidelines for reducing the total SEC in the liquefaction structure.[176] Currently, LN$_2$ produced from the air separation system is the most common refrigerant in the precooling step of the H$_2$ liquefaction factory because of its developed technology and proper temperature condition. According to the international demand for pure oxygen, LN$_2$ will not be available as an inexpensive refrigerant for large-scale H$_2$ liquefaction plants in the future.[184] For large H$_2$ liquefaction factories, the high-temperature difference in low temperatures prevents using LN$_2$; using LN$_2$ for precooling up to 80 K is less efficient. Also, the minimum exergy required to produce LN$_2$ is twice the amount required to refrigerate the feed H$_2$ to 80 K.[185] Therefore, using a closed-loop nitrogen cooling cycle and mixed refrigerants can solve this problem. Moreover, expanders can be used to lower the temperature of H$_2$ during an isentropic expansion process, which always reduces the temperature of ideal and nonideal gases.[186] Considering that the H$_2$ liquefaction process uses the pressure expansion or reduction phenomenon to decrease the temperature of H$_2$ gas, a compression process using a compressor for the incoming H$_2$ gas is necessary. Part of the cooling can be done at a higher temperature by compressing the feed to a greater pressure, which reduces the power consumption to provide the needed refrigeration but boosts the cost of condensation at ambient temperature.[185] H$_2$, helium, and Ne are the candidates used separately and in mixtures for the cooling and liquefaction steps.[187] The small- to medium-scale H$_2$ liquefaction structure for easy use of LN$_2$ is often located adjacent to cryogenic air separation units. Helium is the only element with a lower boiling temperature than H$_2$. However, its availability and price can be the main challenges. H$_2$ temperature can be decreased to 90 K by liquid oxygen recovery in the precooling section, but this component can encounter the same
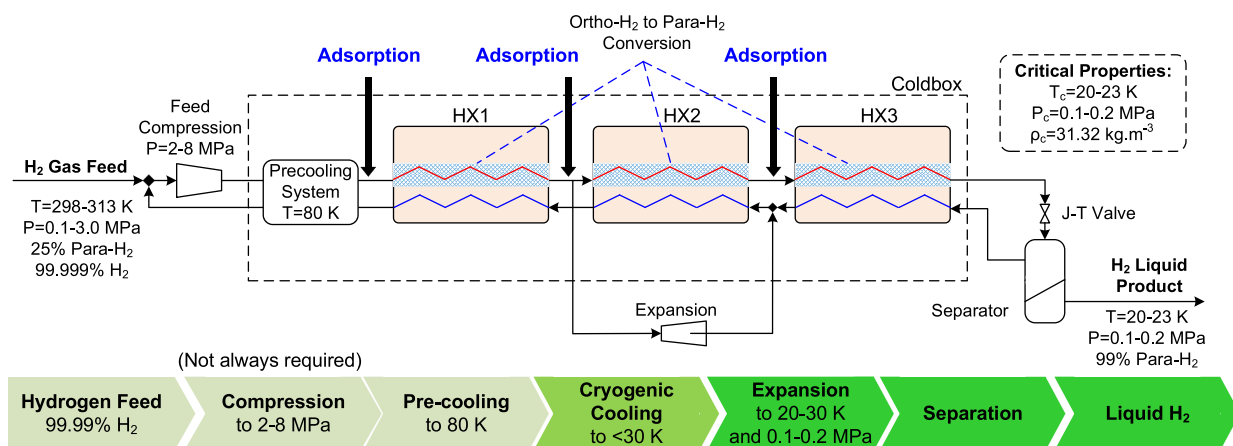
Figure 5. Schematic of the H_2 liquefaction system according to various temperatures in a Claude simple process. Modified from ref 59.
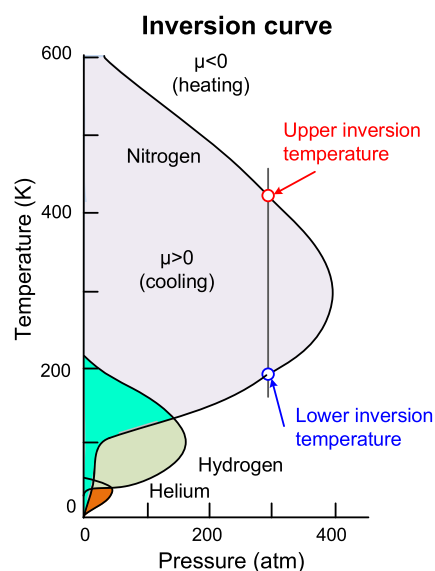
Figure 6. Joule−Thomson diagram of several different gases and their inversion point. Modified from ref 183.

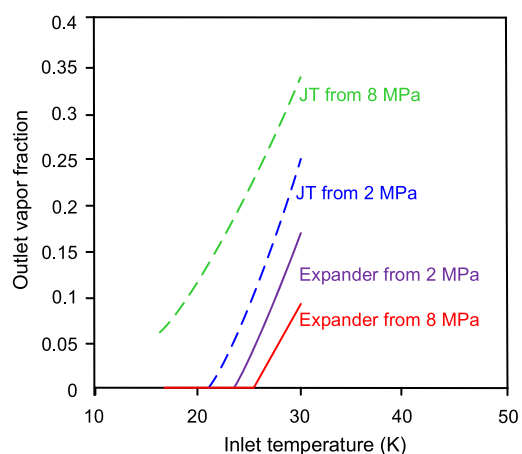**Figure 7.** Variations of the steam fraction at different pressures and temperatures after the J−T valve and expander. Modified from ref 185.

problems as LN_2 cold recovery. In contrast, the LNG cold recovery (i.e., liquid methane) for the precooling section has a promising prospect considering availability and price.[80] Several mixed refrigerants have been developed with various precooling temperatures because the boiling point of the mixture depends on the composition.[80,184] Figure 7 displays the importance of using expanders instead of the J−T valve, especially in high-pressure compression.

In H_2 liquefaction with the Claude and L−H methods, cooling is achieved by isentropic expansion through the expander and isothermal expansion by the J−T valve.[185] Also, in the reverse Brayton cycle, the refrigerant flow expansion is done only by the turbine expanders. The most significant issue for cryogenic cooling involves the highly fluctuating specific heat of H_2 near the critical temperature, which makes temperature stabilization in heat exchangers difficult. An increase in the input H_2 pressure fixes this problem, somehow. The compression process reduces the cooling load over a wide temperature range, but the variable cooling load should be managed by adjusting the cooling power.[188]

A constant enthalpy process in the J−T valve or a constant entropy process in expanders can liquefy H_2. In the L−H

precooling process, compressors compress H_2 gas to relatively high pressures, and then, it is cooled by passing through exchangers and LN_2. Finally, by passing through a J−T valve and due to a sudden pressure drop, its temperature decreases and part of the H_2 gas liquefies. Part of the H_2 that is in gas form is used as a cold fluid in heat exchangers to cool the hot H_2 gas entering the process because of its relatively low temperature. This gas is finally returned to the beginning of the process to be mixed with fresh H_2 gas, and the process is repeated.[190] In the Claude process, the cold return flow cools part of the H_2 gas, and LN_2 is separated and cooled by passing through an expander. This cooled H_2 is used to cool the rest of the H_2 flow. In the Claude process, similar to the L−H process, a J−T valve is used for liquefaction in the last step.[189] The Claude process has higher liquefaction efficiency and lower power consumption than the L−H process.[170] But, the Claude process uses more complex equipment compared to the L−H process.[191] Helium gas, in addition to LN_2, is used for precooling in the Claude process with a helium precooler. As a result, the pressure required for the compressor's H_2 output as well as its SEC are reduced. In this process, the size of the compressor is smaller than that in the Claude process, but three separate compressors are needed for H_2, nitrogen, and helium.[189] The J−B auxiliary refrigeration systems can be used for similar helium precooling in combination with a simple Claude process to provide intermediate cooling. The refrigerant used in J−B auxiliary
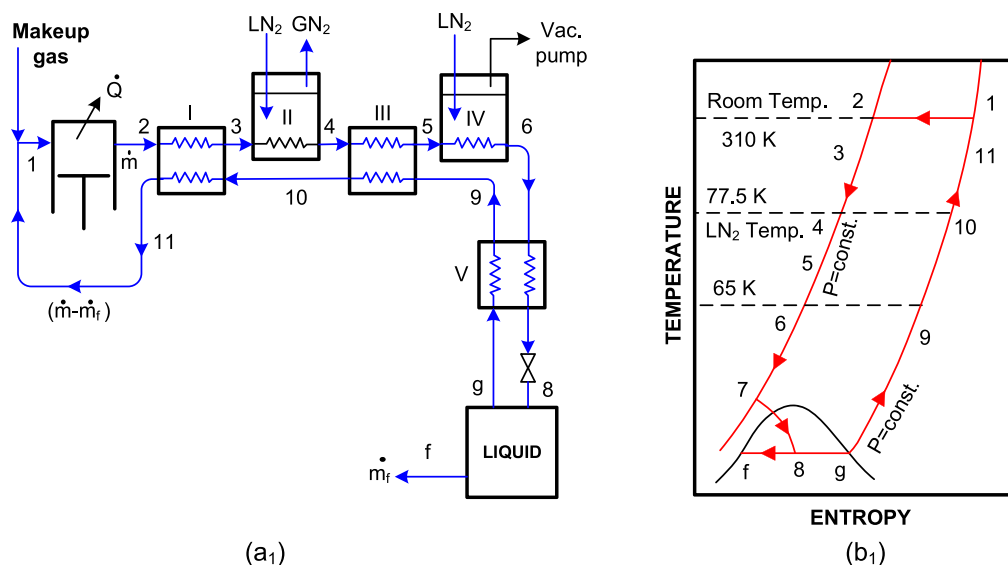
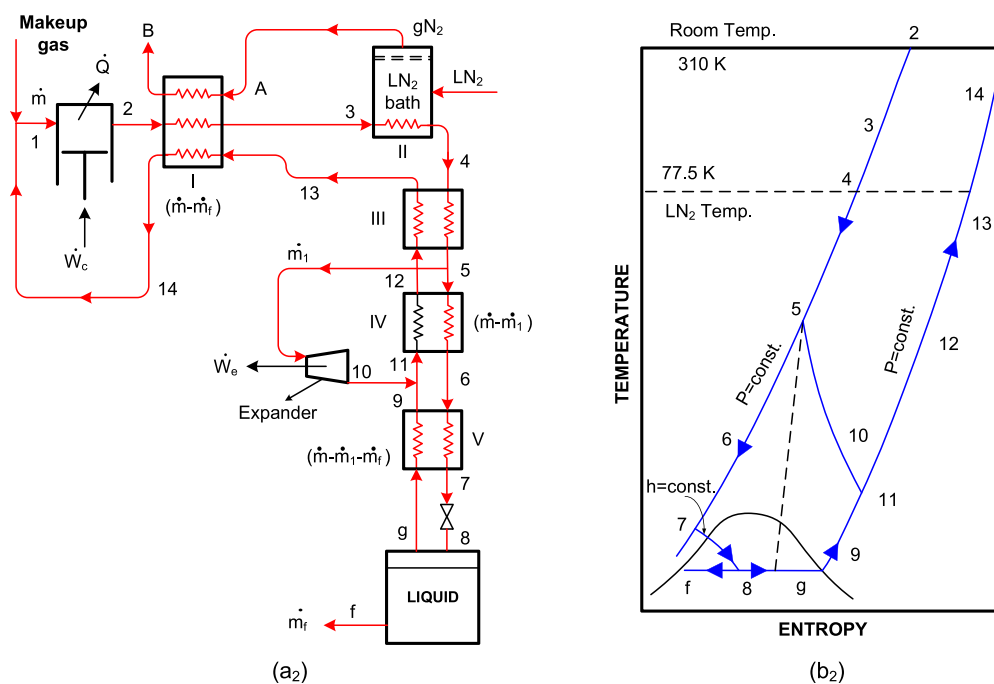(a) Flow diagram and temperature-entropy graph of precooled L-H system

(b) Flow diagram and temperature-entropy graph of Claude process H$_2$ liquefier

Figure 8. Flow diagram and temperature−entropy graph for the precooled L−H system, Claude process H$_2$ liquefier, and Claude process with a helium precooling H$_2$ condensing cycle. Modified from ref 189.

refrigeration systems can be simple or mixed. Mixed refrigerant precooling systems can be used as an auxiliary precooling part of H$_2$ liquefaction systems. These systems consume less power and are more efficient than closed single-component cycles.[175] Figure 8 depicts the flow diagram and temperature−entropy graph for the precooled L−H system, Claude process, and Claude process with helium precooling. Figure 9 depicts the flow diagram of the J−B plant and mixed refrigerant precooling in the Claude systems.

The SEC of current H$_2$ liquefaction systems is 10.8−12.7 kWh/kgLH$_2$ for the Claude system and 12.3−13.4 kWh/kgLH$_2$ for the Brayton structure.[192] Claude processes are the most often

used processes by industrial units compared to other cooling processes.[62] Cooling H$_2$ to temperatures close to its boiling point is done by refrigerants that can reduce the temperature to the boiling temperature without phase change.[193] H$_2$ is the main refrigerant in most of the traditional H$_2$ liquefaction processes. Its application includes drawbacks such as the inability to decrease the temperature below the H$_2$ boiling point, the high SEC of compressors, and high penetration in equipment structure due to low molecular mass and low system efficiency.[165,194] Helium refrigerant and Ne gas were proposed to solve the problems caused by H$_2$; the larger molecular mass of helium significantly reduces the power consumption, and its
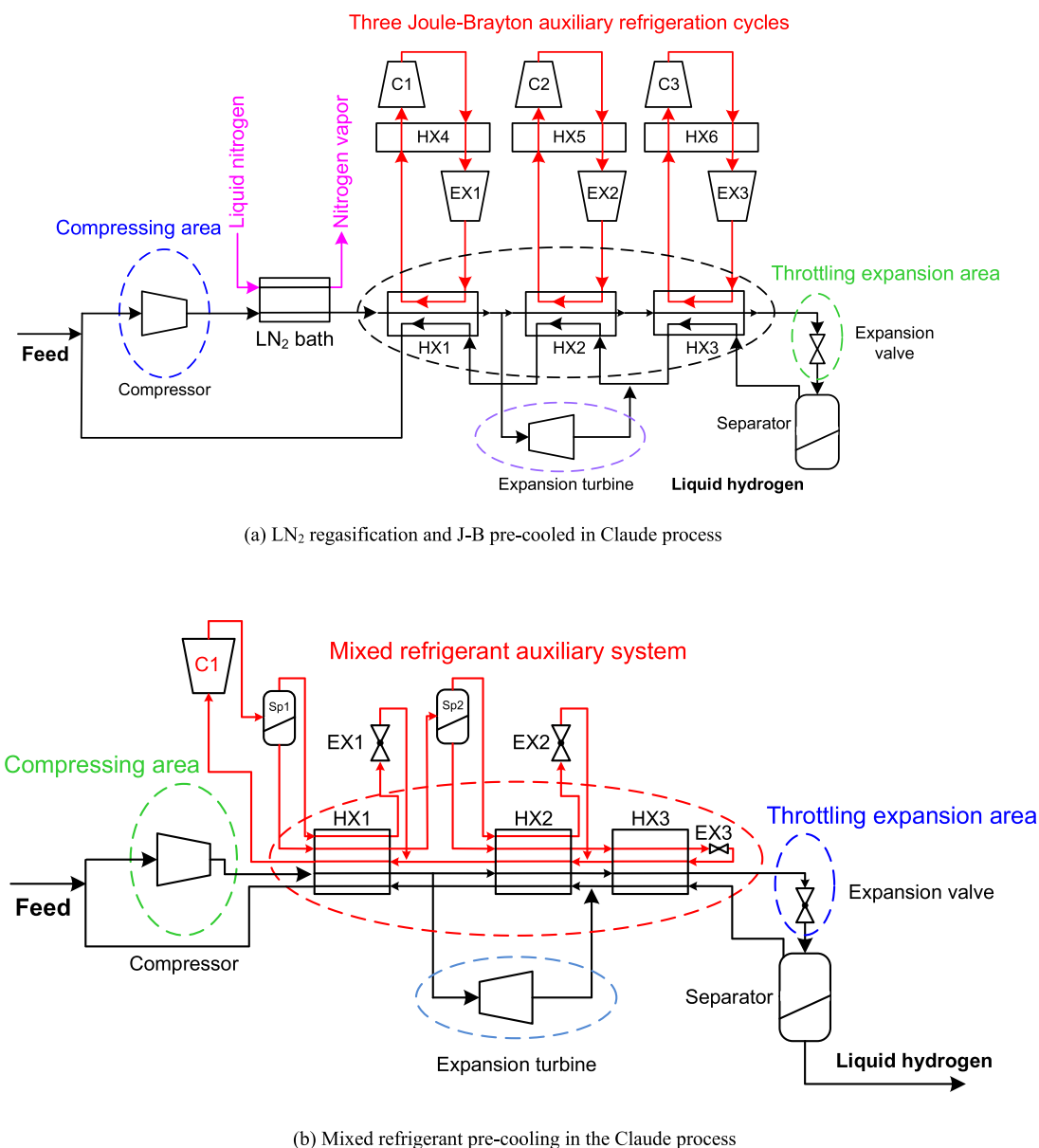
(a) LN$_2$ regasification and J-B pre-cooled in Claude process

(b) Mixed refrigerant pre-cooling in the Claude process

Figure 9. Flow diagram of the J−B process and mixed refrigerant precooling in the Claude systems. Modified from ref 58.

penetration decreases due to the larger molecules of helium.[78,195] Figure 10 depicts the various temperature ranges of low-boiling fluids used as refrigerants for H$_2$ liquefaction. H$_2$ and helium refrigerants are the most suitable options for H$_2$ liquefaction. To prevent the weakening of the thermal properties, the maximum usable amount of Ne was suggested to be 30%.[196]

4. DIFFERENT METHODS TO IMPROVE THE PERFORMANCE OF HYDROGEN LIQUEFACTION SYSTEMS

Systems designed for H$_2$ liquefaction include simple Kapitza, Claude, dual-pressure Claude, precooled L−H, dual-pressure precooled L−H, simple precooled Claude, dual-pressure precooled Claude, helium precooled Claude cycles, and precooled MRCs.[58,66] Also, nitrogen[77] and propane[165] were used to precool the liquefaction cycle. Extensive research has been conducted to reduce the SEC in liquid H$_2$ production units so that it can compete with other energy sources as a portable

clean fuel. Mixed refrigerant cooling systems, absorption/ejector refrigerating cycles, LNG regasification operations for precooling, operational optimization, pinch and exergy analyses, and integration with the same manufacturing process can help to reduce the SEC.

4.1. Mixed Fluid Refrigeration System in the Hydrogen Liquefaction Process. One of the principal challenges of pure H$_2$ storage in large volumes is the low efficiency of the current H$_2$ liquefaction systems. Nowadays, the H$_2$ liquefaction system is expensive and requires much energy to operate. Therefore, the highest cost in the construction of hydrogen liquefaction plants belongs to the refrigeration cycles. Therefore, the proper and optimal design of per-cooling and liquefaction cycles is necessary.[174] By using mixed refrigerants instead of pure refrigerants in the H$_2$ liquefaction structure, it is possible to modify the suitable temperature range of using the refrigeration system with pure refrigerants.[197,198] As a result, the type and percentage of components in multicomponent refrigerants are chosen in such a way that the refrigerant evaporates at a
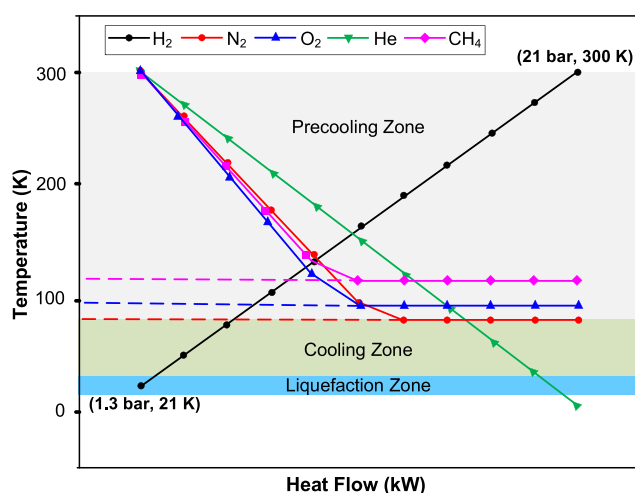
Figure 10. Different temperature ranges of low-boiling fluids involved in refrigerants for H_2 liquefaction. Modified from ref 80.

temperature range close to the process's refrigeration load curve.[199] Due to the high cost of cryogenic systems of low-temperature processes and also their complex interaction with the core of the process, extensive research has focused on their optimization and integration with the core of the process. Podbielniak[200] was the first to introduce the mixed refrigerant process. Then, using Podbielniak's patent, Kleemenko showed that the process efficiency depends on the small temperature difference between the cooled stream and the mixed refrigerants.[201] Next, multiple U.S. patents on this structure were subsequently developed for the LNG process. Gaumer et al.[202] presented one of the most interesting MRCs. Krasae-in et al.[203,204] used small-scale laboratory MRCs for precooling H_2 gas. Krasae-in et al.[89] developed the H_2 liquefaction system with 100 TPD capacity including two-stage MRCs for precooling and four J−B cascades for large-scale liquefaction. The thermodynamic efficiency according to ortho- to para-H_2 conversion and the SEC were obtained at 54.02% and 5.35 kWh/kgLH$_2$, respectively. Also, the SEC and thermodynamic efficiency due to the ortho- to para-H_2 conversion in the basic H_2 liquefaction system in the Ingolstadt factory were 13.58 kWh/kgLH$_2$ and 21.28%, respectively.[205] Also, Krasae-in[91] developed the H_2 liquefaction process with a 100 TPD capacity including two-stage MRCs and four J−B cascade processes with H_2 composition. The SEC in the developed system and the basic H_2 liquefaction system at the Ingolstadt facility are 5.35 and 13.58 kWh/kgLH$_2$, respectively.[205] It is recommended to use MRC for precooling in the LH$_2$ production cycle with a large

size (>50 TPD). Increasing the capacity of the H_2 liquefaction cycle and using the MRC in precooling lead to a reduction of the SEC to less than 7 kWh/kgLH$_2$. Table 3 lists the state of the art H_2 liquefaction technology with various capacities. It shows that H_2 liquefaction cycles can be divided into four sizes of small (1−10 TPD), medium (10−50 TPD), large (50−100 TPD), and extra large (>100 TPD) according to their capacity. Table 4 presents the technical characteristics of the theoretical systems in H_2 liquefaction processes. It is concluded that using MRC increases the exergy efficiency in H_2 liquefaction systems.

4.2. LNG Regasification in the Hydrogen Liquefaction Process. Pure H_2 storage using liquefaction methods is associated with losses due to boil-off gas in liquid H_2 and the high SEC.[100] The SEC in the liquefaction plants currently operating in the world is about 13−15 kWh/kgLH$_2$.[215] Theoretically, the minimum energy needed in the H_2 liquefaction process for gaseous feed H_2 at 25 bar is about 2.7 kWh/kgLH$_2$.[139] To facilitate future energy applications, it is critical to reduce the SEC and enhance exergy efficiency in H_2 liquefaction systems. Also, the H_2 liquefaction cost is about 40−50% of the total investment for a 100 TPD capacity.[216] Therefore, it is necessary to develop methods to reduce the refrigeration used in the system. Liquid natural gas is the most widely utilized raw material for H_2 production. A significant amount of cryogenic energy is released into the water during the regasification process.[217] In general, most of the cold energy of LNG (830 kJ/kg) is lost in seawater as it changes phase from liquid (114 K) to gas or is partially heated before being compressed and entering pipelines. It can also be supplied as regasified natural gas elsewhere. This cold energy is being employed in food storage, separation units, cryogenic CO_2 absorption, desalination, power production, and, more recently, air liquefaction.[218−221] It was suggested to use the regasification refrigeration potential of LNG to precool the H_2 liquefaction system to reduce the SEC. The first related patent was given to Air Products in 2005.[222] Kuendig et al.[86] confirmed the thermodynamic efficiency of this design. The input energy savings was about 30−50% based on the process configuration. Cho et al.[217] utilized cold recovery of LNG and the J−B cascade process to liquefy H_2. They used a combination of a genetic algorithm (GA) and an HYSYS simulator to optimize the offered structure. The results indicated that the modification of the liquefaction structure using regasification of LNG and its optimization decreased the SEC from 4.36 to 4.07 kWh/kgLH$_2$. Also, the capital and operating costs of the offered configuration were reduced by 15.16% and 9.05%, respectively. Figure 11 depicts various process diagrams for employing the LNG recovery in the precooling of the H_2 liquefaction structure. The

Table 3. State of the art H_2 Liquefaction Technology in Terms of Capacity[a]

	state of the art				
	small size	medium size	large size	large size	future extra large
capacity (TPD)	1−10	10−50	50−100	50−100	>100
precooling technology	liquid N_2 or N_2 process	N_2 process	N_2 process	MR process	MR process
liquefaction technology	He process or H_2 process	He process or H_2 process	He process	He process	He process
maturity	references under operation	references under operation	design validated ready for industrialization	design validated ready for industrialization	under study
optimization	CAPEX oriented	CAPEX oriented	CAPEX oriented	OPEX oriented	OPEX oriented
SEC (kWh/kgLH$_2$)	>12 kWh/kg				<7 kWh/kg

[a]Modified from ref 206.

Table 4. Technical Characteristics of the Theoretical Systems in H$_2$ Liquefaction Processes

author	year	SEC (kWh/kgLH$_2$)	exergy efficiency (%)	COP	process details
Baker et al.[76]	1978	10.85	36		number of conversion reactors (NCR): 2, O-H$_2$ to P-H$_2$ (%): 75/51.4/3
					LN$_2$ and J−B precooling Linde
					feed: mass flow (MF), 250 TPD; temperature (T), 35 °C; pressure (P), 1 bar
					MITA: 1−3 °C
Bracha et al.,[77] Gross et al.,[207] Quack,[165,208] Weindorf et al.,[209] and Krasae-In et al.[62,89,203]	1994[77,207]	13.6[77,207]	33[77]		LN$_2$ and J−B precooling Linde
	2002[165,208] 2003[209]	15[165,208]			
		13[209]	21[62,89,203]		
	2010[62,89,203]				
Matsuda et al.[210]	1997	8.416	47.1		Ne with cold pump, 300 TPD
		8.576	46.2		basic Ne Brayton, 300 TPD
		8.688	45.6		helium Brayton, 300 TPD
		8.528	46.4		
					H$_2$ Claude, 300 TPD
Kuz'menko et al.[78]	2008	12.7	34.6		precooling cycle: SRC (LN$_2$)
					cooling and liquefaction cycle: helium refrigeration cycle
					feed: MF, 0.0625 kg/s; T, 42 °C; P, 16 bar
Shimko et al.[211]	2008	8.73	44.6		NCR: 4
					modified Claude cycle with helium refrigeration unit
					feed: MF, 50 TPD
Krasae-In et al.[203]	2010	5.35	54.0	0.1661	precooling cycle: MRC (C$_1$, C$_2$, C$_3$, C$_4$, C$_5$, R14, C$_3$H$_6$, Ne, and N$_2$)
					cooling and liquefaction cycle: helium refrigeration and H$_2$ refrigeration cycles
					feed: MF, 2 kg/h; T, 25 °C; P, 1 bar
Krasae-In et al.[91]	2014	5.91	48.9	0.1490	NCR: 6, O-H$_2$ to P-H$_2$ (%): 100/75/64/52/20/20/5
					precooling cycle: two-stage MRC compression (25 to −198 °C)
					cooling and liquefaction cycle: four H$_2$ J−B cycles, (−198 to −253 °C)
					feed: MF, 1.157 kg/s; T, 25 °C; P, 21 bar
					MITA: 1−3 °C
Yuksel et al.[169]	2017		57.1		NCR: 3
					precooling, cooling and liquefaction cycles: SRC (He) (25 to −252 °C)
					catalyst bed I: −158 °C
					catalyst bed II: −222 °C
					catalyst bed III: −245 °C
Sadaghiani et al.[170]	2017	4.36	55.5	0.1797	NCR: 2, O-H$_2$ to P-H$_2$ (%): 100/50/5
					precooling cycle: MRC (C$_1$, C$_2$, C$_3$, C$_4$, C$_5$, R14, C$_2$H$_4$, H$_2$ and N$_2$), (25 to −193 °C)
					cooling and liquefaction cycle: SRC (H$_2$) (−193 to −253 °C)
					feed: MF, 3.45 kg/s; T, 25 °C; P, 21 bar
					MITA: 1−3 °C
Asadnia et al.[87]	2017	7.69	39.5	0.1710	precooling cycle I: MRC (C$_1$, C$_2$, C$_4$, H$_2$, and N$_2$) (25 to −198 °C)
					cooling and liquefaction cycle: MRC (He, H$_2$, and Ne) (−198 to −252.9 °C)
					feed: MF, 1.157 kg/s; T, 25 °C; P, 21 bar
					MITA: 1−3 °C
Sadaghiani et al.[171]	2017	7.65	32.0	0.0672	NCR: 4
					precooling, cooling, and liquefaction cycles: MRC (C$_2$, C$_3$, C$_5$, C$_2$H$_4$, H$_2$, and N$_2$) (25 to −252 °C)
					feed: MF, 1.5 kg/s; T, 25 °C; P, 21 bar
					MITA: 1−2 °C
Asadnia et al.[71]	2018	6.47	45.5	0.2034	NCR: 5

Table 4. continued

author	year	SEC (kWh/kgLH$_2$)	exergy efficiency (%)	COP	process details
					precooling cycle I: MRC (C$_1$, C$_2$, C$_3$, C$_4$, C$_5$, R14, NH$_3$, H$_2$, and N$_2$)
					precooling cycle II: SRC (H$_2$) (25 to −196.2 °C)
					cooling and liquefaction cycles: MRC (H$_2$ and Ne) (−196.2 to −249.3 °C)
					feed: MF, 1.157 kg/s; T, 25 °C; P, 21 bar
					MITA: 1−2 °C
Qyyum et al.[147]	2021	6.45	47.2	0.204	NCR: 2
					precooling cycle I: MRC (C$_1$, C$_2$, C$_3$, C$_4$, and N$_2$) (25 to −160 °C)
					cooling cycle (−160 to −230 °C), MRC (C$_1$, C$_2$, C$_3$, H$_2$, and N$_2$)
					liquefaction cycle: MRC (Ne and H$_2$) (−230 to −248.1 °C)
					feed: MF, 1 kg/h; T, 25 °C; P, 21 bar
					MITA: 1−3 °C
Zhang et al.[178]	2021	5.742	55.3	0.1574	NCR: 3, O-H$_2$ to P-H$_2$ (%): 0/51/3
					precooling cycle I: MRC (C$_1$, C$_2$, C$_3$, C$_5$, and N$_2$)
					precooling cycle II: SRC (N$_2$), (25 to −160 °C)
					cooling cycle: MRC (H$_2$ and Ne) (−160 to −230 °C)
					liquefaction cycle: MRC (N$_2$, Ne, and H$_2$) (−230 to −248.1 °C)
					feed: MF, 3.344 kg/s; T, 25 °C; P, 21 bar
Naquash et al.[161]	2022	7.63	31.4	0.1600	NCR 3, O-H$_2$ to P-H$_2$ (%): 75/65/25/5
					precooling cycle I: SRC (CO$_2$)
					precooling cycle II: MRC (C$_1$, C$_2$, C$_3$, and N$_2$) (25 to −160 °C)
					cooling cycle: MRC (C$_1$, C$_2$, H$_2$, and N$_2$) (−160 to −230 °C)
					liquefaction cycle: MRC (He and H$_2$) (−230 to −248.1 °C)
					unit production price: 5.18 $/kg LH$_2$ for 1 TPD
					feed: MF, 1.157 kg/s; T, 25 °C; P, 21 bar
					MITA: 1 °C
Sun et al.[164]	2022	6.43			NCR: 2, O-H$_2$ to P-H$_2$ (%): 75/50/1
					precooling cycle: MRC (C$_1$, C$_2$, C$_3$, C$_4$, C$_5$, H$_2$, R14, C$_2$H$_4$, N$_2$), (25 to −195 °C)
					cooling and liquefaction cycles: MRC (N$_2$, He, and H$_2$) (−195 to −253 °C)
					feed: MF, 345 kg/s; T, 25 °C; P, 21 bar
					MITA: 1−3 °C
Naquash et al.[212]	2022	9.62	31.5	0.1	NCR: 3, Fe$_2$O$_3$
					precooling cycle: MRC (C$_1$, C$_2$, C$_3$, and N$_2$) (25 to −160 °C)
					cooling cycle: MRC (C$_1$, C$_2$, N$_2$, and H$_2$) (−160 to −235 °C)
					liquefaction cycle: MRC (N$_2$, He, and H$_2$) (−235 to −252 °C)
					TEC, 196 MM$; TAC, 52.8 MM$/year
					feed: MF, 100 kg/s; T, 35 °C; P, 5 bar
					MITA: 1−2 °C
Lee et al.[213]	2022	4.55	67	0.289	NCR: 3, IONEX
					precooling cycle I: MRC (C$_2$, C$_3$, C$_4$, and HFO)
					precooling cycle II: MRC (C$_1$, C$_2$, C$_3$, C$_4$, and N$_2$) (25 to −153 °C)
					cooling cycle: MRC (C$_1$, C$_2$, C$_3$, H$_2$, and N$_2$) (−153 to −235 °C)
					liquefaction cycle: MRC (He and H$_2$) (−235 to −252 °C)
					unit production price: 5.18 $/kg LH$_2$ for 1 TPD
					feed: MF, 1 kg/s; T, 25 °C; P, 21 bar
					MITA: 1−3 °C
Kim et al.[214]	2022	9.477	34	0.23	NCR: 2, O-H$_2$ to P-H$_2$ (%): 75/25/0.5

Table 4. continued

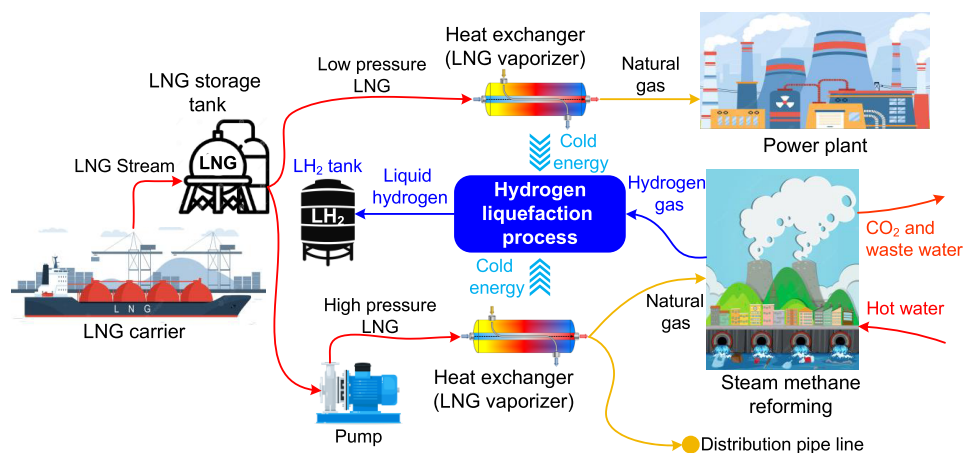| author	year	SEC (kWh/kgLH$_2$)	exergy efficiency (%)	COP	process details
					precooling cycle: MRC (C$_1$, C$_2$, C$_3$, and N$_2$) (25 to −160 °C)
					cooling cycle: MRC (C$_1$, C$_2$, N$_2$, and H$_2$) (−160 to −230 °C)
					liquefaction cycle: MRC (N$_2$, He, and H$_2$) (−230 to −252.1 °C)
					unit production price: 5.54 \$/kg LH$_2$ for 1 TPD
					feed: MF, 1 TPD; T, 25 °C; P, 25 bar
					MITA: 1−2 °C

Figure 11. Layout of a hybrid H$_2$ liquefaction system with an SMR plant integrated with the LNG cold recovery terminal. Modified from ref 152.

LNG cold recovery process in the precooling of the H$_2$ liquefaction cycle can be used alone or integrated with other precooling cycles (MRC and SRC precooling). Noh et al.[223] designed two new configurations of H$_2$ liquefaction using the regasification recovery of LNG in the precooling stage. To precool the H$_2$ liquefaction system, the first structure alone employs the regasification process, while the second employs a combination of the regasification operation and mixed refrigerant systems. Similar results demonstrated that the SEC in the first and second structures has decreased by 5.14% and 8.13%, respectively, compared to the basic cycle. Also, the capital and operating costs of the second structure decreased by 31.76% and 11.55%, respectively, compared to the basic cycle. Riaz et al.[80] employed LNG cold recovery in the precooling stage to reduce the SEC in the H$_2$ liquefaction system. This structural modification reduced the total amount of refrigerant by 50% and the SEC by 40%. The exergy efficiency of the hybrid design was reported to be 42.25%. In addition, the COP of this structure was 40.2% higher than the basic system. The suggested system has the prospect of a cost-effective LNG and LH$_2$ supply chain. Chang et al.[83] designed a novel thermodynamic structure for H$_2$ liquefaction using LNG cold recovery. The LNG cold recovery system refrigerated the H$_2$ gas which then entered a closed Brayton cooling system. The SEC for a laboratory-scale structure with 0.5 TPD capacity was 12.6−13.6 kWh/kgLH$_2$. Yang et al.[84] investigated the H$_2$ liquefaction cycle with 300 TPD capacity, including the LN2 and LNG cold recovery for H$_2$ precooling. The analysis demonstrated that the LNG cold recovery system for H$_2$ precooling reduces the LN$_2$ mass flow rate and improves the structure efficiency. Furthermore, the SEC decreased from 13.58 to 11.05 kWh/kgLH$_2$ in the modified structure. A hybrid system for H$_2$ liquefaction and storage was

proposed using the LNG cold recovery system for precooling and four MRCs for liquefaction. Fuel cells unit, gas turbine power plants, two-stage organic Rankine cycles (ORC), and a CO$_2$ power system were utilized to provide power.[224] The power consumption, COP, and SEC for the proposed system were calculated to be 3.872 kWh/kgLH$_2$, 0.175, and 4.772 kWh/kgLH$_2$, respectively. According to the findings, employing the chilling process of the LNG regasification operation for precooling decreases the exergy yield of the H$_2$ liquefaction unit from 39.4% to 38% and the power consumption from 6.642 to 3.822 kWh/kgLH$_2$. Yun[225] presented a H$_2$ liquefaction plant that used LN$_2$ and LNG regasification in the precooling step. According to their study, energy savings of about 75% were obtained.

Zarsazi et al.[226] designed a hybrid refrigeration structure for wind energy storage to liquid H$_2$ using water electrolysis, the L−H liquefaction cycle, and LNG regasification for precooling. The optimization outcomes showed that the energy and exergy yields of the cryogenic structure were 17.51% and 55.43%, respectively. Using the GA algorithm increased the exergy yield of the cryogenic energy storage system to 58.29%.

About 76% of the H$_2$ generated globally is from SMR hydrocarbons. The SMR systems integrated with CO$_2$ capture, utilization, and storage have low CO$_2$ emissions with affordable cost and developed technology compared with other H$_2$ generation techniques (i.e., coal and renewable energy).[105,227,228] Integrating this method to produce H$_2$ in systems that use LNG regasification for precooling can reduce the SEC. Figure 12 illustrates the layout of a hybrid H$_2$ liquefaction system with an SMR plant integrated with the LNG cold recovery terminal. Farmarzi et al.[152] developed a new integrated unit to produce 369 TPD of liquid H$_2$ using LNG

(a) Two-stage MRC and cryogenic J-B cycle

(b) LNG cold recovery, two-stage MRC and cryogenic J-B cycle

(c) LNG cold recovery and cryogenic J-B cycle

Figure 12. Various process diagrams for using the LNG cold recovery in the H$_2$ liquefaction system.

Table 5. Technical Characteristics of Some H_2 Liquefaction Systems Using LNG Cold Recovery

author	year	SEC in the base case (kWh/kgLH$_2$)	exergy efficiency in the base case (%)	relative energy saving (%)	process details in modified case
Yang et al.[84]	2019	13.72		19.46	SEC of the modified case: 11.05 kWh/kgLH$_2$ reducing capital costs (RCC): 35.2% reducing operating costs (ROC): 34.6% selling price of LH$_2$ (SPLH$_2$) in base case: 5.13 \$/kgLH$_2$ SPLH$_2$ in modified case: 2.53 \$/kgLH$_2$ in base case: LN$_2$- and GH$_2$-Brayton cycles in modified case: LNG cold energy, LN$_2$- and GH$_2$-Brayton cycles NCR: 3 feed: MF, 300 TPD; T, 27 °C; P, 20 bar
Cho et al.[217]	2021	4.36		6.65	SEC of the modified case: 4.07 kWh/kgLH$_2$ RCC: 15.16% ROC: 9.05% in base case: two-stage MRC and cryogenic J−B cycle in modified case: LNG cold energy, MRC and cryogenic J−B cycle NCR: 2, O-H$_2$ to P-H$_2$ (%): 100/50/5 precooling cycle: MRC (C$_1$, C$_2$, C$_3$, C$_4$, C$_5$, R14, C$_2$H$_4$, H$_2$, and N$_2$) (25 to −193 °C) cooling and liquefaction units: MRC (Ne, He, and H$_2$) (−193 to −253 °C) feed: MF, 300 TPD; T, 25 °C; P, 21 bar
Faramarzi et al.[152]	2021	13.48		34.34	SEC of the modified case: 8.85 kWh/kgLH$_2$ RCC: 32.7% SPLH$_2$ in base case: 2.54 \$/kgLH$_2$ SPLH$_2$ in modified case: 2.07 \$/kgLH$_2$ ROC: 12.58% in base case: MRC and cryogenic J−B cycle in modified case: LNG cold energy and cryogenic J−B cycle NCR: 4 precooling cycle: MRC (C$_1$, C$_3$, C$_2$H$_4$, and N$_2$) cooling and liquefaction cycles: MRC (Ne, He, and H$_2$) feed: MF, 300 TPD; T, 25 °C; P, 20 bar
Riaz et al.[80]	2021	11.19	28.64	31.72	SEC of the modified case: 7.64 kWh/kgLH$_2$ exergy efficiency of the modified case: 42.25% COP of the base case: 0.196 COP of the modified case: 0.286 in base case: three MRC in modified case: LNG cold energy and three MRC NCR: 3 precooling cycle: MRC (C$_1$, C$_2$, C$_3$, and N$_2$) cooling cycle: MRC (C$_1$, N$_2$, and H$_2$) liquefaction cycle: MRC (He and H$_2$) feed: MF, 31.71 kg/s; T, 25 °C; P, 21 bar
Bian et al.[229]	2021	6.60	47.0		SEC of case I: 6.88 kWh/kgLH$_2$ SEC of case II: 6.91 kWh/kgLH$_2$ exergy efficiency of case I: 45.1% exergy efficiency of case II: 44.9% in base case I: LNG cold energy and four combined J−B cascade cycles in base case II: LNG cold energy and four-stage Brayton cascade cycles in modified case: LNG cold energy and dual-pressure Brayton cycles NCR: 4 feed: MF, 120 TPD; T, 25 °C; P, 21 bar
Ghorbani et al.[224]	2022	6.642	39.4	28.15	SEC of the modified case: 4.772 kWh/kgLH$_2$ exergy efficiency of the modified case: 38% COP of the base case, 0.164; COP of the modified case, 0.171 in base case: two-stage MRC and cryogenic J−B cycle

Table 5. continued

author	year	SEC in the base case (kWh/kgLH$_2$)	exergy efficiency in the base case (%)	relative energy saving (%)	process details in modified case
					in modified case: LNG cold energy and cryogenic J−B cycle
					NCR: 2
					precooling cycle: MRC (C$_1$, C$_2$, C$_3$, C$_4$, C$_5$, R14, C$_2$H$_4$, H$_2$ and N$_2$)
					cooling and liquefaction cycles: MRC (He, H$_2$, and Ne)
					feed: MF, 1766 kmol/h; T, 25 °C; P, 21 bar

(a) Single-stage ACC

(b) Two-stage ACC

(c) Three-stage ACC
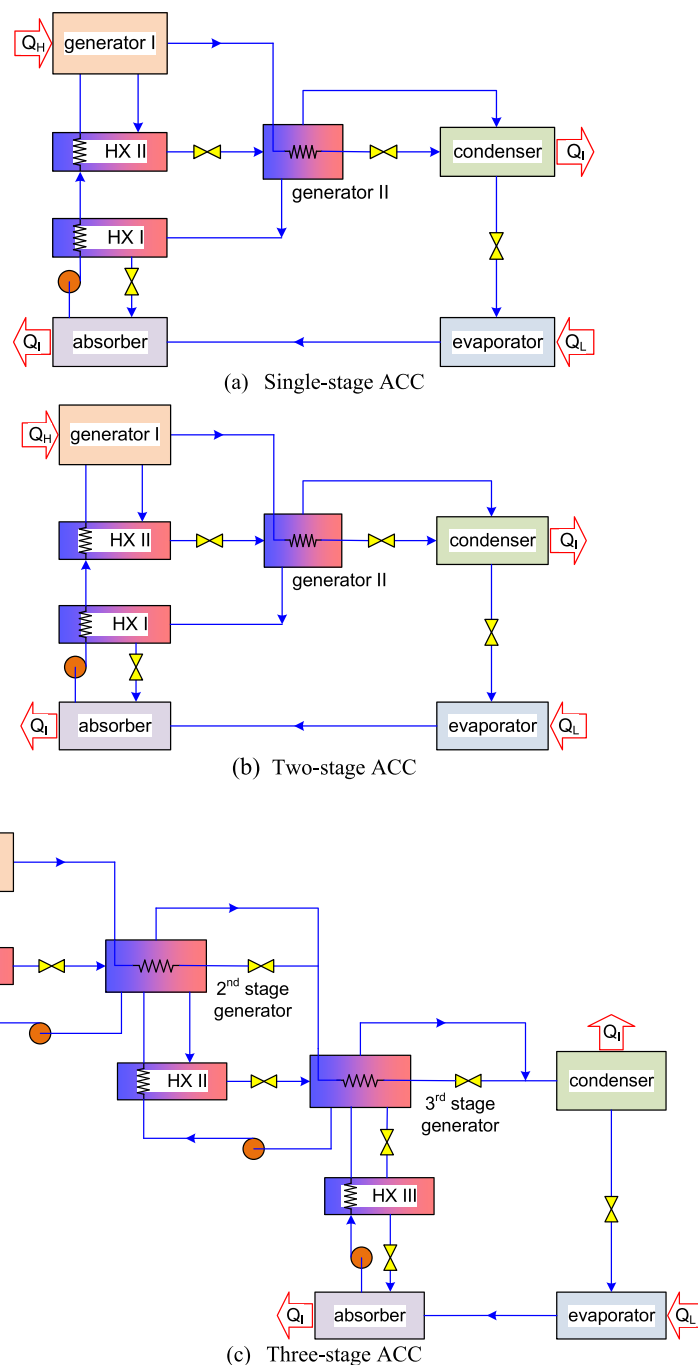
Figure 13. Schematic of multieffect absorption cooling cycles (ACCs) used in integrated systems. Modified from ref 235.

regasification and a SMR process. When compared to the base system, using the refrigeration potential of the regasification process to liquefy natural gas in the H$_2$ liquefaction system lowered the total annual cost by 13.43% and the SEC by 19.9%. The minimum cost of liquid H$_2$ in the market and the investment return period were estimated to be 2.07 $/kg and 3
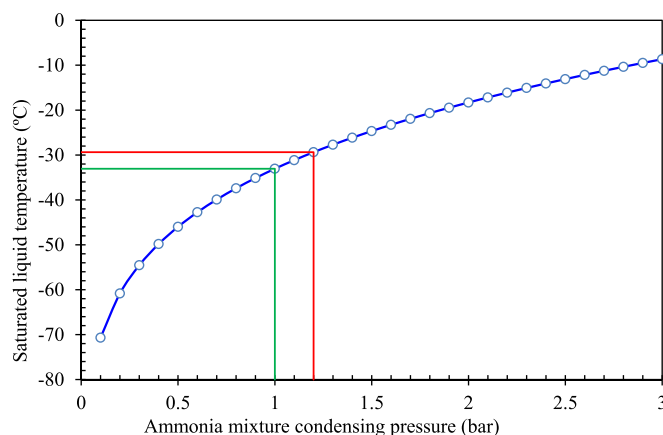
(a) Effect of the NH_3 saturated mixture pressure with a purity of 99.9% on the temperature of the mixture in the evaporator
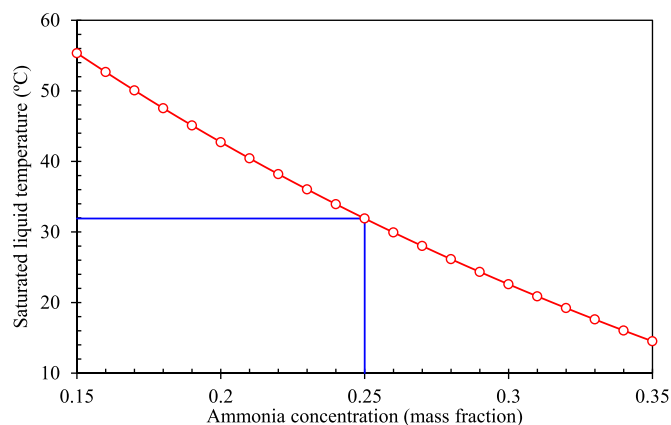
(b) Impact of NH_3 concentration on saturated liquid temperature of NH_3/H_2O mixture in absorber

Figure 14. Effect of NH_3/H_2O mixture parameters to determine evaporator temperature and pressure. Modified from ref 256.

years, respectively. Bae et al.[82] utilized an LNG cold recovery procedure for precooling in the H_2 liquefaction configuration. The regasified natural gas was used to produce H_2 by a steam methane reforming strategy. This system is optimized to reduce the SEC and CO_2 emissions. The CO_2 emissions can be reduced by 38% compared to the initial process, but it increases the system cost. Bi et al.[176] developed a liquefaction H_2 process with 5 tonnes capacity using the SMR unit, LNG, and LN_2 cold energy. Helium gas is a generally safe refrigerant in the precooling and refrigeration industry, and it operates well in small- and medium-scale H_2 liquefaction cycles. The data shows that the hybrid system SEC declines from 10.78 to 7.948 kWh/kgLH_2, the efficiency increased from 0.1205 to 0.1634, and the exergy efficiency increased from 42.16% to 57.17%. Table 5 lists the technical characteristics of some H_2 liquefaction systems using LNG cold recovery. The results indicate that the SEC, capital, and operational costs are reduced by employing the LNG regasification instead of the precooling refrigerants in the H_2 liquefaction cycle.

4.3. Absorption and Ejector Refrigeration Units in Hydrogen Liquefaction Process. Absorption cooling systems are used as an alternative to compression cooling systems in H_2 liquefaction processes to reduce the needed energy. The high SEC in these units is reduced as a result of deleting part of the condensation cooling systems in H_2 liquefaction cycles employing this construction alteration. It is also feasible to use the unit's squandered energy by utilizing ACCs.[232−234] The most famous working fluids for single-stage ACCs are water/

lithium bromide ($LiBr/H_2O$) and ammonia/water (NH_3/H_2O).[235] In addition, much research has been conducted on the performance of ACCs using other working fluids such as ammonia/lithium nitrate ($LiNO_3/NH_3$), lithium bromide + zinc bromide/methoxide ($LiBr + ZnBr_2/CH_3O$), and calcium chloride/water ($H_2O/CaCl_2$).[235,236] There are studies on the use of this technology, especially in power plants,[237] food industries,[238,239] and oil and gas industries.[240,241] In particular, some studies have been conducted for the indirect use of ACCs to improve cooling performance in the LNG industry.[242−245] Also, diffusion−absorption[246−249] and absorption−compression[250−253] refrigeration process cycles are used to provide refrigeration in integrated structures. Figure 13 illustrates a schematic of multieffect ACCs used in integrated systems. The COP of multistage systems does not increase directly with increasing the number of stages; instead, a large number of stages in the system makes it more complicated. Therefore, the two-stage ACC is the most widely used type of multistage system in the absorption cooling industry, and the three- and four-stage cooling units are more studied and investigated in the laboratory.[254]

NH_3/H_2O absorption units are widely used in industrial and commercial structures in which the evaporating temperature is near the freezing temperature of water or below 0 °C. The system can also be used for low-temperature applications, and the possibility of cooling to temperatures close to −60 °C has been reported.[255,256] For cooling at temperatures below −33 °C, the ACC pressure after the relief valves must be less than 100

Table 6. Technical Characteristics of Some H$_2$ Liquefaction Systems According to Absorption and Ejector Refrigeration Units

author	year	SEC (kWh/kgLH$_2$)	exergy efficiency (%)	relative energy saving (%)	process details
Kanoglu et al.[70]	2016	15.08	67.9	25.4	SEC of base case: 20.22 kWh/kgLH$_2$
					in base case: LN$_2$ and Claude liquefaction cycle
					in modified case: ACC, LN$_2$ and Claude liquefaction cycle
					feed: MF, 25.53 kg/s; T, 25 °C; P, 1 bar
					evaporator temperature: −26.9 °C
Yilmaz et al.[73]	2018	11.52	69.44	43.02	SEC of base case: 20.22 kWh/kgLH$_2$
					in base case: LN$_2$ and Claude liquefaction cycle
					liquefaction cost: 1.349 $/kgLH$_2$
					relative cost saving (RCS): 11.4%
					in modified case: ACC, LN$_2$, and Claude liquefaction cycle
					feed: MF, 6.028 kg/s; T, 25 °C; P, 1 bar
					evaporator temperature: −26.9 °C
Yilmaz et al.[72]	2018	10.06	78.3	49.95	SEC of base case: 20.1 kWh/kgLH$_2$
					in base case: LN$_2$ and Claude liquefaction cycle
					liquefaction cost: 1.114 $/kgLH$_2$
					RCS: 32.4%
					in modified case: ACC, LN$_2$, and Claude liquefaction cycle
					feed: MF, 5.878 kg/s; T, 25 °C; P, 1 bar
					evaporator temperature: −26.9 °C
Mehrpooya et al.[71]	2018	6.47	45.5	15.86	SEC of base case: 7.69 kWh/kgLH$_2$
					exergy efficiency of base case: 39.5%
					in base case: two-stage MRC and cryogenic J−B cycle
					in modified case: two-stage MRC and combined cascade cryogenic J−B cycle with an ACC
					NCR: 5
					feed: MF, 90 TPD; T, 25 °C; P, 21 bar
					MITA: 1−2 °C
Aasadnia et al.[75]	2019	12.7	31.6		COP of developed case: 9.56
					in developed case: Claude liquefaction cycle combined with two ACCs
					feed: MF, 261 TPD; T, 25 °C; P, 1 bar
					MITA: 1−2 °C
Ghorbani et al.[74]	2019	4.016	73.75	8.934	SEC of base case: 4.410 kWh/kgLH$_2$
					exergy efficiency of base case: 55.47%
					in base case: two-stage MRC and cryogenic J−B cycle
					in modified case: two-stage MRC and combined cascade cryogenic J−B cycle with an ACC
					NCR, 2; O-H$_2$ to P-H$_2$ (%): 100/50/5
					feed: MF, 290 TPD; T, 25 °C; P, 21 bar
					MITA: 1−3 °C
Azizabadi et al.[265]	2021	4.5		40.96[92]	in base case: two-stage MRC and cryogenic J−B cycle
					in modified case: two-stage MRC and combined cascade cryogenic J−B cycle with an ACC
				38.23[170]	
				15.14[89]	NCR: 3
				15.14[71]	
					feed: MF, 4 kg/s; T, 25 °C; P, 21 bar
					MITA: 1−2 °C
Jouybari et al.[177]	2022	7.405	23.56	3.706	EC of base case: 7.690 kWh/kgLH$_2$
					exergy efficiency of base case: 39.5%
					in base case: two-stage MRC and cryogenic J−B cycle
					in modified case: combined cascade cryogenic J−B cycle with ejector-compression refrigeration unit
					NCR: 2
					feed: MF, 22.34 kg/s; T, 25 °C; P, 21 bar
					evaporator temperature: −125 °C
Zhang et al.[266]	2022	5.413	88.99		in developed case: Claude precooling refrigeration system (two-stage MRC) and combined cascade cryogenic J−B cycle with a two-stage ACC
					NCR: 3
					feed: MF, 3.344 kg/s; T, 25 °C; P, 21 bar
Noh et al.[223]	2022	6.110	69.95	5.14 and 8.13	SEC of the modified case I: 5.798 kWh/kgLH$_2$
					SEC of modified case II: 5.613 kWh/kgLH$_2$
					exergy efficiency of the modified case I: 68.63%

Table 6. continued

author	year	SEC (kWh/kgLH$_2$)	exergy efficiency (%)	relative energy saving (%)	process details
					exergy efficiency of modified case II: 67.24%
					RCC in case I: 12.66%
					RCC in case II: 31.76%
					ROC in case I: 5.76%
					ROC in case II: 11.55%
					in base case: two-stage MRC and cryogenic J−B cycle
					in modified case I: LNG cold energy, two-stage MRC, and cryogenic J−B cycle
					in modified case II: LNG cold energy and cryogenic J−B cycle
					precooling cycle: MRC (C$_1$, C$_2$, C$_3$, C$_4$, C$_5$, R14, C$_2$H$_4$, H$_2$ and N$_2$) (25 to −193 °C)
					cooling and liquefaction cycles: MRC (He, H$_2$, and Ne), (−193 to −252.5 °C)
					feed: MF, 31.71 TPD; T, 25 °C; P, 21 bar
Faramarzi et al.[230]	2022	6.59	46		RCC in optimized case: 3.225%
					ROC in optimized case: 3.973%
					in developed case: LNG cold energy, MRC, and cryogenic J−B cycle
					precooling cycle: MRC (C$_1$, C$_3$, C$_5$, C$_2$H$_4$, and N$_2$) (27 to −195 °C)
					cooling and liquefaction cycles: MRC (He, H$_2$, and Ne) (−193 to −253 °C)
					feed: MF, 4.38 kg/s; T, 27 °C; P, 20 bar
Yang et al.[231]	2023	6.59		47.0	in developed case: LNG cold energy and dual-pressure J−B cycle
					NCR: 3
					precooling cycle: LNG cold energy (27 to −154.9 °C)
					cooling and liquefaction cycles: dual-pressure J−B cycle (He) (−154.9 to −252.5 °C)
					feed: MF, 12 TPD LH$_2$; T, 25 °C; P, 21 bar

kPa (Figure 14a). Therefore, parts of the NH$_3$/H$_2$O process containing the absorber, evaporator, and pump must work in a relative vacuum state. Working in a vacuum state necessitates extra precautions, such as utilizing a vacuum pump and N$_2$ purging to keep air from entering the system, designing a device with vacuum-resistant materials, and increasing the cost of equipment and pipes.[256] In the research conducted, working in pressures less than 100 kPa has been avoided, and the ammonia flow pressure after the valves has been taken as 1.2 bar, including the margin of 0.2 bar from the minimum level.[75,257−259] The temperature of the saturated mixture of ammonia at a pressure of 1.2 bar is equal to −29.4 °C, and considering the minimum temperature of 3 °C in the evaporator, this flow can cool down to a temperature of −26.4 °C (as shown in Figure 14b).[256]

Table 6 reports the technical characteristics of some H$_2$ liquefaction systems based on absorption and ejector refrigeration units. Figure 15 displays the block flow diagram of two hybrid concepts of MRC/ACC/Claude and MRC/ACC/J−B refrigeration processes for H$_2$ liquefaction. Ghorbani et al.[74] developed a novel configuration for H$_2$ liquefaction and investigated it thermodynamically. The modified configuration, which generates about 290 TPD, includes a primary H$_2$ liquefaction plant, an ORC unit, an ACC, and solar trough collectors. The ACC was used to decrease the refrigerants' temperature entering the compressors in the cooling supply unit of the H$_2$ liquefaction process. The H$_2$ liquefaction system consists of an MRC and a combined J−B unit to supply precooling and cooling duty. The SEC and exergy efficiency of the natural gas liquefaction cycle of 4.022 kWh/kgLH$_2$ and 73.75%, respectively. The results showed that the developed process' SEC decreased from 4.410 to 4.022 kWh/kgLH$_2$ compared to the basic plant,[170] and its exergy efficiency increased from 55.47% to 73.75%. Asadnia et al.[92] used the ACC to decrease the temperature of the refrigerants entering the compressors in the precooling and cooling supply cycle of the H$_2$

liquefaction process with 90 TPD capacity. To supply precooling and cooling of the H$_2$ liquefaction cycle, they used an MRC and combined J−B unit. The SEC, COP, and exergy yield of the H$_2$ liquefaction system were 6.47 kWh/kgLH$_2$, 0.2034, and 45.5%, respectively. The SEC, COP, and exergy yield in the basic H$_2$ liquefaction process[71] were 7.69 kWh/kgLH$_2$, 0.1710, and 39.5%, respectively. An ACC cycle and LAC recovery cycle were used to provide precooling for the liquid H$_2$ production system.[26] Then, the partial refrigerant cycle is used to cool and liquefy the precooled H$_2$ to −180 °C. The SEC, COP, and exergy yield of the H$_2$ liquefaction system are 6.71 kWh/kgLH$_2$, 0.18 and 35.7%, respectively.

Using geothermal energy in combination with ACCs for H$_2$ liquefaction has been examined in three different cases: (1) applying a geothermal power plant in the liquefaction process, (2) utilizing geothermal in the ACC to precooling, and (3) employing part of the geothermal for the precooling system with other parts to produce work in the liquefaction process. It was found that employing geothermal power in the ACC reduces the power required for H$_2$ liquefaction and is more advantageous than using geothermal power output in a liquefaction process.[260] Cao et al.[261] designed a system to produce power and liquid H$_2$ from geothermal sources. The generated energy is compared using an ORC or an ACC to find the best cycle performance. The system showed better performance when the ACC was used to produce refrigeration. The cost of liquid H$_2$ produced by the ORC and ACC was 3.8 and 3.6 $/kgLH$_2$, respectively. Yilmaz[72] investigated a H$_2$ liquefaction process with an ACC and geothermal energy. The geothermal power was used for the ACC in the precooling and to produce work in the liquefaction system. The SEC in the H$_2$ liquefaction unit was calculated to be 10.06 kWh/kgLH$_2$. The unit exergetic liquefaction price of H$_2$ in the optimal state was 1.114 $/kgLH$_2$. A triple-effect ACC combined with solar thermal/photovoltaic, geothermal energy, and L−H cycles was considered for H$_2$ liquefaction. With the
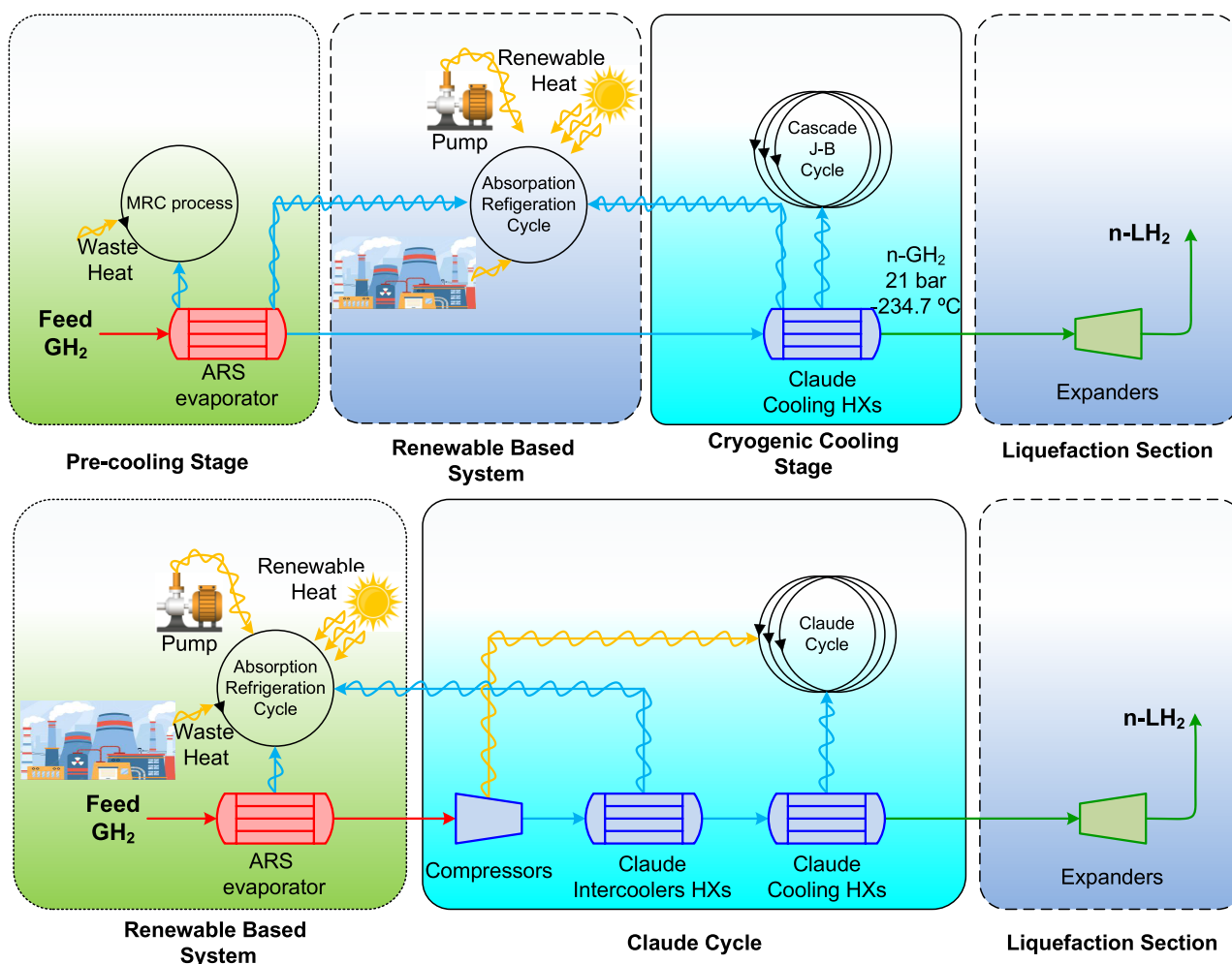
Figure 15. Block flow diagram of two hybrid concepts of MRC/ACC/Claude and MRC/ACC/J−B refrigeration processes for H_2 liquefaction. Modified from refs 71 and 75.

increment in geothermal rate, the exergy and energy utilization factors of the hybrid structure decline from 0.21 to 0.13 and from 0.059 to 0.037, respectively.[262]

An H_2 liquefaction cycle with a geothermal-assisted ACC and a Claude liquefaction system was modeled. A high-temperature geothermal resource and an ACC were used to reduce the SEC in the H_2 liquefaction process. The SEC, COP, and exergy yield in the optimized H_2 liquefaction system were calculated to be 11.52 kWh/kgLH$_2$, 0.346, and 69.44%, respectively. Also, the optimal exergetic cost of liquid H_2 was calculated to be 1.349 $/kgLH$_2$.[73] Asadnia et al.[75] modeled a H_2 liquefaction process with 260 TPD capacity, including a simple Claude cycle with two ACCs. The exergy yield and SEC of the system were calculated to be 31.6% and 12.7 kWh/kgLH$_2$, respectively. A geothermal energy-based water−ammonia ACC for H_2 precooling and a Claude method for H_2 liquefaction were combined to create an integrated H_2 liquefaction system. The ACC's reboiler receives heat from a geothermal source. The ACC could cool H_2 gas to −26.9 °C; the COP of the ACC was 0.556 with an exergy yield of 67.0%. The COP of the Claude liquefaction process was 0.0120, and its exergy yield was 67.3%. Also, the COP and exergy yield of the developed liquefaction process were 0.162 and 67.9%, respectively. Besides, precooling H_2 gas in an ACC with geothermal energy reduced the SEC in the liquefaction cycle by 25.4%.[70] Ratlamwala et al.[263] designed

an innovative configuration for triple production of cooling, power, and liquid H_2 operating an ACC, L−H process, binary power unit, and geothermal energy. They applied energetic and exergetic evaluation to investigate the effect of geothermal power, ambient temperature, and H_2O/NH_3 concentration on the principal factors and efficiency.

Despite the fact that the waste heat from the systems in the ACC is used for precooling in the liquefaction process, the potential of the ejector−compression cooling cycle in H_2 liquefaction has yet to be explored. In this regard, only one simulation study has been reported: the propane−ethylene cooling cycle for H_2 precooling. A hybrid system for H_2 production was developed using a two-stage ejector−compression cooling process for H_2 precooling and six L−H liquefaction units for cooling and liquefaction.[264] The SEC, COP, and exergy yield of the developed structure were calculated to be 7.405 kWh/kgLH$_2$, 0.103, and 0.2359, respectively. The exergy yield, SEC, and COP in the basic H_2 liquefaction process[92] were 39.5%, 7.69 kWh/kgLH$_2$, and 0.1710, respectively.

4.4. Liquid−Air Cold Recovery in Hydrogen Liquefaction Process. Liquid−air is produced utilizing LH$_2$ cold energy in the LH$_2$ regasification step and can be returned to the H_2 gas liquefaction process using the LH$_2$ empty vessel in the LH$_2$ supply chain. Therefore, the LH$_2$ cold energy can be recycled in the LH$_2$ supply chain, even if the H_2 liquefaction and LH$_2$
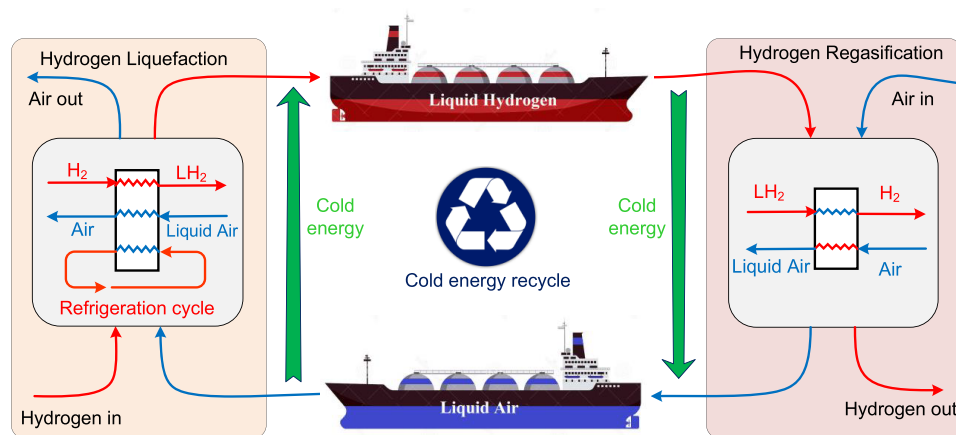
Figure 16. Concept of using liquid−air in the LH$_2$ supply chain for cold energy recovery. Modified from ref 40.

Table 7. Different Optimization Techniques Applied in H$_2$ Liquefaction Systems[a]

author	year	SEC (kWh/kgLH$_2$)	exergy efficiency (%)	optimization techniques
Krasae-In et al.[89]	2010	5.350	54.0	TE
Krasae-In et al.[203]	2010			TE
Krasae-In et al.[204]	2011			TE
Krasae-In et al.[91]	2014	5.910		TE
Cardella et al.[93]	2017	5.930	43.0	SQP
Cardella et al.[289]	2017	5.91		SQP
Yilmaz[72]	2018	10.06	78.3	GA
Seyam et al.[290]	2019	4.74	85.71	TE
Yin et al.[95]	2019	7.133		GA
Qyyum et al.[147]	2021	6.450	47.2	MCD
Zhu et al.[287]	2022	9.810		GA
Son et al.[291]	2022	12.21		GA
Park et al.[292]	2022	5.690		GA
Sun et al.[164]	2022	6.430		PSO
Bi et al.[293]	2022	9.703	39.10	GA
Naquash et al.[294]	2022	5.900	51.37	SQP and BOX
Bi et al.[176]	2022	7.041	54.13	GA
Faramarzi et al.[230]	2022	6.59		GA
Naquash et al.[288]	2022			KBO
Lin et al.[295]	2022		10.52	GA
Li et al.[296]	2022	3.619	82.58	
Ghorbani et al.[297]	2022	6.642	39.40	GA
Mehrenjani et al.[298]	2022		23.34	ANN and GA
Min et al.[299]	2022			ANN and PSO
Meng et al.[300]	2022		9.87−10.95	GW
Geng et al.[215]	2023	5.963	52.61	PSO
Liu et al.[301]	2023		33.34−34.04	GW

[a]Modified from ref 288.

regasification steps occur in remote areas.[40] Figure 16 depicts the use of liquid−air in the LH$_2$ supply chain, specifically for cold energy recovery. Cold liquid−air energy recovery was investigated to provide part of the refrigeration used in LNG[221] and liquid biomethane production systems.[267,268] A limited number of studies have been conducted on applying LAC recovery in the H$_2$ liquefaction cycle.

Taghavi et al.[85] used LAC recovery to precool the H$_2$ liquefaction process. They used the six J−B cascade cycles to cool and liquefy H$_2$. The results revealed that using LAC recovery instead of the two-stage MRC in the H$_2$ liquefaction system reduced the SEC, COP, and exergy yield from 6.42 to 5.955 kWh/kgLH$_2$, 0.1642 to 0.1280, and 39.41% to 29.3%, respectively. Naquash et al.[26] employed the ACC and LAC

recovery to provide precooling for the liquid H$_2$ liquefaction system. An ORC is used to recover the heat loss after the combustion chamber. The SEC, specific CO$_2$ emissions, and exergy yield were calculated to be 6.71 kWh/kgLH$_2$, 2.641 kgCO$_2$/kgLH$_2$, and 35.7%, respectively. The results indicated that the application of the LAC recovery process in H$_2$ liquefaction systems due to the simplicity of the structure has the potential of commercialization in the near future.[269]

4.5. Operational Optimization with Different Algorithms. Refrigerants used in refrigeration cycles are divided into two main categories: pure and mixed refrigerants. Mixed refrigerants can be used in all refrigeration systems, including single-compression refrigeration cycles, CRCs, and multistage refrigeration units.[197] The main advantages of a mixed
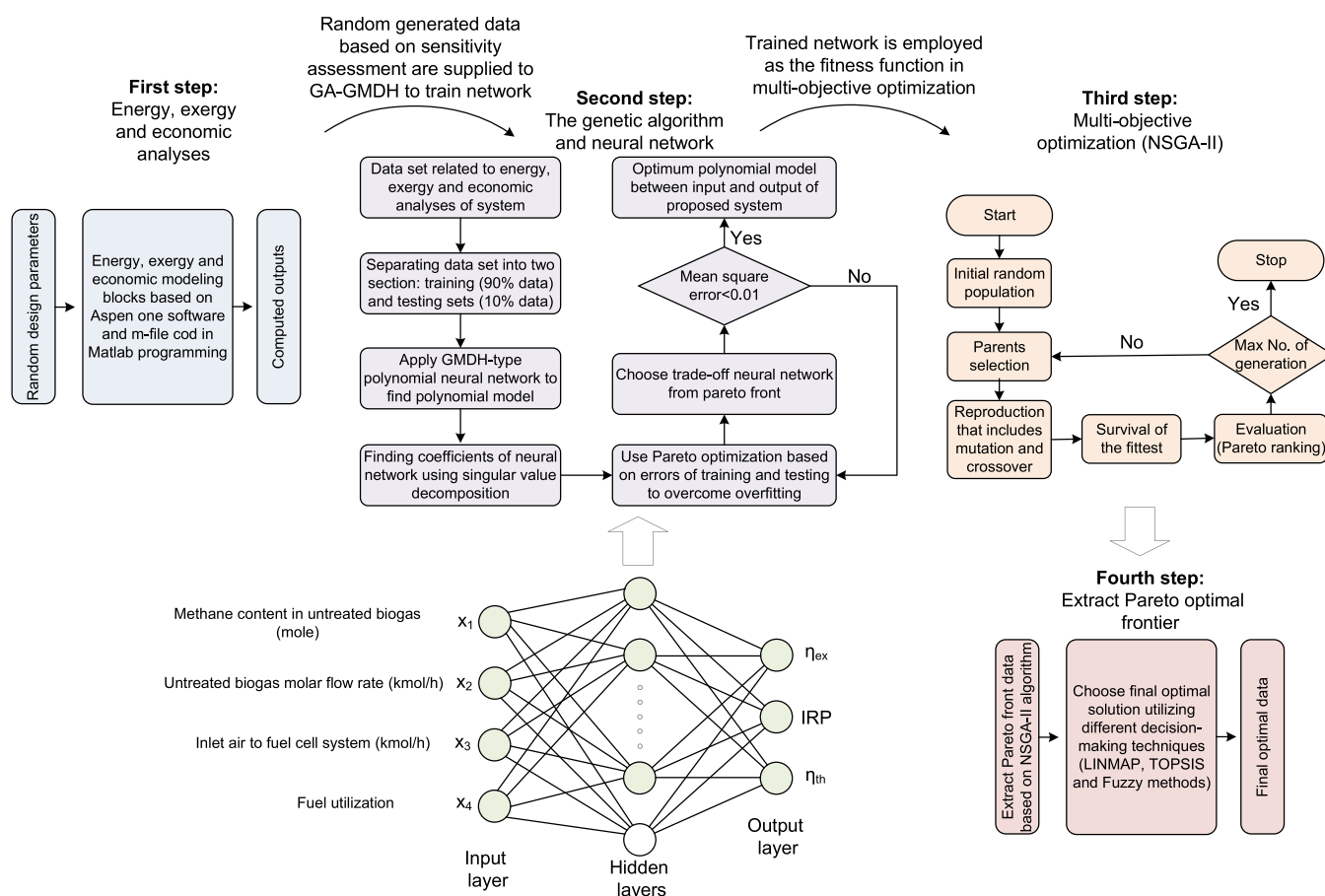
Figure 17. Schematic of the combination of meta-heuristic/ANN algorithms to optimize the H_2 liquefaction cycle. Modified from ref 179.

refrigerant system over pure refrigerant cycles are the simpler arrangement of its cycle equipment, its greater flexibility to provide cooling at different temperature levels by changing the percentage of refrigerant composition, and the system's greater reversibility in a temperature range due to refrigerant evaporation.[181,270,271] The idea of using multicomponent refrigerants goes back many years. In 1936, Podbielniam[272] presented the first mixed refrigerant cryogenic cycle. Later, Haselden et al.,[273,274] Perrett,[275] and Gaumer et al.[276] expanded and developed the idea of utilizing mixed refrigerants for various applications. The ozone layer destruction phenomenon provoked the discussion on replacing CFC-based refrigerants, and many studies have been conducted to use multicomponent refrigerants in domestic and industrial systems. Relevant studies include those by Steed,[277] Lamb et al.,[278] and Duvedi et al.[279] Besides, many studies have focused on using mixed refrigerants to reach low temperatures.[280,281] In all of the mentioned studies, the mathematical programming approach has been used to determine the percentage of the optimal refrigerant composition. Furthermore, in a refrigerant process with a preset layout, these studies focused on maximizing the refrigerant composition percent and the system's operating pressures. Mafi et al.[199,282−284] conducted a comprehensive study on recognizing the behavior of mixed refrigerant refrigerating systems, identifying and investigating their important and key parameters, and optimizing their arrangement using nonlinear mathematical methods. Next, meta-heuristic algorithms were used to reduce the SEC in low-temperature natural gas[285,286] and H_2 liquefaction systems.[82,287] Table 7 lists the character-

istics of the hybrid H_2 liquefaction system that have been optimized using trial and error (TE) methods, sequential quadratic programming (SQP), knowledge-based optimization (KBO), particle swarm optimization (PSO), GA, and modified coordinate descent (MCD) combined with artificial neural networks (ANN).

Recently, a powerful combination of meta-heuristic and artificial intelligence algorithms was developed for multi-objective optimization of H_2 liquefaction cycle parameters. Then, fuzzy Bellman−Zadeh, LINMAP, and TOPSIS methods were employed to make decisions in multiobjective optimization.[179] Figure 17 depicts a schematic of combining a meta-heuristic algorithm and artificial intelligence to optimize the H_2 liquefaction cycle.

4.6. Optimization Based on Pinch Analysis. Pinch technology is introduced as a powerful and effective tool for thermodynamic analysis of process industries and optimization of heat exchanger networks.[302] Thermal systems may be built and optimized in both grassroots and retrofit designs using pinch technology. Thermal systems in operating conditions are being updated in order to conserve the SEC, decrease total expenses, and boost up structural capacity.[303] Linnhoff and Tjoe[304] introduced the first systematic method for modifying and optimizing the thermal systems. In general, modifying the heat exchanger network with the help of pinch analysis includes two stages: targeting and design. Targeting means the prediction before design in such a way that the designer determines the lowest amount of SEC and the lowest required level of the network before any detailed design. Composite curves (CC) and

Table 8. Technical Specifications of Some H_2 Liquefaction Systems with Different Renewable Energy Sources

author	year	hydrogen capacity (kg/h)	exergy efficiency (%)	renewable energy	liquefaction system
Yilmaz et al.[70]	2016	21 700	67.9	geothermal	ACC and Claude liquefaction process
Yuksel et al.[98]	2018	22.3–200.1	38–64	geothermal	LN$_2$ and Linde–Hampson cycle
Corumlu et al.[324]	2018	3.6	0.1955	solar	LN$_2$ and Linde–Hampson cycle
Yilmaz et al.[72]	2018	21 160	27.36	geothermal	LN$_2$ and Linde–Hampson cycle
Yilmaz et al.[325]	2018	95.3	36.5	solar and ocean	LN$_2$ and Linde–Hampson cycle
Yilmaz et al.[73]	2018	31 359	69.44	geothermal	ACC and Claude liquefaction process
Yuksel et al.[326]	2019	216	56.24	solar	Claude liquefaction process
Ghorbani et al.[74]	2019	12 080	73.5	solar	two-stage MRC and combined cascade cryogenic J–B cycle with an ACC
Seyam et al.[327]	2020	1479	23.05	solar	LN$_2$ and Claude liquefaction process
Seyam et al.[290]	2020	12 656	63.7	geothermal	LN$_2$ and Claude liquefaction process
Yilmaz[99]	2020	840.2	38.75	geothermal	LN$_2$ and Claude liquefaction process
Boyaghchi et al.[328]	2021	1770		solar	cascade ORC/ejector refrigeration and cascade cryogenic J–B cycle
Tukenmez et al.[329]	2021	3.992	52.69	geothermal	LN$_2$ and Linde–Hampson cycle
Ghorbani et al.[175]	2021	4234	58.73	wind	two-stage MRC compression and four H$_2$ J–B cycles
Ghorbani et al.[322]	2021	2057	72.41	solar	two-stage MRC and combined cascade cryogenic J–B cycle
Mehrenjani et al.[298]	2022	154.9	23.34	geothermal	Claude liquefaction process
Taghavi et al.[85]	2022	1028	53.22	solar	LAC recovery and six H$_2$ J–B cycles
Meng et al.[300]	2022	532.8–594	9.87–10.95	biomass and geothermal	Claude liquefaction process
Liu et al.[301]	2023	138.2	33.57	biomass	Claude liquefaction process
Khodaparast et al.[323]	2023	3.58	70.52	geothermal	LN$_2$, ACC, and Claude liquefaction processes
		3.93	61.73		LN$_2$, ACC, and reverse Brayton cycles

grand composite curves (GCC) are the essential tools of pinch technology to achieve the desired goals in the goal-setting stage.[305,306] The CCs are used to set goals for correcting the SEC costs and process investment. The GCCs can set goals to determine the appropriate ancillary service levels and the heat load required for each level. The design stage is reviewed after reaching the targeting results. In this stage, the heat exchanger network design is presented.[181] The combined pinch and exergy assessment (CPEA) can be a valuable and practical approach for coinvestigating thermal and power loads. The essential instruments in the targeting phase of CPEA are exergy composite diagrams (ECCs) and exergy grand composite diagrams (EGCCs), which are obtained by replacing the temperature axis in the CCs and GCCs with the Carnot factor $(\eta_C = 1 - \frac{T_o}{T})$.[283,307–310] By integrating mathematical programming approaches and pinch technology, Lee et al.[311] proposed an efficient way for optimizing cryogenic systems. The mechanism for low temperatures was created in two stages. The GCCs were used in the first stage to calculate power consumption, the number of temperature levels, and the suitable ranges. The CPEA was used to identify proper ways to reduce the design's capital and operational expenses. In the second stage, other parameters of the cryogenic system were obtained using the mixed integer nonlinear programming (MINLP) model and disjunctive programming. So, the optimal arrangement of the design was developed using the mathematical method. Introducing a suitable initial guess in the first stage and reducing the examination of all possible modes in optimizing the developed system were the main advantages of the developed method. Mafi et al.[282,284] studied mixed refrigerant refrigeration systems in low-temperature process industries based on mathematical techniques and thermodynamic viewpoints. By combining the NLP/PSO method and the CPEA perspectives, they introduced the optimal arrangement of the refrigeration cycle. A complete knowledge of the cryogenic cycle arrangement

and its distance from the optimal arrangement is gained using the CCs, GCCs, and heat exchanger networks as the qualitative indexes obtained from pinch analysis in H$_2$ liquefaction systems. Next, by altering the design and arrangement of the equipment in the refrigeration process, the optimal arrangement is selected.[101,146,175,179,224,312] It is possible to target the overall costs of the system, including the operational costs of energy supply and the initial costs of providing network equipment using CC and GCC diagrams. Thus, by changing ΔT_{min} and calculating the cost of the required level for the network and the cost of providing utility services, the system total cost is calculated for each ΔT_{min}, and then, the lowest total cost required for the system as the target point is determined. Mehrpooya et al. used the CCs in multistream heat exchangers to reduce the SEC in H$_2$ liquefaction systems.[71,92,170,313–315] The minimum temperature method is essential for choosing the efficient activity of exchangers involved in liquid H$_2$ systems. The ΔT_{min} can be modified by altering the values of the configuration variables. Generally, in H$_2$ liquefaction cycles, ΔT_{min} values are specified to be about 1–2 °C.[26,71,92,212,214] Some researchers reported this value to be between 1 and 3 °C, which is presented in Table 4.

4.7. Combined Hydrogen Liquefaction with Renewable Energy Sources. The dwindling subsurface resources and ramping up pollution are the two main concerns of governments for future generations.[316] Renewable energy sources, such as geothermal, solar, wind, biomass, and tidal, can reduce energy and environmental concerns because they are compatible with the environment and available.[317] The availability and intermittent nature of renewable resources prevent them from immediately meeting the energy demand. Energy storage is the most effective way to solve this issue. Mechanical, electrical, thermal, and chemical energy storage techniques are often used.[318,319] Among these methods, chemical energy storage with carbon-free and low-carbon energy carriers such as H$_2$ has
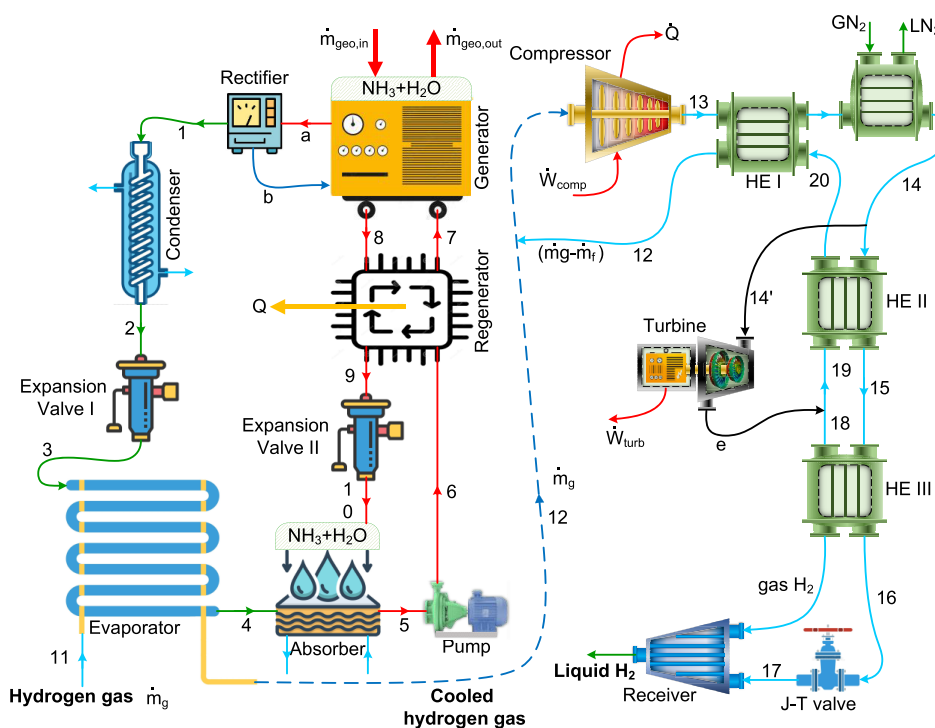
Figure 18. Using the ACC for precooling in the H_2 liquefaction process. Modified from refs 70, 72, and 73.

Table 9. Technical Specifications of Liquid H_2 Production Systems along with Other Side Products

author	year	energy efficiency (%)	exergy efficiency (%)	process details
Mehrpooya et al.[360]	2019		62.54	products: 290 tons of LH_2 and 296 tons of LNG
				COP of the developed system 0.2442
				SEC of the developed system 4.165 kWh/kgLH_2, kg$_{LNG}$
				subsystems: ACC, two-stage MRC, and cascade cryogenic J−B cycle
Yuksel et al.[361]	2019	61.57	58.15	products: H_2, heating, power, cooling, and hot H_2O
				subsystems: waste materials gasification, a single-effect ACC, a PEM electrolyzer, Brayton/Stirling units, and LN_2/L−H in a H_2 liquefaction cycle
Ebrahimi et al.[100]	2020	62.10		products: 0.1660 kg/sLH_2, 5.81 kg/s compressed CO_2 and 8.097 MW power
				subsystems: ASU process, acid gas removal unit, two-stage MRC and combined cascade cryogenic J−B cycle in H_2 liquefaction cycle, and power plant based on gasification
Incer-Valverde et al.[362]	2021		44.0	products: LH_2 and oxygen
				subsystems: PEM electrolyzer and helium refrigeration unit in H_2 liquefaction process
Ghorbani et al.[146]	2021	83.75	62.54	products: 3.756 kg/s liquid fuels, 1.157 kg/sLH_2 and 359.8 kg/s hot H_2O
				subsystems: alkaline electrolyzer, two-stage MRC and combined cascade cryogenic J−B cycle in H_2 liquefaction unit, CO_2 power system, and Fischer−Tropsch reactor
Koc et al.[363]	2022	60.14	58.37	products: LH_2, electrical energy, heating−cooling, and fresh water
				subsystems: Brayton/ORC units, distillation plant, ACC, PEM electrolyzer, and LN_2/L−H in a H_2 liquefaction cycle
Ebrahimi et al.[101]	2022	71.4		products: 7116 kg/h LH_2 and 57 597 kg/h oxygen
				subsystems: magnesium−chlorine thermoelectrochemical cycle, single MR cycle in H_2 liquefaction unit, and solar dish collectors
Mehrpooya et al.[313]	2022		70.62	products: 111.3 kg/s N_2, 42 kg/s argon and oxygen, $\geq 132 \times 10^3$ TPD LH_2, and 751 TPD Ne
				subsystems: solar/geothermal ACC, H_2 liquefaction cycle, and ASU process
Lin et al.[295]	2022		10.52	products: 14.80 kg/h LH_2 and 3377 net power output
				subsystems: biomass gasification unit, Rankine system, PEM electrolyzer and LN_2/L−H in H_2 liquefaction cycle

significant potential to substitute fossil fuels and reduce CO_2 emissions. H_2 is a clean fuel that can support stationary and mobile applications.[320,321] Renewable energies can be used to provide power directly and indirectly in H_2 liquefaction cycles. Thermal energy can be directly used in power generation cycles and ACCs to achieve refrigeration.[261,315] Table 8 lists the

technical specifications of some H_2 liquefaction systems with different renewable energy sources. Wind turbines[175] and photovoltaic panels[322] can be used directly to power compressors of H_2 liquefaction cycles. The analysis of H_2 liquefaction processes integrated with geothermal energy revealed that using heat duty in ACCs for precooling H_2 is

more beneficial than using geothermal power and was associated with a reduction in power consumption.[97] Figure 18 depicts using the ACC for precooling in the H_2 liquefaction process. Mehrenjani et al.[298] designed a novel integrated system of liquid H_2 production using a PEM electrolyzer, an ORC unit based on geothermal energy, LNG regasification, and the Claude process. The combined ANN and GA were used for thermoeconomic optimization. The exergy efficiency, liquid H_2 rate, and LCOH were calculated to be 23.34%, 154.95 kg/h, and 1.827 \$/kg, respectively. An integrated system of liquid H_2 production employing a Kalina power unit, wind turbines, an alkaline electrolyzer, and a H_2 liquefaction process was developed.[175] The SEC, COP, and total exergy yield were obtained to be 5.462 kWh/kgLH$_2$, 0.1384, and 58.73%. The results showed that thermal integration in the system reduced power consumption by 8.61%. Khodaparast et al.[323] investigated two H_2 liquefaction systems with inverse Brayton and Claude cycles. They used a combination of LN_2 and an ACC with a geothermal heat source for precooling. The results indicated that the Claude process is more suitable than the inverse Brayton cycle considering cost and exergy rates. The LH_2 cost rate and total exergy efficiency based on the inverse Brayton cycle were calculated to be 7.03 \$/kg and 61.73%, respectively. Also, the LH_2 cost rate and total exergy efficiency based on the Claude cycle were calculated to be 7.03 \$/kg and 70.52%, respectively.

4.8. Hybrid Process for Hydrogen Liquefaction.

Cogeneration systems provide a clear potential path for clean energy supply chains due to their high efficiency and low energy waste.[330] H_2 is the supply chain's most promising clean and green energy fuel. H_2 production, storage, and usage systems can be integrated with cogeneration plants.[331,332] This integration leads to higher efficiency, lower environmental influence, and lower expenses.[175,333] Also, some integrated structures were developed for H_2 purification, but no solutions were provided for its storage.[246,334] The H_2 production and storage processes can be integrated with nuclear power plants,[335–340] renewable heat sources,[341–348] and waste heat from industries (i.e., chemical plants, furnaces, and incinerators).[349–355] Besides, several combined structures were developed for H_2 purification and its liquefaction from coke oven gas (COG) and LNG production.[157,356–359] Xu et al.[157] developed four cycles for producing LNG and liquid H_2, containing closed-loop N_2, closed-loop H_2, open-loop N_2, and open-loop H_2. The outcomes demonstrated that the system purity and SEC were 99.99% and 18.01−41.2 kWh/kmol, respectively. Xu et al.[358] investigated three innovative systems for cogenerating liquid H_2 and LNG based on the COG. A two-step helium expansion process supplied the cooling needed to liquefy H_2. The exergy yield of the hybrid system was reported to be 13−66.5%. Table 9 presents the technical specifications of liquid H_2 production systems and other byproducts. Waste heat from fuel cells, Fischer−Tropsch reactors, and oxy−fuel power plants can be used to produce and liquefy H_2.[146,174,179,224] Besides, the precooling process can be substituted by using inexpensive LN_2 that comes directly from the air separation system to generate liquid oxygen.[102]

5. ECONOMIC, SAFETY, AND ENVIRONMENTAL ASPECTS OF LIQUID HYDROGEN

The costs of the H_2 liquefaction process can be separated into energy supply, capital, and maintenance costs. Investment costs for liquid H_2 production systems are relatively high. Although larger units are more efficient, the risk of investing in

constructing large (>100 TPD) industrial units is a challenge because of the lack of demand. Therefore, as long as there is no favorable demand for liquid H_2 in a region, it will be difficult to invest in this sector.[159,364] The amount of H_2 demanded to meet existing climate commitments by governments and to reach net-zero carbon emission goals is predicted to be 200 and 621 million tonnes in 2030 and 2060, respectively.[25] The costs of H_2 liquefaction for various systems depend on the price of energy (electricity) and the scale of the developed system. The LCOH in the production, storage, and transmission systems associated with the whole chain must be reduced in the coming years with the growth of hydrogen demand compared to the current conditions.[59] Figure 19 illustrates the investment cost of the H_2
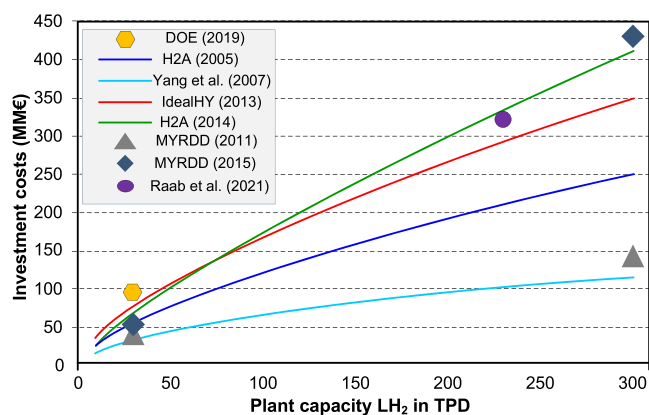

Figure 19. Investment required for the H_2 liquefaction process reported in the literature.[144,365,367−371]

liquefaction system reported in the literature. When the capacity of liquid H_2 manufacturing facilities increases, the rate of investment expenses experience a gradual increase. At capacities larger than 100 TPD, this growth is followed by a gentler slope. When compared to lower scales, large-scale manufacturers are more cost effective and efficient at capacities higher than 100 TPD.[365,366] Table 10 lists the supply chain costs of liquid H_2 at different capacities and conditions. Facility costs for H_2 liquefaction systems for capacities 6−200 TPD were estimated to be \$50−800 million. The capital investment includes land and equipment, H_2 production based on the SMR process, the liquefaction system, and the distribution terminal. According to the DOE,[366] the reported cost of electricity is 42.68 \$/MWh, and the costs of production, terminal, trucking, liquefaction, station, and levelized cost for liquid H_2 supply chain (27 TPD) are 2.24, 0.39, 0.68, 2.75, 8.18, and 14.24 \$/kgH$_2$, respectively. Figure 20 depicts the effect of increasing H_2 liquefaction cycle capacity on the supply chain investment cost and SEC. The results demonstrate that the investment cost of the supply chain increases slowly with the increase of H_2 liquefaction cycle capacity. Also, when the liquefaction cycle capacity increases, the investment cost per capacity and SEC go down. Figure 21 depicts the price share of equipment utilized in a 1 TPD H_2 liquefaction system based on three multicomponent refrigerant refrigeration cycles. The cost (\$/kgH$_2$) of heat exchangers (3.40), supplements (0.7), and electricity (0.57) accounted for most of the costs. The cost of H_2 liquefaction for the capacities of 1, 5, 10, and 50 TPD were reported to be 5.54, 4.75, 4.20, and 3.20 \$/kgH$_2$, respectively.[214]

From well to wheel, the H_2 prices at the filling station can be reduced to 5−7 €/kgH$_2$ with a supply chain of liquid H_2

**Table 10. Supply Chain Costs of Liquid H$_2$ at Different Capacities and Conditions**

author	year	SEC (kWh/kgLH$_2$)	capacity (TPD)	process details
Reuß et al.[371]	2017	6.78	50	electricity cost: 60 $/MWh
				cost (€/kgH$_2$): electrolysis 3.69, liquefaction 1.89−1.98
				MRC precooled Brayton for liquefaction
Heuser et al.[372]	2019	6.78	50	electricity cost: 1.122 €/kgH$_2$
				cost (€/kgH$_2$): electrolysis 0.94, compression 0.03, pipeline transport 0.54, liquefaction 0.4, liquid H$_2$ storage 0.18, ship transport 1.13, LCOH 4.44.
				MRC precooled Brayton for liquefaction
DOE H$_2$ and Fuel Cells Program Record[366]	2019	11.5	27	electricity cost: 42.68 $/MWh
				cost ($/kgH$_2$): production 2.24, terminal 0.39, trucking 0.68, liquefaction 2.75, station 8.18, LCOH 14.24
				SMR in the United States
				LN$_2$ precooled Claude
Li et al.[373]	2020	12	27−30	electricity cost: 50 $/MWh
				cost ($/kgH$_2$): production cost 2.2−4.2 + 1.0, transport 0.2−0.5, liquefaction 0.7−2, station 0.9−2.3, LCOH 4.3−8
				SMR with CCS in the United States and liquid truck transport
European Commission[59,374]	2020	11.5	27	electricity cost: 30−50 $/MWh
				cost ($/kgH$_2$): production 1.61−4.07, transport 1.64−2.43, liquefaction 2.76, distribution 1.19−2.35, LCOH 7.2−8.85
				LH$_2$ imported into Europe
Raab et al.[375]	2021	7	676.5	electricity cost: 78.69 €/kgH$_2$
				cost (€/kgH$_2$): production 5, liquefaction 1.76, regasification 0.3, transport 0.41, LCOH 7.47
				LH$_2$ imported from Australia to Japan
Kim et al.[214]	2022	5.54	1	liquefaction cost: 5.54 $/kgH$_2$
				cost ($/kgH$_2$): compressor 3.40, expander 0.006, heat exchanger 0.045, supplement 0.7, electricity 0.57, labor 0.0105, maintenance 0.55, other 0.28
				MRC for liquefaction

compared to 8−10 €/kgH$_2$ with compressed H$_2$.[376] H$_2$ liquefaction systems with a capacity of 20−50 TPD are economically feasible according to the present technologies to achieve this price. Minor changes in equipment can be used based on optimization methods to further decrease the H$_2$ liquefaction cost and improve the factory capacity.[102] A schematic of the liquid hydrogen delivery infrastructure and LH$_2$ delivery cost contribution is shown in Figure 22. The total cost of transmission and distribution for liquid hydrogen (30−100 Mt/day) was considered to be 2.5−3 $/kgH$_2$. Also, the total cost of hydrogen liquefaction (30−100 Mt/day) was calculated to be 2−2.5 $/kgH$_2$.

Storing H$_2$ as a liquid instead of a gas lowers the storage capacity. Moreover, large-scale liquid H$_2$ storage systems have emerged as a viable solution for efficiently increasing the capacity of H$_2$ fuel stations.[379] The design of the liquid H$_2$ storage system must consider the risks caused by low temperatures (−243 °C), fireball, aerosol puff, gas puff (ignited), missile ejection, gas jet (ignited), pool dispersion, flashfire, pool formation, gas dispersion, fire, aerosol puff (ignited), overpressure generation, two-phase jet, jet fire, pool (ignited), and vapor cloud explosion.[380−386] The three main factors for the development of the main standards of H$_2$ fueling stations based on risk assessment techniques include (i) the various contexts and infrastructures involved, (ii) the probability of leakage, failure, and combustion, and (iii) the physical behavior of H$_2$ in release, combustion, and accumulation.[387] For risk assessment, various data/information should be provided. The number of operational stations using liquid H$_2$ fuel is much lower than the number of operating stations using gaseous H$_2$. As a result, the risk analysis associated with running stations using liquid H$_2$ fuel is restricted.[388] Design failure, incorrect

operation, equipment failure, road traffic accidents, contamination, escalation, and natural causes were assumed to be the main factors of possible accidents in the risk assessment of the H$_2$ liquefaction scenarios by Lowesmith et al.[389] Also, two other studies were performed based on the investigation of accident scenarios in the delivery of liquid H$_2$ to fueling stations[390] and the risk assessment of liquid H$_2$ and gas.[391] Impurities in feed entering H$_2$ liquefaction systems can freeze at low temperatures and cause blockage of exchangers. Existing liquefaction systems use adsorbents to remove impurities, which may not be suitable for large systems (i.e., >50 TPD).[59] Exposure of ortho- to para-H$_2$ conversion reactors to impurities can lead to catalyst poisoning and its gradual deactivation.[322] The standards generally establish technical definitions, minimum performance criteria, and fundamental principles for building and testing H$_2$ liquefaction systems; these rules are essential to ensure the safety of commercial H$_2$ equipment and processes.[392] The principal standards for H$_2$ storage and transportation include the European Committee for Standardization (CEN), the International Organization for Standardization (ISO), the American Society of Mechanical Engineers (ASME), the American National Standards Institute (ANSI), the Standardization Administration of the People's Republic of China (SAC), Canadian National Standards (CNS), the Compressed Gas Association (CGA), the National Fire Protection Association (NFPA), the American Institute of Aeronautics and Astronautics (AIAA), and the Japanese Industrial Standards Committee (JISC).[393−400] Table 11 lists the main standards related to liquid H$_2$ in various industries.

Moreover, liquid H$_2$ is held in containers with double walls and a high vacuum between them to reduce the rate of heat transmission by convection and conduction.[403] Using polyester
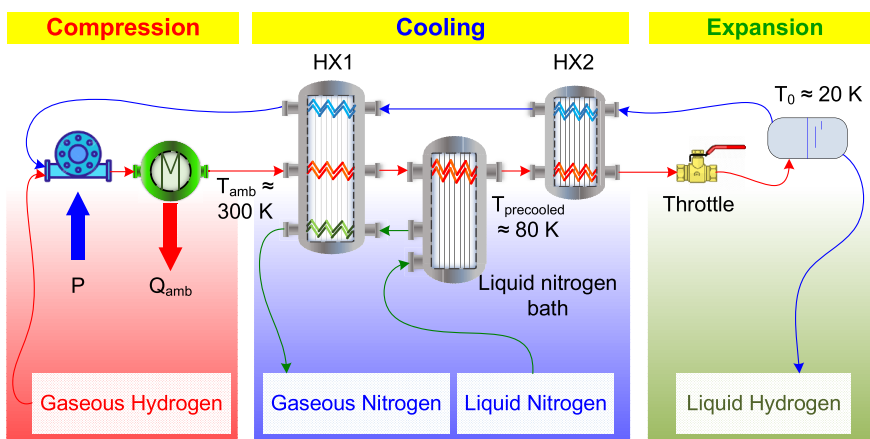
(a) Process diagram of H₂ liquefaction cycle
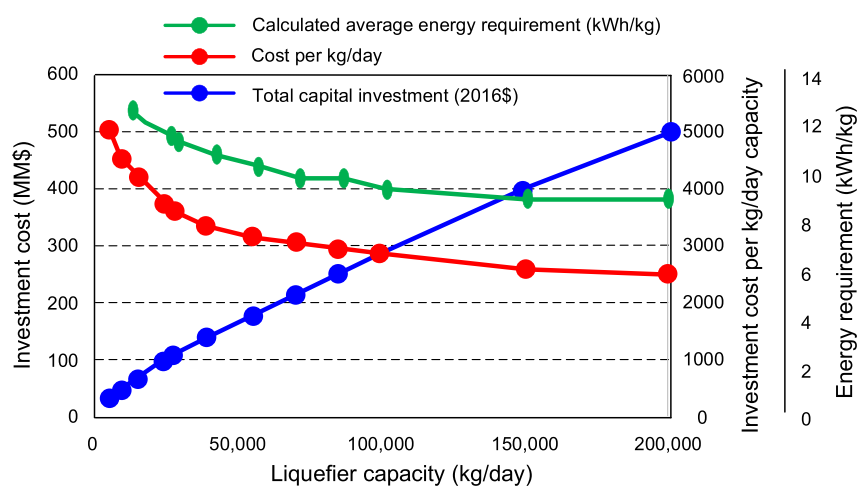
(b) Sensitivity analysis of key parameters

Figure 20. Effect of increasing H₂ liquefaction cycle capacity on the supply chain investment cost and SEC. Modified from ref 366.
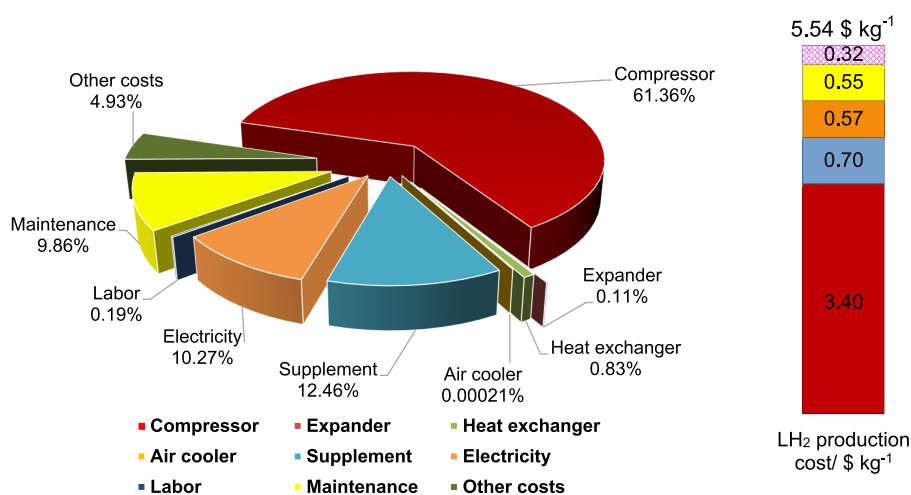
Figure 21. Price share of equipment used in a H₂ liquefaction structure based on three multicomponent refrigerant refrigeration cycles (1 TPD). Modified from ref 214.

sheets covered with alumina, changing coatings of glass fiber and aluminum foil, or perlite particles, silica, and aluminum as protection against heat transfer through radiation are utilized.[404]

Numerous researchers have paid attention to reducing the value of the SEC in H₂ liquefaction systems, while the total price, relative complexity, and emission levels have been ignored. The

(a) Infrastructure of liquid hydrogen delivery

(b) Cost contribution of LH$_2$ delivery
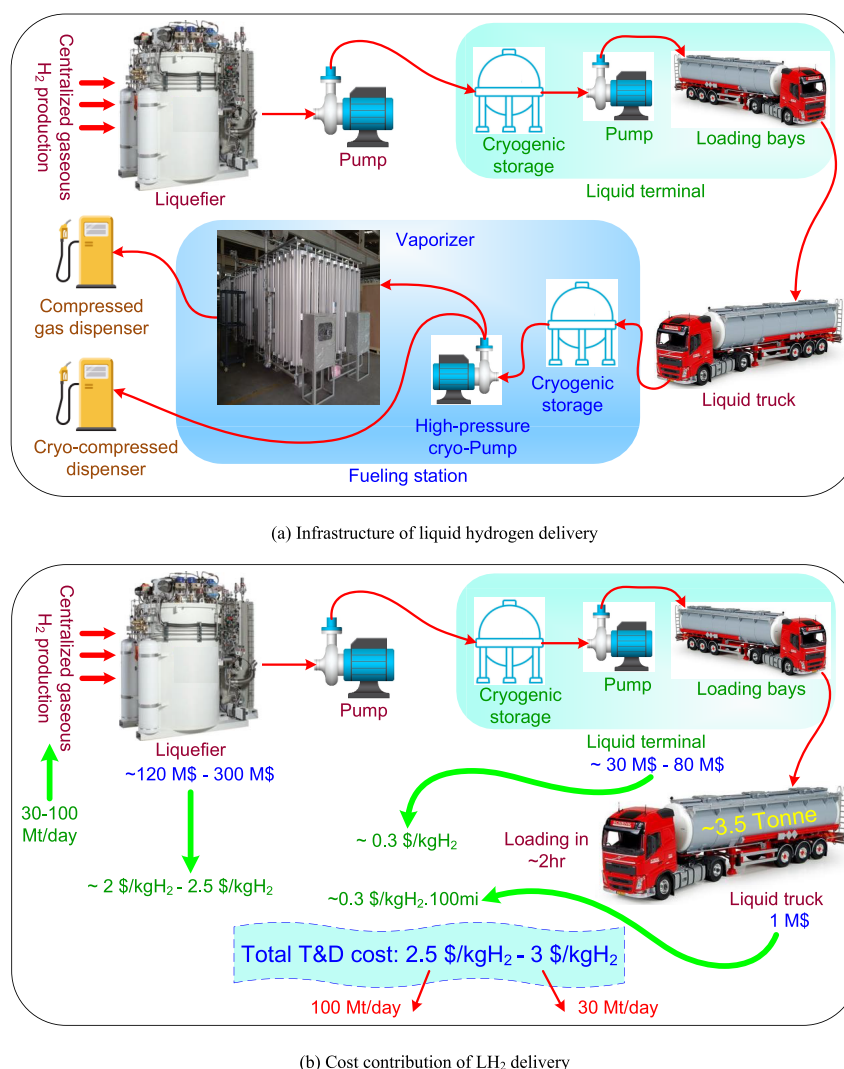
Figure 22. A schematic of the liquid hydrogen delivery infrastructure and LH$_2$ delivery cost contribution. Modified from refs 377 and 378.

life cycle analysis of the structure modeled by Kim et al.[214] estimated 67.85 and 0.253 kgCO$_{2eq}$ emissions for the LH$_2$ production process first and second day, respectively. The refrigerants employed in the liquid cycle contribute significantly to the first-day emissions. During the second day, however, the power supply systems are responsible for the majority of CO$_2$ emissions. Two-objective optimization was investigated to reduce the CO$_2$ emissions and payback period in a liquid H$_2$ production structure.[82] The payback period, the levelized cost of H$_2$, and the CO$_2$ emissions were reported to be 8.40 years, 4.5 $/kg LH$_2$, and 2441 TPD, respectively. LN$_2$, LNG regasification, the H$_2$ Brayton process, and the SMR plant were used to produce liquid H$_2$ in the combination structure. The environmental investigation of a liquid H$_2$ production system integrated with an ACC, a LAC recovery, and an ORC plant demonstrated that the CO$_2$ emission and its total specific were reported to be 96372 TPD and 2.641 kgCO$_2$/kgLH$_2$, respectively.[26] Reuß et al.[371] reported that H$_2$ storage with the LOHC method had the highest CO$_2$ emission (6.29 kgCO$_2$/kgH$_2$) and H$_2$ storage with the liquefaction method had the lowest emission (0.52 kgCO$_2$/kgH$_2$). The SEC and GHG emissions of the hydrogen liquefaction system for 5/33/130 TPD capacity were reported to be 11/9.4/8.2 kWh/kgLH$_2$ and 4.8/4.1/3.6 kgCO$_{2e}$/kgH$_2$, respectively.[377]

6. STATUS AND FUTURE PROSPECTS OF LIQUID HYDROGEN

The SEC and exergy yield in industrial applications are 12.5−15 kWh/kgLH$_2$ and 19.3−23.1%, respectively, such as Praxair (United States) and Linde (Germany).[58] Furthermore, the Linde factory in Germany, with an SEC of 13−15 kWh/kgLH$_2$, is commonly used as a reference for large-scale industrial liquefaction processes.[77,405] Table 12 summarizes the parameters of recent H$_2$ liquefaction units. The majority of these factories are in North American countries. High-temperature geothermal wells located in North America include KS-13 at 1050 °C (Hawaii, United States),[406] Wilson No. 1 at 400 °C (California, United States),[407] H-8,11,12,26,27,29 at >380 °C (Los Humeros, Mexico),[408] Prati-32 at 400 °C (Geysers, California, United States),[409] and IID-14 at 400 °C (Imperial Valley, California, United States).[410] High-temperature wells can be used to produce and store hydrogen. Liquefaction plants with higher production rates, higher efficiency, lower SEC (up to 40% reduction), and lower capital costs are needed to make liquid H$_2$ cost effective for the H$_2$ market.[28,404] The two main purposes for the supply chain of liquid H$_2$ in the future are decreasing the specific liquefaction cost and the SEC to 1−2 US $/kgH$_2$ and 6−8 kWh/kgH$_2$, respectively.[59] Moradi et al.[28] reported an SEC of 6 kWh/kgLH$_2$ for cost-effective H$_2$

Table 11. Standards Related to Liquid H_2 in Various Industries[384,392,401,402]

standard number	standards details
ISO 13984-1999	LH_2, land vehicle fueling structure interface
KS B ISO 13984-2004	
CGA PS-17-2004	position statement on the underground installation of LH_2 storage tanks
DS/ISO 13984-2005	LH_2, land vehicle fueling structure interface
ISO 13985-2006	LH_2, land vehicle fuel tanks
BS ISO 13985-2007	
KS B ISO 13985-2009	
DS/ISO 13985-2012	
GOST R ISO 13985-2013	
GOST R 56248-2014	LH_2, specifications
CGA G-5.5-2014	H_2 vent structures
GB/T 30179-2014	LH_2 land vehicle fueling structure interface
CGA H-5-2014	standard for bulk H_2 store structures
CGA P-28-2014	OSHA system safety management and EPA risk management strategy guidance document for bulk LH_2 supply structures
GOST ISO 13984-2016	LH_2, land vehicle fueling structure interface
CGA PS-48-2016	clarification of available H_2 setback distances and design of novel H_2 setback distances in NFPA55
CGA G-5.3-2017	commodity specification for H_2
CGA P-8.8-2017	safe design and operation of low-temperature enclosures
CGA P-12-2017	safe handling of low-temperature liquids
CGA P-41-2018	locating bulk liquid storage structures in courts
ASME B31.12-2019	pipelines and H_2 piping
CGA H-32019	low-temperature H_2 storage
CGA G-5.4-2019	standards of H_2 piping structures at user locations
NFPA 2-2020	H_2 processes code
NFPA 55-2020	compressed gases and low-temperature fluids code
GB/T 40045-2021	LH_2, fuel specification in H_2 powered vehicles
GB/T 40060-2021	LH_2, technical needs in transportation and storage
GB/T 40061-2021	specialized specification in LH_2 generation structure
MIL-PRF-27201	propellant H_2
GB 50516	specialized codes in fueling station
GB 50156	specialized standards in fueling station
NFPA 50B	LH_2, consumer sites

liquefaction plants. Also, the liquefaction plants' capacity can be improved to about 100 TPD or more to achieve these goals. Currently, the capacity of the H_2 liquefaction plants presented in Table 12 is lower than the 100 TPD as a desired value. Cardella et al.[93,102] introduced two short- to midterm and long-term solutions to achieve a cost-effective H_2 liquefaction system. As a short- to midterm concept, mixed refrigerant cycles in precooling cycles, high-pressure H_2 Claude in cryogenic units, and increasing production capacity up to 150 TPD were implemented. Moreover, the use of mixed refrigerant cycles in precooling cycles, H_2–Ne mixture cycles in cryogenic units, and increasing production capacity to 100 TPD as a long-term idea was examined.[102] The results indicate that H_2 liquefaction costs for 100 TPD can be decreased by about 50% and 67% compared to conventional 25 and 5 TPD liquefier systems, respectively.[93] Also, the results indicated that the design of LH_2 liquefaction cycles of 100 TPD with MRC precooling has the highest exergy efficiency and the lowest liquefaction costs compared to other cycles.[93] Besides, integrating industrial systems and H_2

liquefaction cycles can help decrease the production costs and SEC. Precooling cycles in H_2 liquefaction units can use inexpensive feedstock LN_2 that comes directly from air separation units to produce liquid oxygen.[62,77] Waste refrigeration to sea for LNG at an import terminal can be used for precooling to 130 K temperature.[86] The design of H_2 liquefaction cycles along with industrial H_2 production units at high pressure can lead to the elimination of compressors, reducing the production costs and SEC. The high costs of purchasing special H_2 compressors can be compensated by high-pressure electrolysis.[102,411,412]

A hydrogen liquefaction capacity of 263 MTPD was reported in North America. California, Louisiana, Indiana, New York, Alabama, Ontario, Quebec, and Tennessee were assigned 30, 70, 30, 40, 30, 30, 27, and 6, respectively. Four additional H_2 liquefaction factories have been recently announced to aid the growing H_2 market.[377] Designing liquid hydrogen storage tanks is another major challenge for engineers and researchers in this field. Figure 23 illustrates the development process of liquid hydrogen storage tanks in different projects. The design of large-scale liquid hydrogen storage tanks with capacities of 40 000 to 100 000 m³ for onshore or offshore applications is underway with the DOE budget.[416] All previous research for LH_2 has been based on much smaller tank sizes (<4700 m³) and evacuated insulation units.[417] During the 1960s, a pair of 3200 m³ LH_2 spherical tanks (containing approximately 240 tonnes of LH_2) was built by Chicago Bridge & Iron (CB&I) at NASA's Kennedy Space Center (KSC) launch complex to support the Apollo and space shuttle programs. In 2018, construction began on an additional LH_2 storage tank at Launch Complex 39B (LC-39B). The total on-site storage capacity at LC-39B is about 8000 m³.[417,418] A CB&I preliminary design and feasibility study for 40000 m³ storage space was completed.[416]

7. SUMMARY AND CONCLUSIONS

Hydrogen is a clean and renewable fuel that can replace common fossil fuels. H_2 liquefaction is promising as a physical storage method for large-scale transportation and long-term storage. Liquefaction of H_2 leads to a decrease in volume and an increase in density compared to the gaseous state. Furthermore, the cost of building H_2 generation systems is significant, and it is often difficult to build them in the required area. As a result, the transportation of H_2 from the location of the production system to the place of consumption is justified. H_2 needs to be stored in liquid form because H_2 storage requires a large volume and its transportation is difficult. Liquid H_2 storage systems face problems, including a high SEC, low exergy efficiency, high cost, and boil-off gas losses. This review studies various methods of H_2 liquefaction and its technologies. It discusses several techniques for enhancing H_2 liquefaction performance using an ACC, an ejector refrigeration cycle, LN_2/LNG/LAC energy recovery, CRCs, a mixed refrigerant system, integration with other hybrid structures, optimization algorithms, combined with renewable energy sources, and the pinch methodology. It presents the economic, safety, and environmental factors of different techniques for H_2 liquefaction systems along with standards and codes for various technologies. Additionally, the review presents the current status and prospects of H_2 liquefaction cycles. The principal results of the study are summarized as follows.

(1) When the number of ortho- to para-H_2 conversion steps increases, the SEC of the H_2 liquefaction process declines

Table 12. H₂ Liquefaction Factories Constructed in the Past Years [58,59,62,205,413−415]

country	constructed	location	owner	capacity (TPD)	country	constructed	location	owner	capacity (TPD)
United States	1952	Colorado	NBS[a]	0.5	United States	1994	Pace, FL	APCI	30
United States	1956	Ohio	APCI[b]	1	United States	1995	McIntosh, AL	Praxair	24
United States	1957	Painsville	APS[c]	3	China	1995	Beijing	CALT	0.6
United States	1957	West Palm Beach	APS	3.2	United States	1997	East Chicago, IN	Praxair	30
United States	1957	Florida	APCI	3.5	Japan	2003	Kimitsu	APS	0.3
United States	1957	California	SRMC[d]	1.5	India	2004	Saggonda	Andhra Sugars	1.2
United States	1958	Florida	APCI	30	India	2004	Kimitsu	KSC[l]	0.2
United States	1959	West Palm Beach	APS	27	Japan	2006	Osaka	Iwatani	11.3
United States	1960	Mississippi	APS	32.7	Germany	2008	Leuna	Linde	5
United States	1960	California	SRMC	7	Japan	2008	Tokyo	Iwatani	10
United States	1962	Ontario, CA	Praxair	20	Japan	2009	Chiba	ICL[i]	5
United States	1962	California	SRMC	26	India			Asiatic Oxygen	1.2
United States	1963	California	APCI	32.5	United States		California	SRMC	62.5
United States	1964	Sacramento	Union Carbide	54	United States		New Jersey	ARSC[j]	6
United States	1977	New Orleans, LA	APCI	34	United States		Ashtabula, OH	Praxair	
United States	1978	New Orleans, LA	APCI	34	Japan	2013	Yamaguchi	ICL	5
Japan	1978	Amagasaki	Iwatani	1.2	Japan	2014	Akashi	KHI[k]	5
United States	1981	Niagara Falls, NY	Praxair	18	Japan	2017	Yamaguchi	Iwatani and Tokuyama	10
Canada	1982	Sarnia Ontario,	APCI	30	Australia	2020	Port of Hastings	HESC[h]	0.25
Japan	1984	Tashiro	MHI[f]	0.6	United States	2020	Las Vegas	Air Liquid	27.2
Japan	1985	Akita Prefecture	Tashiro	0.7	Germany	2021	Leuna	Linde	10
United States	1986	Sacramento, CA	APCI	6	United States	2021	La Porte	APS	27.2
Japan	1986	Tane-Ga-Shima	Japan LH₂	1.4	United States	2021	La Porte	Praxair	27.2
Japan	1986	Oita	Pacific H₂	1.9	United States	2021	California	APS	
Canada	1986	Montreal	Air Liquide	10	Korea	2022	Ulsan	Hyosung and Linde	13
Holland	1987	Rosenburg	APCI	5					
France	1987	Waziers, Lille	Air Liquide	10					
Japan	1987	Minamitane	Japan LH₂	2.2					
Canada	1988	Becancour, Quebec	Air Liquide	12					
United States	1989	Niagara Falls, NY	Praxair	18					
Canada	1989	Magog, Quebec	BOC[e]	15					
Guyana	1990	Kouru F	Air Liquide	5					
Canada	1990	Montreal	BOC	14					
Germany	1991	Ingolstadt	Linde	4.4					
India	1992	Mahendragiri	ISRO[g]	0.3					

[a]National Bureau of Standards (NBS). [b]Air Products and Chemicals, Inc. [c]Air Products (APS). [d]Stearns-Roger Manufacturing Company (SRMC). [e]British Oxygen Company (BOC). [f]Mitsubishi Heavy Industries (MHI). [g]Indian Space Research Organisation (ISRO). [h]Hydrogen Energy Supply Chain (HESC). [i]Iwatani Constructed by Linde (ICL). [j]Air Reduction Sales Company (ARSC). [k]Kawasaki Heavy Industries (KHI). [l]Nippon Steel Corporation (KSC).

and the investment cost goes up. When a second reactor is added, the SEC decreases and then decreases gradually with each reactor added. Using 2−3 reactors can be effective in achieving a balance between reducing the SEC and increasing the cost of conversion reactors.

(2) The SEC is reduced when mixed refrigerant cycles are used in H₂ liquefaction operations. The use of mixed refrigerant cycle controllers causes an increase in the capital cost. Moreover, leakage in a section of the cycle alters the percentage of refrigerants, which is difficult to manage. For mixed refrigerants in H₂ liquefaction operations, risk assessments is critical.

(3) Using LNG regasification in H₂ liquefaction cycles reduces the SEC. In the reported liquefaction structures, the capital and operating costs are reduced. In the cycles in which the LNG regasification process replaces mixed refrigerant cycles, the whole configuration exergy yield and the refrigeration cycle COP decrease. Also, LNG regasification substitution of the precooling cycle is associated with a lower SEC and cost compared to the hybrid of LNG regasification with the precooling cycle.

(4) Using ACCs in H₂ liquefaction cycles decreases the SEC. The capital and operating costs of several liquefaction structures reviewed in this article are reduced by using an ACC for precooling; however, more research is needed to provide firm comments/tips on the impact of this replacement on economic prospect. When the ACC replaces the mixed refrigerant cycles, the overall configuration exergy yield and refrigeration cycle COP are reduced. Although the use of an ejector cooling system lowers the SEC in liquefaction systems, additional research is needed to evaluate the economic aspects.

(5) The geothermal ACC for gas precooling significantly saves the power required for H₂ liquefaction and is more beneficial than utilizing geothermal power output in a liquefaction process. In the reported liquefaction structures, the SEC, capital, and operating costs are reduced.

(6) Because the degree of freedom of the precooling cycle is greater than that of the cryogenic cycle, optimization methods prioritize the precooling cycles. Optimization choices include refrigerant mixture, pinch point, and high/low pressure of the refrigeration cycle.
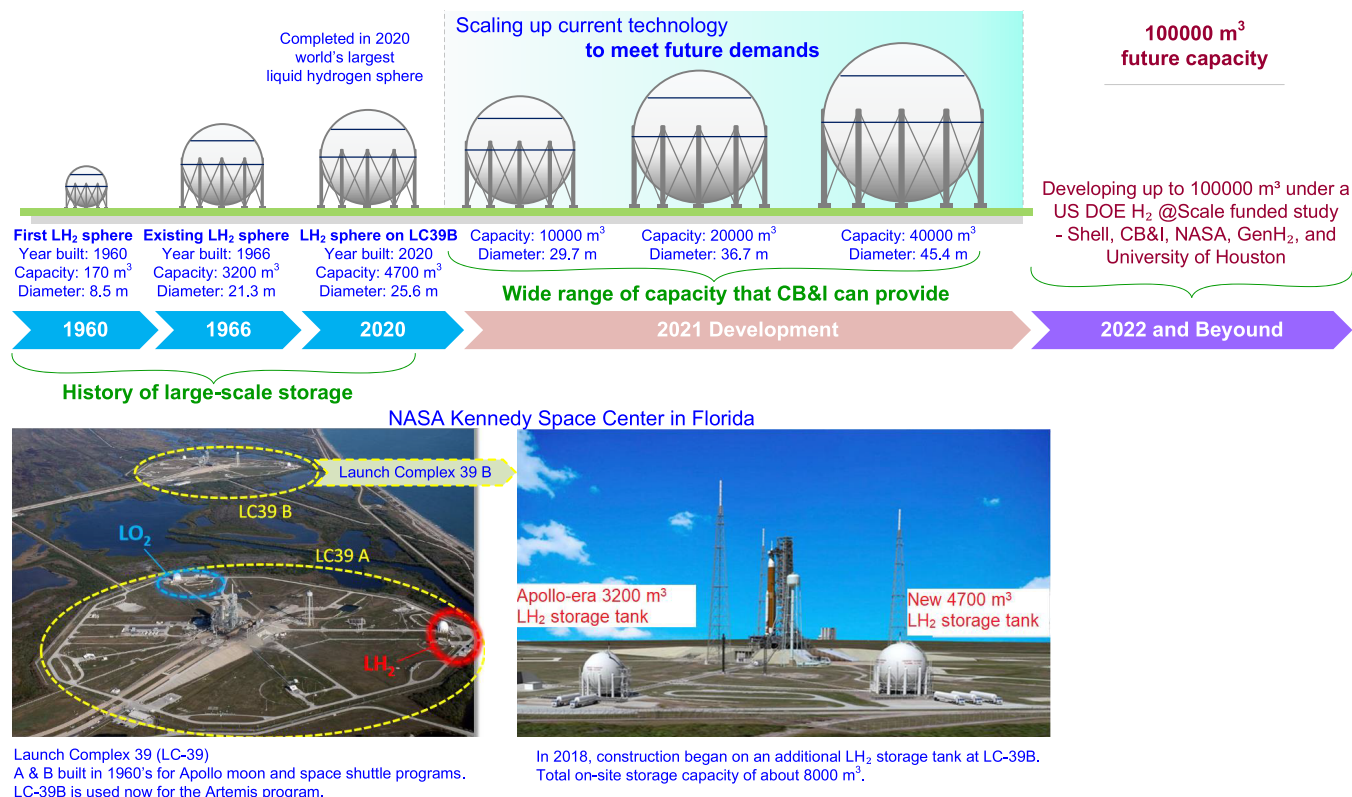
Figure 23. Development process of liquid hydrogen storage tanks in different projects. Modified from refs 416 and 417.

(7) The H_2 liquefaction plants with higher production rates (>100 tonne/day), higher efficiency (>40%), lower SEC (<6 kWh/kgLH$_2$), and lower investment costs (1−2 $/kgLH$_2$) can be economical. Compressors can be eliminated from H_2 production and liquefaction plants, lowering the production costs and SEC. Further research and engineering investigations should focus on the environmental impact of H_2 liquefaction cycles based on refrigerants utilized, electricity consumption, and equipment type.

(8) The impact of various strategies to increase the performance of H_2 liquefaction systems on the supply chain of liquid H_2, environmental aspects, and risk parameters can be investigated. Codes and standards for large-scale H_2 liquefaction storage processes can be assessed and updated.

■ AUTHOR INFORMATION

Corresponding Author

Sohrab Zendehboudi − *Faculty of Engineering and Applied Science, Memorial University, St. John's, Newfoundland and Labrador A1B 3X5, Canada;* ⊚ orcid.org/0000-0001-8527-9087; Email: szendehboudi@mun.ca

Authors

Bahram Ghorbani − *Faculty of Engineering and Applied Science, Memorial University, St. John's, Newfoundland and Labrador A1B 3X5, Canada*

Noori M. Cata Saady − *Faculty of Engineering and Applied Science, Memorial University, St. John's, Newfoundland and Labrador A1B 3X5, Canada*

Xili Duan − *Faculty of Engineering and Applied Science, Memorial University, St. John's, Newfoundland and Labrador A1B 3X5, Canada;* ⊚ orcid.org/0000-0001-5554-0758

Talib M. Albayati − *Department of Chemical Engineering, University of Technology—Iraq, Baghdad 10071, Iraq*

Complete contact information is available at:
https://pubs.acs.org/10.1021/acsomega.3c01072

Notes

The authors declare no competing financial interest.

■ NOMENCLATURE

Acronyms

ACC	absorption cooling cycle
NH$_3$	ammonia
ANN	artificial neural network
C$_4$	butane
CaCl$_2$	calcium chloride
CO$_2$	carbon dioxide
CRC	cascade refrigeration cycle
COP	coefficient of performance
COG	coke oven gas
CPEA	combined pinch and exergy assessment
CC	composite curve
DOE	Department of Energy
D	deuterium
C$_2$	ethane

C_2H_4	ethylene
ECC	exergy composite diagram
EGCC	exergy grand composite diagram
GA	genetic algorithm
GCC	grand composite curve
He	helium
H_2	hydrogen
IPCC	International Conference on Climate Change
J−B	Joule−Brayton
J−T	Joule−Thomson
K	Kelvin
KBO	knowledge-based optimization
LCOH	levelized cost of liquid H_2
L−H	Linde−Hampson
LAC	liquid−air cold
LH_2	liquid hydrogen
LNG	liquid natural gas
LN_2	liquid nitrogen
LOHC	liquid organic H_2 carrier
LiBr	lithium bromide
MF	mass flow
C_1	methane
CH_3OH	methanol
CH_3O	methoxide
C_7H_{14}	methylcyclohexane
MINLP	mixed integer nonlinear programming
MRC	mixed refrigerant cycle
MCD	modified coordinate descent
Ne	neon
N_2	nitrogen
NCR	number of conversion reactors
ORC	organic Rankine cycle
$O\text{-}H_2$	ortho-hydrogen
$P\text{-}H_2$	para-hydrogen
PSO	particle swarming optimization
C_5	pentane
PH	potential of hydrogen
C_3	propane
C_3H_6	propene
RCC	reducing capital costs
ROC	reducing operating costs
RCS	relative cost saving
$SPLH_2$	selling price of liquid hydrogen
SQP	sequential quadratic programming
SRC	single refrigerant cycle
SEC	specific energy consumption
SMR	steam methane reforming
R14	tetrafluoromethane
TPD	tons per day
TE	trial and error
T	tritium
H_2O	water
$ZnBr_2$	zinc bromide

Variables/Letters

C	achieved concentrations
C_0	initial concentration
C_{eq}	equilibrium concentrations
HX	heat exchanger
k_v	volume rate constant $(mol/(cm^3\,s))$
P	pressure (bar)
m	mass flow rate (kg/s)
n	feed molar flow rate (mol/s)
T	temperature (°C)

V	volume of the catalyst (cm^3)

Greek Letters

μ	Joule−Thomson coefficient
ρ	fluid density

Subscripts and superscripts

f	feed
l	liquid

■ REFERENCES

(1) Rastegari, A. A.; Yadav, A. N.; Gupta, A. *Prospects of renewable bioprocessing in future energy systems*; Springer, 2019.

(2) Ghazvini, M.; Sadeghzadeh, M.; Ahmadi, M. H.; Moosavi, S.; Pourfayaz, F. Geothermal energy use in hydrogen production: A review. *Int. J. Energy Res.* **2019**, *43* (14), 7823−7851.

(3) Azarpour, A.; Mohammadzadeh, O.; Rezaei, N.; Zendehboudi, S. Current status and future prospects of renewable and sustainable energy in North America: Progress and challenges. *Energy Convers Manag.* **2022**, *269*, 115945.

(4) Tazikeh, S.; Zendehboudi, S.; Ghafoori, S.; Lohi, A.; Mahinpey, N. Algal bioenergy production and utilization: Technologies, challenges, and prospects. *J. Environ. Chem. Eng.* **2022**, *10*, 107863.

(5) Wang, J.; Ai, K.; Lu, L. Flame-retardant porous hexagonal boron nitride for safe and effective radioactive iodine capture. *J. Mater. Chem. A Mater.* **2019**, *7* (28), 16850−16858.

(6) Zohuri, B. Nuclear fuel cycle and decommissioning. *Nuclear Reactor Technology Development and Utilization*; Elsevier, 2020; pp 61−120.

(7) Møller, K. T.; Jensen, T. R.; Akiba, E.; Li, H.-w. Hydrogen-A sustainable energy carrier. *Prog. Nat. Sci.: Mater. Int.* **2017**, *27* (1), 34−40.

(8) Hassan, I. A.; Ramadan, H. S.; Saleh, M. A.; Hissel, D. Hydrogen storage technologies for stationary and mobile applications: Review, analysis and perspectives. *Renew Sustain Energy Rev.* **2021**, *149*, 111311.

(9) Joseph, A.; Shahidehpour, M. Battery storage systems in electric power systems. *2006 IEEE Power Engineering Society General Meeting*, Montreal, Quebec; IEEE, 2006, p 8 DOI: 10.1109/PES.2006.1709235.

(10) AlShafi, M.; Bicer, Y. Assessment of various energy storage methods for implementation in hot and arid climates. *Energy Storage* **2020**, *2* (6), e191.

(11) Carnegie, R.; Gotham, D.; Nderitu, D.; Preckel, P. V. Utility scale energy storage systems. *State Utility Forecasting Group*; Purdue University, 2013; Vol. *1*.

(12) Kharel, S.; Shabani, B. Hydrogen as a long-term large-scale energy storage solution to support renewables. *Energies.* **2018**, *11* (10), 2825.

(13) Valenti, G. Hydrogen liquefaction and liquid hydrogen storage. *Compendium of hydrogen energy*; Elsevier, 2016; pp 27−51.

(14) *Global Hydrogen Review 2021*; IEA, www.iea.org (Accessed Jan 2023).

(15) Nandapala, K.; Chandra, M. S.; Halwatura, R. Effectiveness of a discretely supported slab insulation system in terms of thermal performance. *Conference Sustainability for People—Envisaging Multi Disciplinary Solution*, Galle, Sri Lanka, 2018; pp 91−98.

(16) Aditya, L.; Mahlia, T.; Rismanchi, B.; Ng, H.; Hasan, M.; Metselaar, H.; Muraza, O.; Aditiya, H. A review on insulation materials for energy conservation in buildings. *Renew Sustain Energy Rev.* **2017**, *73*, 1352−1365.

(17) Neeteson, J.; Verhagen, A. Climate change and agriculture: mitigation and adaptation. *Acta Hortic.* **2010**, *852*, 19−26.

(18) Verma, S. C.; Thakur, M.; Bhardwaj, S. Climate Change and Horticulture Crop Production. *Int. J. Econ. Plants* **2015**, *2* (2), 70−78.

(19) Orr, F. M., Jr CO_2 capture and storage: are we ready? *Energy Environ. Sci.* **2009**, *2* (5), 449−458.

(20) Lou, Y.; Ye, Y.; Yang, Y.; Zuo, W. Long-term carbon emission reduction potential of building retrofits with dynamically changing electricity emission factors. *Build Environ.* **2022**, *210*, 108683.

(21) Hong, W. Y. A techno-economic review on carbon capture, utilisation and storage systems for achieving a net-zero CO_2 emissions future. *Carbon Capture Sci. Technol.* **2022**, *3*, 100044.

(22) IEA 2021. Net Zero by 2050 A Roadmap for the Global Energy Sector, Paris, https://www.iea.org/reports/world-energy-outlook-2022/an-updated-roadmap-to-net-zero-emissions-by-2050 (Accessed Jan 2023).

(23) Ocko, I. B.; Sun, T.; Shindell, D.; Oppenheimer, M.; Hristov, A. N.; Pacala, S. W.; Mauzerall, D. L.; Xu, Y.; Hamburg, S. P. Acting rapidly to deploy readily available methane mitigation measures by sector can immediately slow global warming. *Environ. Res. Lett.* **2021**, *16* (5), 054042.

(24) Koneczna, R.; Cader, J. Hydrogen in the strategies of the european Union member states. *Gospod. Surowcami Miner.* **2021**, *37* (3), 53−74.

(25) Global Hydrogen Review, International Energy Agency 2021, https://iea.blob.core.windows.net/assets/5bd46d7b-906a-4429-abda-e9c507a62341/GlobalHydrogenReview2021.pdf (Accessed Jan 2023).

(26) Naquash, A.; Qyyum, M. A.; Islam, M.; Sial, N. R.; Min, S.; Lee, S.; Lee, M. Performance enhancement of hydrogen liquefaction process via absorption refrigeration and organic Rankine cycle-assisted liquid air energy system. *Energy Convers Manag.* **2022**, *254*, 115200.

(27) Salehabadi, A.; Ahmad, M. I.; Ismail, N.; Morad, N.; Enhessari, M. *Energy, Society and the Environment: Solid-State Hydrogen Storage Materials*; Springer Nature, 2020.

(28) Moradi, R.; Groth, K. M. Hydrogen storage and delivery: Review of the state of the art technologies and risk and reliability analysis. *Int. J. Hydrogen Energy* **2019**, *44* (23), 12254−12269.

(29) Crotogino, F. Large-scale hydrogen storage. *Storing energy*; Elsevier, 2022; pp 613−632.

(30) Kayfeci, M.; Keçebaş, A. Hydrogen storage. In *Solar Hydrogen Production*; Calise, F., D'Accadia, M. D., Santarelli, M., Lanzini, A., Ferrero, D., Eds.; Academic Press, 2019; Chapter 4, pp 85−110.

(31) Langmi, H. W.; Engelbrecht, N.; Modisha, P. M.; Bessarabov, D. Hydrogen storage. In *Electrochemical Power Sources: Fundamentals, Systems, and Applications*; Smolinka, T., Garche, J., Eds.; Elsevier, 2022; Chapter 13, pp 455−486.

(32) Schlapbach, L.; Züttel, A. Hydrogen-storage materials for mobile applications. *Materials for Sustainable Energy*; World Scientific, 2010; pp 265−270; DOI: 10.1142/9789814317665_0038.

(33) Rusman, N. A. A.; Dahari, M. A review on the current progress of metal hydrides material for solid-state hydrogen storage applications. *Int. J. Hydrogen Energy* **2016**, *41* (28), 12108−12126.

(34) Landi, D.; Vita, A.; Borriello, S.; Scafà, M.; Germani, M. A methodological approach for the design of composite tanks produced by filament winding. *Comput.-Aided Des. Appl.* **2020**, *17* (6), 1229−1240.

(35) Berro Ramirez, J. P.; Halm, D.; Grandidier, J.-C.; Villalonga, S.; Nony, F. 700 bar type IV high pressure hydrogen storage vessel burst−Simulation and experimental validation. *Int. J. Hydrogen Energy* **2015**, *40* (38), 13183−13192.

(36) Leh, D.; Saffré, P.; Francescato, P.; Arrieux, R. Multi-sequence dome lay-up simulations for hydrogen hyper-bar composite pressure vessels. *Compos Part A Appl. Sci. Manuf.* **2013**, *52*, 106−117.

(37) Department of Energy, Materials-based hydrogen storage, https://energy.gov/eere/fuelcells/materials-based-hydrogen-storage (Accessed Jan 2023).

(38) Department of Energy, Materials-based hydrogen storage, https://energy.gov/eere/fuelcells/materials-based-hydrogen-storage (Accessed May 2022).

(39) Zhang, J.; Fisher, T. S.; Ramachandran, P. V.; Gore, J. P.; Mudawar, I. A review of heat transfer issues in hydrogen storage technologies. *J. Heat Transfer.* **2005**, *127* (12), 1391−1399.

(40) Taghavi, M.; Salarian, H.; Ghorbani, B. Economic Evaluation of a Hybrid Hydrogen Liquefaction System Utilizing Liquid Air Cold Recovery and Renewable Energies. *Renewable Energy Res. Appl.* **2023**, *4* (1), 125−143.

(41) Züttel, A. Materials for hydrogen storage. *Mater. Today.* **2003**, *6* (9), 24−33.

(42) Sheffield, J. W.; Martin, K. B.; Folkson, R. 5-Electricity and hydrogen as energy vectors for transportation vehicles. In *Alternative Fuels and Advanced Vehicle Technologies for Improved Environmental Performance*, Folkson, R., Ed.; Woodhead Publishing, 2014; pp 117−137.

(43) Aceves, S. M.; Petitpas, G.; Espinosa-Loza, F.; Matthews, M. J.; Ledesma-Orozco, E. Safe, long range, inexpensive and rapidly refuelable hydrogen vehicles with cryogenic pressure vessels. *Int. J. Hydrogen Energy* **2013**, *38* (5), 2480−2489.

(44) Rusman, N.; Dahari, M. A review on the current progress of metal hydrides material for solid-state hydrogen storage applications. *Int. J. Hydrogen Energy* **2016**, *41* (28), 12108−12126.

(45) Bruch, L. W.; Cole, M. W.; Zaremba, E. *Physical adsorption: forces and phenomena*; Courier Dover Publications, 2007.

(46) Zhou, L. Progress and problems in hydrogen storage methods. *Renew Sustain Energy Rev.* **2005**, *9* (4), 395−408.

(47) Gupta, A.; Baron, G. V.; Perreault, P.; Lenaerts, S.; Ciocarlan, R.-G.; Cool, P.; Mileo, P. G. M.; Rogge, S.; Van Speybroeck, V.; Watson, G.; et al. Hydrogen Clathrates: Next Generation Hydrogen Storage Materials. *Energy Storage Mater.* **2021**, *41*, 69−107.

(48) Hassan, I.; Ramadan, H. S.; Saleh, M. A.; Hissel, D. Hydrogen storage technologies for stationary and mobile applications: Review, analysis and perspectives. *Renew Sustain Energy Rev.* **2021**, *149*, 111311.

(49) Hong, S.-H.; Song, M. Y. Hydrogen desorption and absorption properties of Pd and MgO or nano-sized Ni-added MgH2+ LiBH4 composites. *Mater. Res. Bull.* **2013**, *48* (9), 3453−3458.

(50) Lee, S.-Y.; Lee, J.-H.; Kim, Y.-H.; Kim, J.-W.; Lee, K.-J.; Park, S.-J. Recent progress using solid-state materials for hydrogen storage: a short review. *Processes.* **2022**, *10* (2), 304.

(51) Niermann, M.; Beckendorff, A.; Kaltschmitt, M.; Bonhoff, K. Liquid Organic Hydrogen Carrier (LOHC)−Assessment based on chemical and economic properties. *Int. J. Hydrogen Energy* **2019**, *44* (13), 6631−6654.

(52) Niermann, M.; Timmerberg, S.; Drünert, S.; Kaltschmitt, M. Liquid Organic Hydrogen Carriers and alternatives for international transport of renewable hydrogen. *Renew Sustain Energy Rev.* **2021**, *135*, 110171.

(53) Singh, R.; Singh, M.; Gautam, S. Hydrogen economy, energy, and liquid organic carriers for its mobility. *Mater. Today Proc.* **2021**, *46*, 5420−5427.

(54) Klerke, A.; Christensen, C. H.; Nørskov, J. K.; Vegge, T. Ammonia for hydrogen storage: challenges and opportunities. *J. Mater. Chem.* **2008**, *18* (20), 2304−2310.

(55) Wulf, C.; Zapp, P. Assessment of system variations for hydrogen transport by liquid organic hydrogen carriers. *Int. J. Hydrogen Energy* **2018**, *43* (26), 11884−11895.

(56) Mukherjee, S.; Devaguptapu, S. V.; Sviripa, A.; Lund, C. R.; Wu, G. Low-temperature ammonia decomposition catalysts for hydrogen generation. *Appl. Catal., B* **2018**, *226*, 162−181.

(57) Ghorbani, B.; Zendehboudi, S.; Afrouzi, Z. A. Thermo-economic optimization of a novel hybrid structure for power generation and portable hydrogen and ammonia storage based on magnesium−chloride thermochemical process and liquefied natural gas cryogenic energy. *J. Clean Prod.* **2023**, *403*, 136571.

(58) Aasadnia, M.; Mehrpooya, M. Large-scale liquid hydrogen production methods and approaches: A review. *Appl. Energy.* **2018**, *212*, 57−83.

(59) Al Ghafri, S. Z.; Munro, S.; Cardella, U.; Funke, T.; Notardonato, W.; Trusler, J. P. M.; Leachman, J.; Span, R.; Kamiya, S.; Pearce, G.; Swanger, A.; Rodriguez, E. D.; Bajada, P.; Jiao, F.; Peng, K.; Siahvashi, A.; Johns, M. L.; May, E. F. Hydrogen liquefaction: a review of the fundamental physics, engineering practice and future opportunities. *Energy Environ. Sci.* **2022**, *15*, 2690−2731.

(60) Wijayanta, A. T.; Oda, T.; Purnomo, C. W.; Kashiwagi, T.; Aziz, M. Liquid hydrogen, methylcyclohexane, and ammonia as potential hydrogen storage: Comparison review. *Int. J. Hydrogen Energy* **2019**, *44* (29), 15026−15044.

(61) Bell, T.; Torrente-Murciano, L. H 2 production via ammonia decomposition using non-noble metal catalysts: A review. *Top Catal.* **2016**, *59*, 1438−1457.

(62) Krasae-in, S.; Stang, J. H.; Neksa, P. Development of large-scale hydrogen liquefaction processes from 1898 to 2009. *Int. J. Hydrogen Energy* **2010**, *35* (10), 4524−4533.

(63) Dewar, J. Preliminary note on the liquefaction of hydrogen and helium. *Science* **1898**, *8* (183), 3−5.

(64) Yin, L.; Ju, Y. Review on the design and optimization of hydrogen liquefaction processes. *Front. Energy.* **2020**, *14* (3), 530−544.

(65) YILMAZ, C. Thermodynamic performance analysis of gas liquefaction cycles for cryogenic applications. *J. Therm. Eng.* **2019**, *5* (1), 62−75.

(66) Qi, M.; Park, J.; Lee, I.; Moon, I. Liquid air as an emerging energy vector towards carbon neutrality: A multi-scale systems perspective. *Renew Sustain Energy Rev.* **2022**, *159*, 112201.

(67) Veziroglu, T. N.; Sherif, S.; Barbir, F. Hydrogen energy solutions. *Environmental solutions*; Elsevier, 2005; pp 143−180.

(68) Khodaparast, S. H.; Zare, V.; Mohammadkhani, F. Geothermal assisted hydrogen liquefaction systems integrated with liquid nitrogen precooling; Thermoeconomic comparison of Claude and reverse Brayton cycle for liquid nitrogen supply. *Process Saf. Environ. Prot.* **2023**, *171*, 28−37.

(69) Lee, D.; Quarme Gbadago, D.; Jo, Y.; Hwang, G.; Jo, Y.; Smith, R.; Hwang, S. Integrating hydrogen liquefaction with steam methane reforming and CO_2 liquefaction processes using techno-economic perspectives. *Energy Convers. Manage.* **2021**, *245*, 114620.

(70) Kanoglu, M.; Yilmaz, C.; Abusoglu, A. Geothermal energy use in absorption precooling for Claude hydrogen liquefaction cycle. *Int. J. Hydrogen Energy* **2016**, *41* (26), 11185−11200.

(71) Aasadnia, M.; Mehrpooya, M. Conceptual design and analysis of a novel process for hydrogen liquefaction assisted by absorption precooling system. *J. Clean Prod.* **2018**, *205*, 565−588.

(72) Yilmaz, C. A case study: Exergoeconomic analysis and genetic algorithm optimization of performance of a hydrogen liquefaction cycle assisted by geothermal absorption precooling cycle. *Renew Energy.* **2018**, *128*, 68−80.

(73) Yilmaz, C.; Kaska, O. Performance analysis and optimization of a hydrogen liquefaction system assisted by geothermal absorption precooling refrigeration cycle. *Int. J. Hydrogen Energy* **2018**, *43* (44), 20203−20213.

(74) Ghorbani, B.; Mehrpooya, M.; Aasadnia, M.; Niasar, M. S. Hydrogen liquefaction process using solar energy and organic Rankine cycle power system. *J. Clean Prod.* **2019**, *235*, 1465−1482.

(75) Aasadnia, M.; Mehrpooya, M.; Ansarinasab, H. A 3E evaluation on the interaction between environmental impacts and costs in a hydrogen liquefier combined with absorption refrigeration systems. *Appl. Therm Eng.* **2019**, *159*, 113798.

(76) Baker, C.; Shaner, R. A study of the efficiency of hydrogen liquefaction. *Int. J. Hydrogen Energy* **1978**, *3* (3), 321−334.

(77) Bracha, M.; Lorenz, G.; Patzelt, A.; Wanner, M. Large-scale hydrogen liquefaction in Germany. *Int. J. Hydrogen Energy* **1994**, *19* (1), 53−59.

(78) Kuz'menko, I.; Morkovkin, I.; Gurov, E. Concept of building medium-capacity hydrogen liquefiers with helium refrigeration cycle. *Chem. Pet. Eng.* **2004**, *40* (1), 94−98.

(79) Garceau, N. M.; Baik, J. H.; Lim, C. M.; Kim, S. Y.; Oh, I.-H.; Karng, S. W. Development of a small-scale hydrogen liquefaction system. *Int. J. Hydrogen Energy* **2015**, *40* (35), 11872−11878.

(80) Riaz, A.; Qyyum, M. A.; Min, S.; Lee, S.; Lee, M. Performance improvement potential of harnessing LNG regasification for hydrogen liquefaction process: Energy and exergy perspectives. *Appl. Energy.* **2021**, *301*, 117471.

(81) Faramarzi, S.; Nainiyan, S. M. M.; Mafi, M.; Ghasemiasl, R. A novel hydrogen liquefaction process based on LNG cold energy and mixed refrigerant cycle. *Int. J. Refrig.* **2021**, *131*, 263.

(82) Bae, J.-E.; Wilailak, S.; Yang, J.-H.; Yun, D.-Y.; Zahid, U.; Lee, C.-J. Multi-objective optimization of hydrogen liquefaction process

integrated with liquefied natural gas system. *Energy Convers Manag.* **2021**, *231*, 113835.

(83) Chang, H.-M.; Kim, B. H.; Choi, B. Hydrogen liquefaction process with Brayton refrigeration cycle to utilize the cold energy of LNG. *Cryogenics.* **2020**, *108*, 103093.

(84) Yang, J.-H.; Yoon, Y.; Ryu, M.; An, S.-K.; Shin, J.; Lee, C.-J. Integrated hydrogen liquefaction process with steam methane reforming by using liquefied natural gas cooling system. *Appl. Energy.* **2019**, *255*, 113840.

(85) Taghavi, M.; Salarian, H.; Ghorbani, B. Thermodynamic and exergy evaluation of a novel integrated hydrogen liquefaction structure using liquid air cold energy recovery, solid oxide fuel cell and photovoltaic panels. *J. Clean Prod.* **2021**, *320*, 128821.

(86) Kuendig, A.; Loehlein, K.; Kramer, G. J.; Huijsmans, J. Large scale hydrogen liquefaction in combination with LNG re-gasification. *Proceedings of the 16th World Hydrogen Energy Conference*; WHEC, 2006; pp 3326−3333.

(87) Ansarinasab, H.; Mehrpooya, M.; Mohammadi, A. Advanced exergy and exergoeconomic analyses of a hydrogen liquefaction plant equipped with mixed refrigerant system. *J. Clean Prod.* **2017**, *144*, 248−259.

(88) Ansarinasab, H.; Mehrpooya, M.; Sadeghzadeh, M. An exergy-based investigation on hydrogen liquefaction plant-exergy, exergoeconomic, and exergoenvironmental analyses. *J. Clean Prod.* **2019**, *210*, 530−541.

(89) Krasae-In, S.; Stang, J. H.; Neksa, P. Simulation on a proposed large-scale liquid hydrogen plant using a multi-component refrigerant refrigeration system. *Int. J. Hydrogen Energy* **2010**, *35* (22), 12531−12544.

(90) Stang, J.; Neksa, P.; Brendeng, E. On the design of an efficient hydrogen liquefaction process. *Proceedings of the 16th World Hydrogen Energy Conference*; WHEC, 2006.

(91) Krasae-In, S. Optimal operation of a large-scale liquid hydrogen plant utilizing mixed fluid refrigeration system. *Int. J. Hydrogen Energy* **2014**, *39* (13), 7015−7029.

(92) Asadnia, M.; Mehrpooya, M. A novel hydrogen liquefaction process configuration with combined mixed refrigerant systems. *Int. J. Hydrogen Energy* **2017**, *42* (23), 15564−15585.

(93) Cardella, U.; Decker, L.; Sundberg, J.; Klein, H. Process optimization for large-scale hydrogen liquefaction. *Int. J. Hydrogen Energy* **2017**, *42* (17), 12339−12354.

(94) Koc, M.; Tukenmez, N.; Ozturk, M. Development and thermodynamic assessment of a novel solar and biomass energy based integrated plant for liquid hydrogen production. *Int. J. Hydrogen Energy* **2020**, *45* (60), 34587−34607.

(95) Yin, L.; Ju, Y. Process optimization and analysis of a novel hydrogen liquefaction cycle. *Int. J. Refrig.* **2020**, *110*, 219−230.

(96) Jackson, S.; Brodal, E. Optimization of a Mixed Refrigerant Based H2 Liquefaction Pre-Cooling Process and Estimate of Liquefaction Performance with Varying Ambient Temperature. *Energies.* **2021**, *14* (19), 6090.

(97) Yilmaz, C.; Kanoglu, M.; Bolatturk, A.; Gadalla, M. Economics of hydrogen production and liquefaction by geothermal energy. *Int. J. Hydrogen Energy* **2012**, *37* (2), 2058−2069.

(98) Yuksel, Y. E.; Ozturk, M.; Dincer, I. Analysis and performance assessment of a combined geothermal power-based hydrogen production and liquefaction system. *Int. J. Hydrogen Energy* **2018**, *43* (22), 10268−10280.

(99) Yilmaz, C. Optimum energy evaluation and life cycle cost assessment of a hydrogen liquefaction system assisted by geothermal energy. *Int. J. Hydrogen Energy* **2020**, *45* (5), 3558−3568.

(100) Ebrahimi, A.; Ghorbani, B.; Ziabasharhagh, M. Pinch and sensitivity analyses of hydrogen liquefaction process in a hybridized system of biomass gasification plant, and cryogenic air separation cycle. *J. Clean Prod.* **2020**, *258*, 120548.

(101) Ebrahimi, A.; Saharkhiz, M. H. M.; Ghorbani, B. Thermodynamic investigation of a novel hydrogen liquefaction process using thermo-electrochemical water splitting cycle and solar collectors. *Energy Convers Manag.* **2021**, *242*, 114318.

(102) Cardella, U.; Decker, L.; Klein, H. Roadmap to economically viable hydrogen liquefaction. *Int. J. Hydrogen Energy* **2017**, *42* (19), 13329−13338.

(103) Najjar, Y. S.; Mashareh, S. Hydrogen leakage sensing and control. *Biomed. J. Sci. Tech. Res.* **2019**, *21* (5), 16228−16240.

(104) Schlapbach, L.; Züttel, A. Hydrogen-storage materials for mobile applications. *Mater. Sustainable Energy* **2010**, 265−270.

(105) Madadi Avargani, V.; Zendehboudi, S.; Cata Saady, N. M.; Dusseault, M. B. A comprehensive review on hydrogen production and utilization in North America: Prospects and challenges. *Energy Convers. Manage.* **2022**, *269*, 115927.

(106) Hwang, J.-J. Sustainability study of hydrogen pathways for fuel cell vehicle applications. *Renew Sustain Energy Rev.* **2013**, *19*, 220−229.

(107) El-Shafie, M.; Kambara, S.; Hayakawa, Y. Hydrogen production technologies overview. *J. Power Energy Eng.* **2019**, *07*, 107.

(108) Kumar, R.; Kumar, A.; Pal, A. An overview of conventional and non-conventional hydrogen production methods. *Mater. Today Proc.* **2021**, *46*, 5353−5359.

(109) Nikolaidis, P.; Poullikkas, A. A comparative overview of hydrogen production processes. *Renew Sustain Energy Rev.* **2017**, *67*, 597−611.

(110) Chai, S.; Zhang, G.; Li, G.; Zhang, Y. Industrial hydrogen production technology and development status in China: a review. *Clean Technol. Environ. Policy.* **2021**, *23* (7), 1931−1946.

(111) Priyanka, D. Eco-Friendly Energy Resources. *Environment Conservation, Challenges Threats in Conservation of Biodiversity*; Scieng Publications, 2022; Vol. *IV*, pp 87−98.

(112) Mehrpooya, M.; Habibi, R. A review on hydrogen production thermochemical water-splitting cycles. *J. Clean Prod.* **2020**, *275*, 123836.

(113) Safari, F.; Dincer, I. A review and comparative evaluation of thermochemical water splitting cycles for hydrogen production. *Energy Convers Manag.* **2020**, *205*, 112182.

(114) Wang, Z.; Naterer, G.; Gabriel, K.; Gravelsins, R.; Daggupati, V. Comparison of sulfur−iodine and copper−chlorine thermochemical hydrogen production cycles. *Int. J. Hydrogen Energy* **2010**, *35* (10), 4820−4830.

(115) Naterer, G.F.; Suppiah, S.; Stolberg, L.; Lewis, M.; Wang, Z.; Rosen, M.A.; Dincer, I.; Gabriel, K.; Odukoya, A.; Secnik, E.; Easton, E.B.; Papangelakis, V. Progress in thermochemical hydrogen production with the copper−chlorine cycle. *Int. J. Hydrogen Energy* **2015**, *40* (19), 6283−6295.

(116) Ozcan, H.; Dincer, I. Thermodynamic modeling of a nuclear energy based integrated system for hydrogen production and liquefaction. *Comput. Chem. Eng.* **2016**, *90*, 234−246.

(117) Balta, M. T.; Dincer, I.; Hepbasli, A. Performance assessment of solar-driven integrated Mg−Cl cycle for hydrogen production. *Int. J. Hydrogen Energy* **2014**, *39* (35), 20652−20661.

(118) Balta, M. T.; Dincer, I.; Hepbasli, A. Energy and exergy analyses of magnesium-chlorine (Mg-Cl) thermochemical cycle. *Int. J. Hydrogen Energy* **2012**, *37* (6), 4855−4862.

(119) Habibi, R.; Mehrpooya, M.; Pourmoghadam, P. Integrated Mg-Cl hydrogen production process and CaO/CaCO₃-CaCl₂ thermochemical energy storage phase change system using solar tower system. *Energy Convers Manag.* **2021**, *245*, 114555.

(120) Safari, F.; Dincer, I. A study on the Fe−Cl thermochemical water splitting cycle for hydrogen production. *Int. J. Hydrogen Energy* **2020**, *45* (38), 18867−18875.

(121) Razi, F.; Hewage, K.; Sadiq, R. A Comparative Assessment of Thermodynamic and Exergoeconomic Performances of Three Thermochemical Water-Splitting Cycles of Chlorine Family for Hydrogen Production. *Energy Convers Manag.* **2022**, *271*, 116313.

(122) Karaca, A. E.; Qureshy, A. M.; Dincer, I. An overview and critical assessment of thermochemical hydrogen production methods. *J. Clean Prod.* **2023**, *385*, 135706.

(123) Ahangar, N.; Mehrpooya, M. Thermaly integrated five-step ZnSI thermochemical cycle hydrogen production process using solar energy. *Energy Convers Manag.* **2020**, *222*, 113243.

(124) Xu, L.; Li, Y.; Zhang, P.; Chen, S.; Wang, L. Preparation and characterization of bimetallic Ni−Ir/C catalysts for HI decomposition in the thermochemical water-splitting iodine−sulfur process for hydrogen production. *Int. J. Hydrogen Energy* **2019**, *44* (45), 24360−24368.

(125) Ying, Z.; Zhang, Y.; Zheng, X.; Dou, B.; Cui, G. Simulation study on the microscopic characteristics of electrochemical Bunsen reaction in the sulfur−iodine cycle for renewable hydrogen production. *Appl. Therm Eng.* **2019**, *152*, 437−444.

(126) Behzadi, A.; Gholamian, E.; Alirahmi, S. M.; Nourozi, B.; Sadrizadeh, S. A comparative evaluation of alternative optimization strategies for a novel heliostat-driven hydrogen production/injection system coupled with a vanadium chlorine cycle. *Energy Convers Manag.* **2022**, *267*, 115878.

(127) Al-Rashed, A. A.; Alsarraf, J.; Alnaqi, A. A. A comparative investigation of syngas and biofuel power and hydrogen plant combining nanomaterial-supported solid oxide fuel cell with vanadium-chlorine thermochemical cycle. *Fuel.* **2023**, *331*, 125910.

(128) Verhelst, S.; Wallner, T. Hydrogen-fueled internal combustion engines. *Prog. Energy Combust. Sci.* **2009**, *35* (6), 490−527.

(129) Kovač, A.; Paranos, M.; Marciuš, D. Hydrogen in energy transition: A review. *Int. J. Hydrogen Energy* **2021**, *46*, 10016.

(130) Ogden, J. M.; Williams, R. H.; Larson, E. D. Societal lifecycle costs of cars with alternative fuels/engines. *Energy policy.* **2004**, *32* (1), 7−27.

(131) Atilhan, S.; Park, S.; El-Halwagi, M. M.; Atilhan, M.; Moore, M.; Nielsen, R. B. Green hydrogen as an alternative fuel for the shipping industry. *Curr. Opin Chem. Eng.* **2021**, *31*, 100668.

(132) Anderson, P.; Sharkey, J.; Walsh, R. Calculation of the research octane number of motor gasolines from gas chromatographic data and a new approach to motor gasoline quality control. *J. Inst. Pet.* **1972**, *58* (560), 83.

(133) Tashie-Lewis, B. C.; Nnabuife, S. G. Hydrogen production, distribution, storage and power conversion in a hydrogen economy-a technology review. *Chem. Eng. J. Adv.* **2021**, *8*, 100172.

(134) Najjar, Y. S. H. Hydrogen safety: The road toward green technology. *Int. J. Hydrogen Energy* **2013**, *38* (25), 10716−10728.

(135) Dincer, I.; Ishaq, H. Introduction. In *Renewable Hydrogen Production*, Dincer, I., Ishaq, H., Eds.; Elsevier, 2022; Chapter 1, pp 1−33.

(136) Taipabu, M. I.; Viswanathan, K.; Wu, W.; Hattu, N.; Atabani, A. E. A critical review of the hydrogen production from biomass-based feedstocks: Challenge, solution, and future prospect. *Process Saf. Environ. Prot.* **2022**, *164*, 384−407.

(137) Seddon, D. *The Hydrogen Economy: Fundamentals, Technology, Economics*; World Scientific, 2022.

(138) Naterer, G. F.; Dincer, I.; Zamfirescu, C. *Hydrogen production from nuclear energy*; Springer, 2013.

(139) Aziz, M. Liquid hydrogen: A review on liquefaction, storage, transportation, and safety. *Energies.* **2021**, *14* (18), 5917.

(140) Veziroğlu, T. N.; Şahin, S. 21st Century's energy: Hydrogen energy system. *Energy Convers. Manage.* **2008**, *49* (7), 1820−1831.

(141) Balat, M. Potential importance of hydrogen as a future solution to environmental and transportation problems. *Int. J. Hydrogen Energy* **2008**, *33* (15), 4013−4029.

(142) Mazloomi, K.; Gomes, C. Hydrogen as an energy carrier: Prospects and challenges. *Renew Sustain Energy Rev.* **2012**, *16* (5), 3024−3033.

(143) Trevisani, L.; Fabbri, M.; Negrini, F.; Ribani, P. Advanced energy recovery systems from liquid hydrogen. *Energy Convers Manag.* **2007**, *48* (1), 146−154.

(144) Yang, C.; Ogden, J. Determining the lowest-cost hydrogen delivery mode. *Int. J. Hydrogen Energy* **2007**, *32* (2), 268−286.

(145) Al-Hallaj, S.; Wilke, S.; Schweitzer, B. Energy storage systems for smart grid applications. *Water, Energy & Food Sustainability in the Middle East*; Springer, 2017; pp 161−192.

(146) Ghorbani, B.; Ebrahimi, A.; Rooholamini, S.; Ziabasharhagh, M. Integrated Fischer−Tropsch synthesis process with hydrogen liquefaction cycle. *J. Clean Prod.* **2021**, *283*, 124592.

(147) Qyyum, M. A.; Riaz, A.; Naquash, A.; Haider, J.; Qadeer, K.; Nawaz, A.; Lee, H.; Lee, M. 100% saturated liquid hydrogen production: Mixed-refrigerant cascaded process with two-stage ortho-to-para hydrogen conversion. *Energy Convers Manag.* **2021**, *246*, 114659.

(148) Chen, L.; Xiao, R.; Cheng, C.; Tian, G.; Chen, S.; Hou, Y. Thermodynamic analysis of the para-to-ortho hydrogen conversion in cryo-compressed hydrogen vessels for automotive applications. *Int. J. Hydrogen Energy* **2020**, *45* (46), 24928−24937.

(149) Timmerhaus, K. D.; Flynn, T. M. *Cryogenic process engineering*; Springer Science & Business Media, 2013.

(150) Buntkowsky, G.; Walaszek, B.; Adamczyk, A.; Xu, Y.; Limbach, H.-H.; Chaudret, B. Mechanism of nuclear spin initiated para-H2 to ortho-H 2 conversion. *Phys. Chem. Chem. Phys.* **2006**, *8* (16), 1929−1935.

(151) Fukai, Y. *The metal-hydrogen system: basic bulk properties*; Springer Science & Business Media, 2006.

(152) Faramarzi, S.; Nainiyan, S. M. M.; Mafi, M.; Ghasemiasl, R. A novel hydrogen liquefaction process based on LNG cold energy and mixed refrigerant cycle. *Int. J. Refrig.* **2021**, *131*, 263−274.

(153) Baker, C. *Economics of Hydrogen Production and Liquefaction updated to 1980*; Langley Research Center, 1979.

(154) Valenti, G. 2-Hydrogen liquefaction and liquid hydrogen storage. In *Compendium of Hydrogen Energy*; Gupta, R. B., Basile, A., Veziroğlu, T. N., Eds.; Woodhead Publishing, 2016; pp 27−51.

(155) Gursu, S.; Lordgooei, M.; Sherif, S. A.; Veziroğlu, T. N. An optimization study of liquid hydrogen boil-off losses. *Int. J. Hydrogen Energy* **1992**, *17* (3), 227−236.

(156) Weitzel, D. H.; Loebenstein, W.; Draper, J.; Park, O. E. Ortho−para catalysis in liquid-hydrogen production. *J. Res. Natl. Bur. Std* **1958**, *60*, 221−227.

(157) Xu, J.; Lin, W. Research on systems for producing liquid hydrogen and LNG from hydrogen-methane mixtures with hydrogen expansion refrigeration. *Int. J. Hydrogen Energy* **2021**, *46* (57), 29243−29260.

(158) Felderhoff, M.; Weidenthaler, C.; von Helmolt, R.; Eberle, U. Hydrogen storage: the remaining scientific and technological challenges. *Phys. Chem. Chem. Phys.* **2007**, *9* (21), 2643−2653.

(159) Sherif, S.; Zeytinoglu, N.; Veziroğlu, T. Liquid hydrogen: Potential, problems, and a proposed research program. *Int. J. Hydrogen Energy* **1997**, *22* (7), 683−688.

(160) Jensen, J.; Stewart, R. G.; Tuttle, W.; Brechna, H. *Brookhaven national laboratory selected cryogenic data notebook: sections I-IX*; Brookhaven National Laboratory, 1980.

(161) Naquash, A.; Qyyum, M. A.; Min, S.; Lee, S.; Lee, M. Carbon-dioxide-precooled hydrogen liquefaction process: An innovative approach for performance enhancement−Energy, exergy, and economic perspectives. *Energy Convers Manag.* **2022**, *251*, 114947.

(162) Zhuzhgov, A.; Krivoruchko, O.; Isupova, L.; Mart'yanov, O.; Parmon, V. Low-temperature conversion of ortho-hydrogen into liquid para-hydrogen: Process and catalysts. review. *Catal. Ind.* **2018**, *10* (1), 9−19.

(163) Teng, J.; Wang, K.; Zhu, S.; Bao, S.; Zhi, X.; Zhang, X.; Qiu, L. Comparative study on thermodynamic performance of hydrogen liquefaction processes with various ortho-para hydrogen conversion methods. *Energy.* **2023**, *271*, 127016.

(164) Sun, H.; Geng, J.; Wang, C.; Rong, G.; Gao, X.; Xu, J.; Yang, D. Optimization of a hydrogen liquefaction process utilizing mixed refrigeration considering stages of ortho-para hydrogen conversion. *Int. J. Hydrogen Energy* **2022**, *47* (39), 17271−17284.

(165) Quack, H. Conceptual design of a high efficiency large capacity hydrogen liquefier. *AIP Conference Proceedings*; American Institute of Physics, 2002; Vol. *613*, pp 255−263.

(166) Staats, W. L. Analysis of a supercritical hydrogen liquefaction cycle. S.M. Thesis, Massachusetts Institute of Technology, 2008.

(167) Valenti, G.; Macchi, E. Proposal of an innovative, high-efficiency, large-scale hydrogen liquefier. *Int. J. Hydrogen Energy* **2008**, *33* (12), 3116−3121.

(168) Berstad, D. O.; Stang, J. H.; Nekså, P. Large-scale hydrogen liquefier utilising mixed-refrigerant pre-cooling. *Int. J. Hydrogen Energy* **2010**, *35* (10), 4512−4523.

(169) Yuksel, Y. E.; Ozturk, M.; Dincer, I. Analysis and assessment of a novel hydrogen liquefaction process. *Int. J. Hydrogen Energy* **2017**, *42* (16), 11429−11438.

(170) Sadaghiani, M. S.; Mehrpooya, M. Introducing and energy analysis of a novel cryogenic hydrogen liquefaction process configuration. *Int. J. Hydrogen Energy* **2017**, *42* (9), 6033−6050.

(171) Sadaghiani, M. S.; Mehrpooya, M.; Ansarinasab, H. Process development and exergy cost sensitivity analysis of a novel hydrogen liquefaction process. *Int. J. Hydrogen Energy* **2017**, *42* (50), 29797−29819.

(172) Hammad, A.; Dincer, I. Analysis and assessment of an advanced hydrogen liquefaction system. *Int. J. Hydrogen Energy* **2018**, *43* (2), 1139−1151.

(173) Chang, H.-M.; Ryu, K. N.; Baik, J. H. Thermodynamic design of hydrogen liquefaction systems with helium or neon Brayton refrigerator. *Cryogenics.* **2018**, *91*, 68−76.

(174) Nouri, M.; Miansari, M.; Ghorbani, B. Exergy and economic analyses of a novel hybrid structure for simultaneous production of liquid hydrogen and carbon dioxide using photovoltaic and electrolyzer systems. *J. Clean Prod.* **2020**, *259*, 120862.

(175) Ghorbani, B.; Zendehboudi, S.; Moradi, M. Development of an integrated structure of hydrogen and oxygen liquefaction cycle using wind turbines, Kalina power generation cycle, and electrolyzer. *Energy.* **2021**, *221*, 119653.

(176) Bi, Y.; Yin, L.; He, T.; Ju, Y. Optimization and analysis of a novel hydrogen liquefaction process for circulating hydrogen refrigeration. *Int. J. Hydrogen Energy* **2022**, *47* (1), 348−364.

(177) Jouybari, A. K.; Ilinca, A.; Ghorbani, B.; Rooholamini, S. Thermodynamic and exergy evaluation of an innovative hydrogen liquefaction structure based on ejector-compression refrigeration unit, cascade multi-component refrigerant system, and Kalina power plant. *Int. J. Hydrogen Energy* **2022**, *47* (62), 26369−26393.

(178) Zhang, S.; Liu, G. Design and performance analysis of a hydrogen liquefaction process. *Clean Technol. Environ. Policy.* **2022**, *24* (1), 51−65.

(179) Ghorbani, B.; Zendehboudi, S.; Afrouzi, Z. A. Multi-objective optimization of an innovative integrated system for production and storage of hydrogen with net-zero carbon emissions. *Energy Convers Manag.* **2023**, *276*, 116506.

(180) Mukhopadhyay, M. *Fundamentals of cryogenic engineering*; PHI Learning Pvt. Ltd.: New Delhi, India, 2010.

(181) Mafi, M. Development in mixed refrigerant cycles for separation systems of petrochemical industries and thermo-economical optimiza-tion through combined pinch and exergy analysis. Doctoral dissertation, PhD Thesis, Department of Mechanical Engineering, Khajeh Nasir Toosi University of Technology, Tehran, 2009.

(182) Weisend, J. G.; Weisend, J. *Handbook of cryogenic engineering*; Taylor & Francis: Philadelphia, PA, 1998.

(183) How to get down to microkelvin, https://indico.cern.ch/event/602052/contributions/2429708/attachments/1460515/2256925/HighRR_Krantz_2017.pdf (Accessed Jan 2023).

(184) Wilhelmsen, Ø.; Berstad, D.; Aasen, A.; Nekså, P.; Skaugen, G. Reducing the exergy destruction in the cryogenic heat exchangers of hydrogen liquefaction processes. *Int. J. Hydrogen Energy* **2018**, *43* (10), 5033−5047.

(185) Walnum, H. T.; Berstad, D.; Drescher, M.; Neksa, P.; Quack, H.; Haberstroh, C.; Essler, J. Principles for the liquefaction of hydrogen with emphasis on precooling processes. *Refrig. Sci. Technol.* **2012**, *2012*, 273−280.

(186) Maytal, B.-Z.; Pfotenhauer, J. M. *Miniature Joule-Thomson cryocooling: principles and practice*; Springer Science & Business Media, 2012.

(187) Chang, H.-M.; Park, M. G. Cascade JT systems with single-component refrigerants for hydrogen liquefaction. *Cryogenics.* **2022**, *121*, 103410.

(188) Brookhaven National Laboratory selected cryogenic data notebook. *Brookhaven National Laboratory Report BNL 10200-R*; Brookhaven National Laboratory, 1980; Vol. *I*.

(189) Nandi, T.; Sarangi, S. Performance and optimization of hydrogen liquefaction cycles. *Int. J. Hydrogen Energy* **1993**, *18* (2), 131−139.

(190) Peschka, W. *Liquid hydrogen: fuel of the future*; Springer Science & Business Media, 2012.

(191) Sham, R.; Jindal, T.; Pabla, B. Cryogenic processes- a review. *Int. J. Eng. Sci. Technol.* **2011**, *3* (1), 601−609.

(192) Ohlig, K.; Decker, L. The latest developments and outlook for hydrogen liquefaction technology. *AIP Conference Proceedings*; American Institute of Physics, 2014; Vol. *1573*, pp 1311−1317.

(193) Mukhopadhyay, M. *Fundamentals of cryogenic engineering*; PHI Learning Pvt. Ltd., 2010.

(194) Notardonato, W. U. Analysis and testing of an integrated refrigeration and storage system for liquid hydrogen zero boil-off, liquefaction, and densification. Ph.D. Dissertation, University of Florida, 2006.

(195) Belyakov, V.; Krakovskii, B.; Popov, O.; Step, G. K.; Udut, V. Low-capacity hydrogen liquefier with a helium cycle. *Chem. Pet. Eng.* **2002**, *38* (3), 150−153.

(196) Quack, H.; Essler, J.; Haberstroh, C.; Walnum, H.; Berstad, D.; Drescher, M.; Neksaa, P. Search for the best processes to liquefy hydrogen in very large plants. *12th cryogenic-IIR Conference*, Dresden, Germany; International Institute of Refrigeration, 2012.

(197) Smith, R. *Chemical process: design and integration*; John Wiley & Sons, 2005.

(198) Lee, G.-C. Optimal Design and Anaaylsis of Refrigeration Systems For Low Temperature Processes. Thesis Dissertation, The University of Manchester, 2001.

(199) Mafi, M.; Ghorbani, B.; Amidpour, M. Mousavi Naynian, S. M. Design of mixed refrigerant cycle for low temperature processes using thermodynamic approach. *Sci. Iran.* **2013**, *20* (4), 1254−1268.

(200) Podbielniak, W. J. Art of refrigeration. U.S. Patent 2041725, 1936 (Accessed Jan 2023).

(201) Kleemenko, A. P. One flow cascade cycle. *Proceedings of the 10th International Congress of Refrigeration*, 1959; Vol. *1*, pp 34−39.

(202) Gaumer, L. S., Jr.; Newton, C. L. Process for liquefying natural gas employing a multicomponent refrigerant for obtaining low temperature cooling. Google Patents: 1972.

(203) Krasae-In, S.; Stang, J. H.; Neksa, P. Exergy analysis on the simulation of a small-scale hydrogen liquefaction test rig with a multi-component refrigerant refrigeration system. *Int. J. Hydrogen Energy* **2010**, *35* (15), 8030−8042.

(204) Krasae-In, S.; Bredesen, A. M.; Stang, J. H.; Neksa, P. Simulation and experiment of a hydrogen liquefaction test rig using a multi-component refrigerant refrigeration system. *Int. J. Hydrogen Energy* **2011**, *36* (1), 907−919.

(205) Krasae-in, S. Efficient hydrogen liquefaction processes. Doctoral Thesis, NTNU, 2013.

(206) *State of the Art Hydrogen Liquefaction, DOE Workshop 2022, Air Liquide Engineering & Construction*, https://www.energy.gov/sites/default/files/2022-03/Liquid%20H2%20Workshop-Air%20Liquide.pdf (Accessed May 2022).

(207) Gross, R.; Otto, W.; Patzelt, A.; Wanner, M. Liquid hydrogen for europe-the linde plant at ingolstadt. fluessigwasserstoff fuer europa-die linde-anlage in ingolstadt. *Linde Ber. Tech. Wiss.* **1994**, *71*.3642

(208) Quack, H. The key role of the cryotechnology in the hydrogen energy industry (Die Schluesselrolle der Kryotechnik in der Wasserst-off-Energiewirtschaft). Wissenschaftliche Zeitschrift der Technischen Universität Dresden, 2001.

(209) Weindorf, W.; Bünger, U.; Schindler, J. Comments on the paper by Baldur Eliasson and Ulf Bossel "The future of the hydrogen economy: bright or bleak?". *LB-Systemtechnik GmbH, Ottobrunn* **2003**.

(210) Matsuda, H.; Nagami, M. *Study of large hydrogen liquefaction process*; Nippon Sanso Corp.: Kawasaki City, 1997.

(211) Shimko, M.; Gardiner, M.; Bakke, P. Innovative hydrogen liquefaction cycle. *FY 2008 Annual Progress Report, DOE Hydrogen Program*, 2008.

(212) Naquash, A.; Haider, J.; Qyyum, M. A.; Islam, M.; Min, S.; Lee, S.; Lim, H.; Lee, M. Hydrogen enrichment by CO_2 anti-sublimation integrated with triple mixed refrigerant-based liquid hydrogen production process. *J. Clean Prod.* **2022**, *341*, 130745.

(213) Lee, H.; Haider, J.; Abdul Qyyum, M.; Choe, C.; Lim, H. An innovative high energy efficiency−based process enhancement of hydrogen liquefaction: Energy, exergy, and economic perspectives. *Fuel* **2022**, *320*, 123964.

(214) Kim, H.; Haider, J.; Qyyum, M. A.; Lim, H. Mixed refrigerant−based simplified hydrogen liquefaction process: Energy, exergy, economic, and environmental analysis. *J. Clean Prod.* **2022**, *367*, 132947.

(215) Geng, J.; Sun, H. Optimization and analysis of a hydrogen liquefaction process: Energy, exergy, economic, and uncertainty quantification analysis. *Energy.* **2023**, *262*, 125410.

(216) Andersson, J.; Grönkvist, S. Large-scale storage of hydrogen. *Int. J. Hydrogen Energy* **2019**, *44* (23), 11901−11919.

(217) Cho, S.; Park, J.; Noh, W.; Lee, I.; Moon, I. Developed hydrogen liquefaction process using liquefied natural gas cold energy: Design, energy optimization, and techno-economic feasibility. *Int. J. Energy Res.* **2021**, *45* (10), 14745−14760.

(218) He, T.; Lv, H.; Shao, Z.; Zhang, J.; Xing, X.; Ma, H. Cascade utilization of LNG cold energy by integrating cryogenic energy storage, organic Rankine cycle and direct cooling. *Appl. Energy.* **2020**, *277*, 115570.

(219) Kanbur, B. B.; Xiang, L.; Dubey, S.; Choo, F. H.; Duan, F. Finite sum based thermoeconomic and sustainable analyses of the small scale LNG cold utilized power generation systems. *Appl. Energy.* **2018**, *220*, 944−961.

(220) He, T.; Chong, Z. R.; Zheng, J.; Ju, Y.; Linga, P. LNG cold energy utilization: Prospects and challenges. *Energy.* **2019**, *170*, 557−568.

(221) Qi, M.; Park, J.; Kim, J.; Lee, I.; Moon, I. Advanced integration of LNG regasification power plant with liquid air energy storage: Enhancements in flexibility, safety, and power generation. *Appl. Energy.* **2020**, *269*, 115049.

(222) Allam, R. J.; James, P. S. Process and Apparatus for Liquefying Hydrogen. U.S. Patent US007559213B2, 2009.

(223) Noh, W.; Park, S.; Kim, J.; Lee, I. Comparative design, thermodynamic and techno-economic analysis of utilizing liquefied natural gas cold energy for hydrogen liquefaction processes. *Int. J. Energy Res.* **2022**, *46* (9), 12926−12947.

(224) Ghorbani, B.; Zendehboudi, S.; Khatami Jouybari, A. Thermo-economic optimization of a hydrogen storage structure using liquid natural gas regasification and molten carbonate fuel cell. *J. Energy Storage* **2022**, *52*, 104722.

(225) Yun, S.-K. Design and analysis for hydrogen liquefaction process using LNG cold energy. *J. Kor. Inst. Gas.* **2011**, *15* (3), 1−5.

(226) Zarsazi, H.; Sadeghi, S.; Moghimi, M. Investigation of a novel hybrid LNG waste heat-/wind-driven hydrogen liquefaction system: exergoeconomic analysis and multi-criteria optimization. *J. Therm. Anal. Calorim.* **2022**, 1−17.

(227) The future of hydrogen. *International Energy Agency report*; IEA, 2019.

(228) Carapellucci, R.; Giordano, L. Steam, dry and autothermal methane reforming for hydrogen production: A thermodynamic equilibrium analysis. *J. Power Sources.* **2020**, *469*, 228391.

(229) Bian, J.; Yang, J.; Li, Y.; Chen, Z.; Liang, F.; Cao, X. Thermodynamic and economic analysis of a novel hydrogen liquefaction process with LNG precooling and dual-pressure Brayton cycle. *Energy Convers Manag.* **2021**, *250*, 114904.

(230) Faramarzi, S.; Nainiyan, S. M. M.; Mafi, M.; Ghasemiasl, R. Energy, exergy, and economic analyses of an innovative hydrogen liquefaction process utilising liquefied natural gas regasification system. *Int. J. Exergy.* **2022**, *38* (4), 442−456.

(231) Yang, J.; Li, Y.; Tan, H.; Bian, J.; Cao, X. Optimization and analysis of a hydrogen liquefaction process integrated with the liquefied natural gas gasification and organic Rankine cycle. *J. Energy Storage.* **2023**, *59*, 106490.

(232) Wang, R.; Oliveira, R. Adsorption refrigeration—an efficient way to make good use of waste heat and solar energy. *Prog. Energy Combust. Sci.* **2006**, *32* (4), 424−458.

(233) Yan, X.; Chen, G.; Hong, D.; Lin, S.; Tang, L. A novel absorption refrigeration cycle for heat sources with large temperature change. *Appl. Therm Eng.* **2013**, *52* (1), 179−186.

(234) Han, W.; Sun, L.; Zheng, D.; Jin, H.; Ma, S.; Jing, X. New hybrid absorption—compression refrigeration system based on cascade use of mid-temperature waste heat. *Appl. Energy.* **2013**, *106*, 383−390.

(235) Srikhirin, P.; Aphornratana, S.; Chungpaibulpatana, S. A review of absorption refrigeration technologies. *Renew Sustain Energy Rev.* **2001**, *5* (4), 343−372.

(236) Arshi Banu, P.S.; Sudharsan, N.M. Review of water based vapour absorption cooling systems using thermodynamic analysis. *Renewable Sustainable Energy Rev.* **2018**, *82*, 3750−3761.

(237) Ghaebi, H.; Karimkashi, S.; Saidi, M. Integration of an absorption chiller in a total CHP site for utilizing its cooling production potential based on R-curve concept. *Int. J. Refrig.* **2012**, *35* (5), 1384−1392.

(238) Aneke, M.; Agnew, B.; Underwood, C.; Menkiti, M. Thermodynamic analysis of alternative refrigeration cycles driven from waste heat in a food processing application. *Int. J. Refrig.* **2012**, *35* (5), 1349−1358.

(239) Taboas, F.; Bourouis, M.; Vallès, M. Analysis of ammonia/water and ammonia/salt mixture absorption cycles for refrigeration purposes in fishing ships. *Appl. Therm Eng.* **2014**, *66* (1−2), 603−611.

(240) Bruno, J.; Vidal, A.; Coronas, A. Improvement of the raw gas drying process in olefin plants using an absorption cooling system driven by quench oil waste heat. *Energy Convers Manag.* **2006**, *47* (1), 97−113.

(241) Brant, B.; Brueske, S.; Erickson, D.; Papar, R. New waste-heat refrigeration unit cuts flaring, reduces pollution. *Oil Gas J.* **1998**, *96* (20).

(242) Rodgers, P.; Mortazavi, A.; Eveloy, V.; Al-Hashimi, S.; Hwang, Y.; Radermacher, R. Enhancement of LNG plant propane cycle through waste heat powered absorption cooling. *Appl. Therm Eng.* **2012**, *48*, 41−53.

(243) Ghorbani, B.; Hamedi, M.-H.; Amidpour, M.; Shirmohammadi, R. Implementing absorption refrigeration cycle in lieu of DMR and C3MR cycles in the integrated NGL, LNG and NRU unit. *Int. J. Refrig.* **2017**, *77*, 20−38.

(244) Ghorbani, B.; Shirmohammadi, R.; Mehrpooya, M. A novel energy efficient LNG/NGL recovery process using absorption and mixed refrigerant refrigeration cycles—Economic and exergy analyses. *Appl. Therm. Eng.* **2018**, *132*, 283−295.

(245) Zaitsev, A.; Mehrpooya, M.; Ghorbani, B.; Sanavbarov, R.; Naumov, F.; Shermatova, F. Novel integrated helium extraction and natural gas liquefaction process configurations using absorption refrigeration and waste heat. *Int. J. Energy Res.* **2020**, *44* (8), 6430−6451.

(246) Mehrpooya, M.; Mousavi, S. A.; Asadnia, M.; Zaitsev, A.; Sanavbarov, R. Conceptual design and evaluation of an innovative hydrogen purification process applying diffusion-absorption refrigeration cycle (Exergoeconomic and exergy analyses). *J. Clean Prod.* **2021**, *316*, 128271.

(247) Mousavi, S. A.; Mehrpooya, M.; Delpisheh, M. Development and life cycle assessment of a novel solar-based cogeneration configuration comprised of diffusion-absorption refrigeration and organic Rankine cycle in remote areas. *Process Saf. Environ. Prot.* **2022**, *159*, 1019−1038.

(248) Mehrpooya, M.; Amirhaeri, Y.; Hadavi, H. Proposal and investigation of a novel small-scale natural gas liquefaction process using diffusion absorption refrigeration technology. *Chem. Pap.* **2022**, *76* (9), 5901−5927.

(249) Mehrpooya, M.; Mousavi, S. A.; Delpisheh, M.; Zaitsev, A.; Nikitin, A. 4E assessment and 3D parametric analysis of an innovative liquefied natural gas production process assisted by a diffusion−absorption refrigeration unit. *Chem. Pap.* **2022**, *76* (75), 1−22.

(250) Mousavi, S. A.; Mehrpooya, M. A comprehensive exergy-based evaluation on cascade absorption-compression refrigeration system for low temperature applications-exergy, exergoeconomic, and exergoenvironmental assessments. *J. Clean Prod.* **2020**, *246*, 119005.

(251) Ghorbani, B.; Ebrahimi, A.; Skandarzadeh, F.; Ziabasharhagh, M. Energy, exergy and pinch analyses of an integrated cryogenic natural gas process based on coupling of absorption−compression refrigeration system, organic Rankine cycle and solar parabolic trough collectors. *J. Therm Anal Calorim.* **2021**, *145* (3), 925−953.

(252) Ghorbani, B.; Rahnavard, Z.; Ahmadi, M. H.; Jouybari, A. K. An innovative hybrid structure of solar PV-driven air separation unit, molten carbonate fuel cell, and absorption−compression refrigeration system (Process development and exergy analysis). *Energy Rep.* **2021**, *7*, 8960−8972.

(253) Ebrahimi, A.; Ghorbani, B.; Ziabasharhagh, M. Exergy and economic analyses of an innovative integrated system for cogeneration of treated biogas and liquid carbon dioxide using absorption−compression refrigeration system and ORC/Kalina power cycles through geothermal energy. *Process Saf. Environ. Prot.* **2022**, *158*, 257−281.

(254) Ziegler, F.; Kahn, R.; Summerer, F.; Alefeld, G. Multi-effect absorption chillers. *Int. J. Refrig.* **1993**, *16* (5), 301−311.

(255) Langreck, J.; Bassols, J.; Kuckelkorn, B.; Schneider, R.; Veelken, H. Reliability of ammonia absorption refrigeration plants in the chemical and food industry, https://colibris.home.xs4all.nl/pdf_documents/english_docu/reliability_of_ammonia_absorption.pdf (Accessed Sep 2022).

(256) Mehrpooya, M.; Omidi, M.; Vatani, A. Novel mixed fluid cascade natural gas liquefaction process configuration using absorption refrigeration system. *Appl. Therm Eng.* **2016**, *98*, 591−604.

(257) Ansarinasab, H.; Mehrpooya, M. Advanced exergoeconomic analysis of a novel process for production of LNG by using a single effect absorption refrigeration cycle. *Appl. Therm Eng.* **2017**, *114*, 719−732.

(258) Mehrpooya, M.; Ghorbani, B.; Hosseini, S. S. Thermodynamic and economic evaluation of a novel concentrated solar power system integrated with absorption refrigeration and desalination cycles. *Energy Convers Manag.* **2018**, *175*, 337−356.

(259) Afrouzy, Z. A.; Taghavi, M. Thermo-economic analysis of a novel integrated structure for liquefied natural gas production using photovoltaic panels. *J. Therm Anal Calorim.* **2021**, *145* (3), 1509−1536.

(260) Kanoglu, M.; Dincer, I.; Rosen, M. A. Geothermal energy use in hydrogen liquefaction. *Int. J. Hydrogen Energy* **2007**, *32* (17), 4250−4257.

(261) Cao, Y.; Dhahad, H. A.; Togun, H.; Aly, A. A.; Felemban, B. F.; El-Shafay, A.; Rashidi, S.; Farhang, B. Application, comparative study, and multi-objective optimization of a hydrogen liquefaction system utilizing either ORC or an absorption power cycle. *Int. J. Hydrogen Energy* **2022**, *47* (62), 26408−26421.

(262) Ratlamwala, T. A. H.; Dincer, I.; Gadalla, M.; Kanoglu, M. Thermodynamic analysis of a new renewable energy based hybrid system for hydrogen liquefaction. *Int. J. Hydrogen Energy* **2012**, *37* (23), 18108−18117.

(263) Ratlamwala, T. A. H.; Dincer, I.; Gadalla, M. Thermodynamic analysis of a novel integrated geothermal based power generation-quadruple effect absorption cooling-hydrogen liquefaction system. *Int. J. Hydrogen Energy* **2012**, *37* (7), 5840−5849.

(264) Jouybari, A. K.; Ilinca, A.; Ghorbani, B.; Rooholamini, S. Thermodynamic and exergy evaluation of an innovative hydrogen liquefaction structure based on ejector-compression refrigeration unit, cascade multi-component refrigerant system, and Kalina power plant. *Int. J. Hydrogen Energy* **2022**, *47*, 26369.

(265) Rezaie Azizabadi, H.; Ziabasharhagh, M.; Mafi, M. Introducing a proper hydrogen liquefaction concept for using wasted heat of thermal

power plants-case study: Parand gas power plant. *Chin J. Chem. Eng.* **2021**, *40*, 187−196.

(266) Zhang, S.; Li, K.; Liu, G. An efficient hydrogen liquefaction process integrated with a solar power tower and absorption precooling system. *Clean Technol. Environ. Policy* **2022**, *25* (3), 1−27.

(267) Rehman, A.; Qyyum, M. A.; Qadeer, K.; Zakir, F.; Ding, Y.; Lee, M.; Wang, L. Integrated biomethane liquefaction using exergy from the discharging end of a liquid air energy storage system. *Appl. Energy.* **2020**, *260*, 114260.

(268) Ghorbani, B.; Sadeghzadeh, M.; Ahmadi, M. H.; Sharifpur, M. Exergy assessment and energy integration of a novel solar-driven liquid carbon dioxide and liquefied natural gas cogeneration system using liquid air cold energy recovery. *J. Therm. Anal. Calorim.* **2022**, *148* (3), 1−22.

(269) Riaz, A.; Qyyum, M. A.; Kim, G.; Lee, M. Harnessing Liquid Air Cold Energy for Performance Enhancement of Hydrogen Liquefaction Process. *International Conference on Applied Energy*, 2021, https://www.energy-proceedings.org/wp-content/uploads/2022/03/Proceedings-ICAE2021_277.pdf (Accessed Sep 2022).

(270) Mafi, M.; Ghorbani, B.; Salehi, G. R.; Amidpour, M.; MOUSAVI, N. S. The mathematical method and thermodynamic approaches to design Multi-Component refrigeration used in cryogenic process part II: Optimal arrangement. *Gas Process. J.* **2014**, *1* (2), 13−21.

(271) Ghorbani, B.; Mafi, M.; Amidpour, M.; MOUSAVI, N. S.; Salehi, G. R. Mathematical method and thermodynamic approaches to design multi-component refrigeration used in cryogenic process Part I: optimal operating conditions. *Gas Process. J.* **2014**, *2* (1), 1−9.

(272) Podbielniak, W.J. Art of refrigeration. U.S. Patent 2041725, 1986.

(273) Barber, N.; Haselden, G. The liquefaction of naturally occuring methane. *Trans. Inst. Chem. Eng.* **1957**, *35*, 77−86.

(274) Bensafi, A.; Haselden, G. Wide-boiling refrigerant mixtures for energy saving. *Int. J. Refrig.* **1994**, *17* (7), 469−474.

(275) Perret, J. C. Method and apparatus for the cooling and low temperature liquefaction of gaseous mixtures. US Patent 3364685, 1968.

(276) Gaumer, L. S., Jr.; Newton, C. L. Liquefaction of natural gas employing multiple-component refrigerants. U.S. Patent US3593535A, 1971.

(277) Steed, J. Present uses of chlorofluorocarbons and effects due to environmental regulations. *Int. J. Thermophys.* **1989**, *10*, 545−552.

(278) Lamb, R.; Foumeny, E.; Haselden, G. The use of wide boiling refrigerant mixtures in water chiller units for power saving. *ICHEME Research Event* **1996**, 223−225.

(279) Duvedi, A.; Achenie, L. E. On the design of environmentally benign refrigerant mixtures: a mathematical programming approach. *Comput. Chem. Eng.* **1997**, *21* (8), 915−923.

(280) Gong, M.; Wu, J.; Luo, E. Performances of the mixed-gases Joule−Thomson refrigeration cycles for cooling fixed-temperature heat loads. *Cryogenics.* **2004**, *44* (12), 847−857.

(281) Maytal, B.-Z.; Nellis, G.; Klein, S.; Pfotenhauer, J. Elevated-pressure mixed-coolants Joule−Thomson cryocooling. *Cryogenics.* **2006**, *46* (1), 55−67.

(282) Ghorbani, B.; Mafi, M.; Shirmohammadi, R.; Hamedi, M.-H.; Amidpour, M. Optimization of operation parameters of refrigeration cycle using particle swarm and NLP techniques. *J. Nat. Gas Sci. Eng.* **2014**, *21*, 779−790.

(283) Mafi, M.; Amidpour, M.; Mousavi Naeynian, S. Comparison of low temperature mixed refrigerant cycles for separation systems. *Int. J. Energy Res.* **2009**, *33* (4), 358−377.

(284) Amidpour, M.; Hamedi, M.; Mafi, M.; Ghorbani, B.; Shirmohammadi, R.; Salimi, M. Sensitivity analysis, economic optimization, and configuration design of mixed refrigerant cycles by NLP techniques. *J. Nat. Gas Sci. Eng.* **2015**, *24*, 144−155.

(285) Faramarzi, S.; Nainiyan, S. M. M.; Mafi, M.; Ghasemiasl, R. Genetic algorithm optimization of two natural gas liquefaction methods based on energy, exergy, and economy analyses: the case study of

Shahid Rajaee power plant peak-shaving system. *Gas Process. J.* **2021**, *9* (1), 91−108.

(286) Ghorbani, B.; Shirmohammadi, R.; Mehrpooya, M.; Hamedi, M.-H. Structural, operational and economic optimization of cryogenic natural gas plant using NSGAII two-objective genetic algorithm. *Energy.* **2018**, *159*, 410−428.

(287) Zhu, J.; Wang, G.; Li, Y.; Duo, Z.; Sun, C. Optimization of hydrogen liquefaction process based on parallel genetic algorithm. *Int. J. Hydrogen Energy* **2022**, *47* (63), 27038−27048.

(288) Naquash, A.; Riaz, A.; Qyyum, M. A.; Kim, G.; Lee, M. Process knowledge inspired opportunistic approach for thermodynamically feasible and efficient design of hydrogen liquefaction process. *Int. J. Hydrogen Energy* **2022**. DOI: 10.1016/j.ijhydene.2022.11.163

(289) Cardella, U.; Decker, L.; Klein, H. Economically viable large-scale hydrogen liquefaction. *IOP Conference Series: Materials Science and Engineering*; IOP Publishing, 2017; Vol. *171*, p 012013.

(290) Seyam, S.; Dincer, I.; Agelin-Chaab, M. Analysis of a clean hydrogen liquefaction plant integrated with a geothermal system. *J. Clean Prod.* **2020**, *243*, 118562.

(291) Son, H.; Yu, T.; Hwang, J.; Lim, Y. Simulation methodology for hydrogen liquefaction process design considering hydrogen characteristics. *Int. J. Hydrogen Energy.* **2022**, *47* (61), 25662−25678.

(292) Park, S.; Noh, W.; Park, J.; Park, J.; Lee, I. Efficient Heat Exchange Configuration for Sub-Cooling Cycle of Hydrogen Liquefaction Process. *Energies.* **2022**, *15* (13), 4560.

(293) Bi, Y.; Ju, Y. Conceptual design and optimization of a novel hydrogen liquefaction process based on helium expansion cycle integrating with mixed refrigerant pre-cooling. *Int. J. Hydrogen Energy.* **2022**, *47* (38), 16949−16963.

(294) Naquash, A.; Riaz, A.; Lee, H.; Qyyum, M. A.; Lee, S.; Lam, S. S.; Lee, M. Hydrofluoroolefin-based mixed refrigerant for enhanced performance of hydrogen liquefaction process. *Int. J. Hydrogen Energy* **2022**, *47*, 41648.

(295) Lin, H.; Wu, X.; Ayed, H.; Mouldi, A.; Abbas, S. Z.; Ebrahimi-Moghadam, A. A new biomass gasification driven hybrid system for power and liquid hydrogen cogeneration: Parametric study and multi-objective evolutionary optimization. *Int. J. Hydrogen Energy.* **2022**, *47* (62), 26394−26407.

(296) Li, K.; Zhang, S.; Liu, G. Model for analyzing the energy efficiency of hydrogen liquefaction process considering the variation of hydrogen liquefaction ratio and precooling temperature. *Int. J. Hydrogen Energy* **2022**, *47*, 24194.

(297) Ghorbani, B.; Zendehboudi, S.; Khatami Jouybari, A. Thermo-economic optimization of a hydrogen storage structure using liquid natural gas regasification and molten carbonate fuel cell. *J. Energy Storage.* **2022**, *52*, 104722.

(298) Mehrenjani, J. R.; Gharehghani, A.; Sangesaraki, A. G. Machine learning optimization of a novel geothermal driven system with LNG heat sink for hydrogen production and liquefaction. *Energy Convers Manag.* **2022**, *254*, 115266.

(299) Min, S.; Riaz, A.; Qyyum, M. A.; Choe, H.; Moon, S.-g.; Lee, M. Application of machine learning model to optimization of the hydrogen liquefaction process. *Comput.-Aided Chem. Eng.* **2022**, *49*, 961−966.

(300) Meng, Y.; Wu, H.; Zheng, Y.; Wang, K.; Duan, Y. Comparative analysis and multi-objective optimization of hydrogen liquefaction process using either organic Rankine or absorption power cycles driven by dual-source biomass fuel and geothermal energy. *Energy.* **2022**, *253*, 124078.

(301) Liu, X.; Hu, G.; Zeng, Z. Performance characterization and multi-objective optimization of integrating a biomass-fueled brayton cycle, a kalina cycle, and an organic rankine cycle with a claude hydrogen liquefaction cycle. *Energy.* **2023**, *263*, 125535.

(302) Akbarnia, M.; Amidpour, M.; Shadaram, A. A new approach in pinch technology considering piping costs in total cost targeting for heat exchanger network. *Chem. Eng. Res. Des.* **2009**, *87* (3), 357−365.

(303) Ebrahimi, A.; Ziabasharhagh, M. Optimal design and integration of a cryogenic Air Separation Unit (ASU) with Liquefied Natural Gas (LNG) as heat sink, thermodynamic and economic analyses. *Energy.* **2017**, *126*, 868−885.

(304) Tjoe, T. N.; Linnhoff, B. Using pinch technology for process retrofit. *Chem. Eng.* **1986**, *93* (8), 47−60.

(305) Safari, D.; Kasiri, N.; Khalili-Garakani, A.; Mafi, M. Economic Analysis of Separation Unit of Methanol to Propylene Production Based on Optimization of Refrigeration Cycles Using Pinch and Exergy Analysis: Analyse économique de l'unité de séparation de la production de méthanol en propylène basée sur l'optimization des cycles de réfrigération à l'aide de l'analyse Pinch et Exergy. *Int. J. Refrig.* **2023**, *146*, 108−117.

(306) Rezaie Azizabadi, H.; Ziabasharhagh, M.; Mafi, M. Applicability of the common equations of state for modeling hydrogen liquefaction processes in Aspen HYSYS. *Gas Process. J.* **2021**, *9* (1), 11−28.

(307) Mafi, M.; Naeynian, S. M.; Amidpour, M. Exergy analysis of multistage cascade low temperature refrigeration systems used in olefin plants. *Int. J. Refrig.* **2009**, *32* (2), 279−294.

(308) Feng, X.; Zhu, X. Combining pinch and exergy analysis for process modifications. *Appl. Therm Eng.* **1997**, *17* (3), 249−261.

(309) Staine, F.; Favrat, D. Energy integration of industrial processes based on the pinch analysis method extended to include exergy factors. *Appl. Therm Eng.* **1996**, *16* (6), 497−507.

(310) Bütün, H.; Kantor, I.; Maréchal, F. A heat integration method with multiple heat exchange interfaces. *Energy.* **2018**, *152*, 476−488.

(311) Smith, R.; Lee, G.-C.; Zhu, X. Refrigeration System Design by Combined Pinch and Exergy Analysis. *AIChE Spring Meeting*; AIChE, 2000.

(312) Kwon, H.; Do, T. N.; Kim, J. Energy-efficient liquid hydrogen production using cold energy in liquefied natural gas: Process intensification and techno-economic analysis. *J. Clean Prod.* **2022**, *380*, 135034.

(313) Mehrpooya, M.; Saedi, M.; Allahyarzadeh, A.; Mousavi, S. A.; Jarrahian, A. Conceptual design and performance evaluation of a novel cryogenic integrated process for extraction of neon and production of liquid hydrogen. *Process Saf. Environ. Prot.* **2022**, *164*, 228−246.

(314) Pakzad, P.; Mehrpooya, M.; Zaitsev, A. Thermodynamic assessments of a novel integrated process for producing liquid helium and hydrogen simultaneously. *Int. J. Hydrogen Energy.* **2021**, *46* (76), 37939−37964.

(315) Karimi, M.; Mehrpooya, M.; pourfayaz, F. Proposal and investigation of a novel hybrid hydrogen production and liquefaction process using solid oxide electrolyzer, solar energy, and thermoelectric generator. *J. Clean Prod.* **2022**, *331*, 130001.

(316) Safdari Shadloo, M.; Xu, H.; Mahian, O.; Maheri, A. Fundamental and engineering thermal aspects of energy and environment. *J. Therm Anal Calorim.* **2020**, *139* (4), 2395−2398.

(317) Barhoumi, E.; Okonkwo, P.; Zghaibeh, M.; Belgacem, I. B.; Alkanhal, T. A.; Abo-Khalil, A.; Tlili, I. Renewable energy resources and workforce case study Saudi Arabia: review and recommendations. *J. Therm Anal Calorim.* **2020**, *141* (1), 221−230.

(318) Safari, F.; Dincer, I. Assessment and optimization of an integrated wind power system for hydrogen and methane production. *Energy Convers Manag.* **2018**, *177*, 693−703.

(319) Sadeghi, S.; Ghandehariun, S.; Rezaie, B.; Javani, N. An innovative s olar-powered natural g as-based compressed air energy storage system integrated with a liquefied air power cycle. *Int. J. Energy Res.* **2021**, *45* (11), 16294−16309.

(320) Mahlia, T.; Saktisahdan, T.; Jannifar, A.; Hasan, M.; Matseelar, H. A review of available methods and development on energy storage; technology update. *Renew Sustain Energy Rev.* **2014**, *33*, 532−545.

(321) Namar, M. M.; Jahanian, O. Energy and exergy analysis of a hydrogen-fueled HCCI engine. *J. Therm Anal Calorim.* **2019**, *137* (1), 205−215.

(322) Ghorbani, B.; Mehrpooya, M.; Amidpour, M. A novel integrated structure of hydrogen purification and liquefaction using natural gas steam reforming, organic Rankine cycle and photovoltaic panels. *Cryogenics.* **2021**, *119*, 103352.

(323) Khodaparast, S. H.; Zare, V.; Mohammadkhani, F. Geothermal assisted hydrogen liquefaction systems integrated with liquid nitrogen precooling; thermoeconomic comparison of Claude and reverse

Brayton cycle for liquid nitrogen supply. *Process Saf. Environ. Prot.* **2023**, *171*, 28−37.

(324) Corumlu, V.; Ozsoy, A.; Ozturk, M. Thermodynamic studies of a novel heat pipe evacuated tube solar collectors based integrated process for hydrogen production. *Int. J. Hydrogen Energy.* **2018**, *43* (2), 1060−1070.

(325) Yilmaz, F.; Ozturk, M.; Selbas, R. Thermodynamic performance assessment of ocean thermal energy conversion based hydrogen production and liquefaction process. *Int. J. Hydrogen Energy.* **2018**, *43* (23), 10626−10636.

(326) Yuksel, Y. E.; Ozturk, M.; Dincer, I. Energetic and exergetic assessments of a novel solar power tower based multigeneration system with hydrogen production and liquefaction. *Int. J. Hydrogen Energy.* **2019**, *44* (26), 13071−13084.

(327) Seyam, S.; Dincer, I.; Agelin-Chaab, M. Development of a clean power plant integrated with a solar farm for a sustainable community. *Energy Convers Manag.* **2020**, *225*, 113434.

(328) Ahmadi Boyaghchi, F.; Sohbatloo, A. Exergetic, exergoeconomic, and exergoenvironmental assessments and optimization of a novel solar cascade organic Rankine cycle-assisted hydrogen liquefaction. *Sci. Iran.* **2021**, *28* (1), 273−290.

(329) Tukenmez, N.; Yilmaz, F.; Ozturk, M. Thermodynamic performance assessment of a geothermal energy assisted combined system for liquid hydrogen generation. *Int. J. Hydrogen Energy.* **2021**, *46* (57), 28995−29011.

(330) Muradov, N. Z.; Veziroğlu, T. N. Green" path from fossil-based to hydrogen economy: an overview of carbon-neutral technologies. *Int. J. Hydrogen Energy.* **2008**, *33* (23), 6804−6839.

(331) Midilli, A.; Ay, M.; Dincer, I.; Rosen, M. A. On hydrogen and hydrogen energy strategies: I: current status and needs. *Renew Sustain Energy Rev.* **2005**, *9* (3), 255−271.

(332) Jain, I. Hydrogen the fuel for 21st century. *Int. J. Hydrogen Energy.* **2009**, *34* (17), 7368−7378.

(333) Rosen, M. A.; Naterer, G. F.; Chukwu, C. C.; Sadhankar, R.; Suppiah, S. Nuclear-based hydrogen production with a thermochemical copper−chlorine cycle and supercritical water reactor: equipment scale-up and process simulation. *Int. J. Energy Res.* **2012**, *36* (4), 456−465.

(334) Aasadnia, M.; Mehrpooya, M.; Ghorbani, B. A novel integrated structure for hydrogen purification using the cryogenic method. *J. Clean Prod.* **2021**, *278*, 123872.

(335) Ozbilen, A.; Dincer, I.; Rosen, M. A. Environmental evaluation of hydrogen production via thermochemical water splitting using the Cu−Cl Cycle: A parametric study. *Int. J. Hydrogen Energy.* **2011**, *36* (16), 9514−9528.

(336) Ozbilen, A.; Dincer, I.; Rosen, M. A. A comparative life cycle analysis of hydrogen production via thermochemical water splitting using a Cu−Cl cycle. *Int. J. Hydrogen Energy.* **2011**, *36* (17), 11321−11327.

(337) Al-Zareer, M.; Dincer, I.; Rosen, M. A. Analysis and assessment of the integrated generation IV gas-cooled fast nuclear reactor and copper-chlorine cycle for hydrogen and electricity production. *Energy Convers Manag.* **2020**, *205*, 112387.

(338) Al-Zareer, M.; Dincer, I.; Rosen, M. A. Performance analysis of a supercritical water-cooled nuclear reactor integrated with a combined cycle, a Cu-Cl thermochemical cycle and a hydrogen compression system. *Appl. Energy.* **2017**, *195*, 646−658.

(339) Al-Zareer, M.; Dincer, I.; Rosen, M. A. Development and assessment of a novel integrated nuclear plant for electricity and hydrogen production. *Energy Convers Manag.* **2017**, *134*, 221−234.

(340) Orhan, M. F.; Dincer, I.; Rosen, M. A. Investigation of an integrated hydrogen production system based on nuclear and renewable energy sources: a new approach for sustainable hydrogen production via copper−chlorine thermochemical cycles. *Int. J. Energy Res.* **2012**, *36* (15), 1388−1394.

(341) Mehrpooya, M.; Ghorbani, B.; Khodaverdi, M. Hydrogen production by thermochemical water splitting cycle using low-grade solar heat and phase change material energy storage system. *Int. J. Energy Res.* **2022**, *46* (6), 7590−7609.

(342) Mehrpooya, M.; Ghorbani, B.; Ekrataleshian, A. A novel hybrid process for production of cyclohexanone oxime and high temperature hydrogen production using solar energy. *Sustainable Energy Technol. Assess.* **2022**, *50*, 101817.

(343) Siddiqui, O.; Ishaq, H.; Dincer, I. A novel solar and geothermal-based trigeneration system for electricity generation, hydrogen production and cooling. *Energy Convers Manag.* **2019**, *198*, 111812.

(344) Ishaq, H.; Dincer, I.; Naterer, G. F. Development and assessment of a solar, wind and hydrogen hybrid trigeneration system. *Int. J. Hydrogen Energy.* **2018**, *43* (52), 23148−23160.

(345) Ratlamwala, T. A. H.; Dincer, I. Comparative energy and exergy analyses of two solar-based integrated hydrogen production systems. *Int. J. Hydrogen Energy.* **2015**, *40* (24), 7568−7578.

(346) Zhang, B.; Shan, S.; Zhou, Z. A novel clean hydrogen production system combining cascading solar spectral radiation and copper-chlorine cycle: Modeling and analysis. *J. Clean Prod.* **2022**, *380*, 135036.

(347) Onder, G.; Yilmaz, F.; Ozturk, M. Thermodynamic performance analysis of a copper−chlorine thermochemical cycle and biomass based combined plant for multigeneration. *Int. J. Energy Res.* **2020**, *44* (9), 7548−7567.

(348) Temiz, M.; Dincer, I. An integrated bifacial photovoltaic and supercritical geothermal driven copper-chlorine thermochemical cycle for multigeneration. *Sustainable Energy Technol. Assess.* **2021**, *45*, 101117.

(349) Aghahosseini, S.; Dincer, I.; Naterer, G. F. Integrated gasification and Cu−Cl cycle for trigeneration of hydrogen, steam and electricity. *Int. J. Hydrogen Energy.* **2011**, *36* (4), 2845−2854.

(350) Odukoya, A.; Naterer, G. Upgrading waste heat from a cement plant for thermochemical hydrogen production. *Int. J. Hydrogen Energy.* **2014**, *39* (36), 20898−20906.

(351) Ishaq, H.; Dincer, I.; Naterer, G. F. Industrial heat recovery from a steel furnace for the cogeneration of electricity and hydrogen with the copper-chlorine cycle. *Energy Convers Manag.* **2018**, *171*, 384−397.

(352) DinAli, M. N.; Dincer, I. Development of a new trigenerational integrated system for dimethyl-ether, electricity and fresh water production. *Energy Convers Manag.* **2019**, *185*, 850−865.

(353) Ishaq, H.; Dincer, I. Investigation of an integrated system with industrial thermal management options for carbon emission reduction and hydrogen and ammonia production. *Int. J. Hydrogen Energy.* **2019**, *44* (26), 12971−12982.

(354) Ishaq, H.; Dincer, I.; Naterer, G. F. Multigeneration system exergy analysis and thermal management of an industrial glassmaking process linked with a Cu−Cl cycle for hydrogen production. *Int. J. Hydrogen Energy.* **2019**, *44* (20), 9791−9801.

(355) Ishaq, H.; Dincer, I.; Naterer, G. F. New trigeneration system integrated with desalination and industrial waste heat recovery for hydrogen production. *Appl. Therm Eng.* **2018**, *142*, 767−778.

(356) Deng, L.; Adams, T. A., II Techno-economic analysis of coke oven gas and blast furnace gas to methanol process with carbon dioxide capture and utilization. *Energy Convers Manag.* **2020**, *204*, 112315.

(357) Xu, J.; Lin, W.; Xu, S. Hydrogen and LNG production from coke oven gas with multi-stage helium expansion refrigeration. *Int. J. Hydrogen Energy.* **2018**, *43* (28), 12680−12687.

(358) Xu, J.; Lin, W. Integrated hydrogen liquefaction processes with LNG production by two-stage helium reverse Brayton cycles taking industrial by-products as feedstock gas. *Energy.* **2021**, *227*, 120443.

(359) Khatami Jouybari, A.; Ilinca, A.; Ghorbani, B. Thermo-economic optimization of a new solar-driven system for efficient production of methanol and liquefied natural gas using the liquefaction process of coke oven gas and post-combustion carbon dioxide capture. *Energy Convers. Manage.* **2022**, *264*, 115733.

(360) Mehrpooya, M.; Sadaghiani, M. S.; Hedayat, N. A novel integrated hydrogen and natural gas liquefaction process using two multistage mixed refrigerant refrigeration systems. *Int. J. Energy Res.* **2020**, *44* (3), 1636−1653.

(361) Yuksel, Y. E.; Ozturk, M.; Dincer, I. Energy and exergy analyses of an integrated system using waste material gasification for hydrogen production and liquefaction. *Energy Convers Manag.* **2019**, *185*, 718−729.

(362) Incer-Valverde, J.; Mörsdorf, J.; Morosuk, T.; Tsatsaronis, G. Power-to-liquid hydrogen: Exergy-based evaluation of a large-scale system. *Int. J. Hydrogen Energy* **2023**, *48* (31), 11612−11627.

(363) Koc, M.; Yuksel, Y. E.; Ozturk, M. Thermodynamic assessment of a novel multigenerational power system for liquid hydrogen production. *Int. J. Hydrogen Energy* **2022**, *47*, 31806.

(364) Flynn, T. M. *Cryogenic engineering*, 2nd ed.; Marcel Dekker, 2005.

(365) *H2A hydrogen delivery infrastructure analysis models and conventional pathway options analysis results*; 2008.

(366) Connelly, E.; Penev, M.; Elgowainy, A.; Hunter, C. Current Status of Hydrogen Liquefaction Costs. *DOE Hydrogen and Fuel Cells Program Record*; DOE, 2019; pp 1−10.

(367) Reddi, K.; Elgowainy, A.; Brown, D.; Rustagi, N.; Mintz, M.; Gillete, J. *Hydrogen delivery scenario analysis model*; Department of Energy (DOE): Oak Ridge, TN, USA, 2015.

(368) Stolzenburg, K.; Mubbala, R. Hydrogen liquefaction report-whole chain assessment. *Fuel Cells and Hydrogen Joint Undertaking (FCH JU)*; Integrated Design for Demonstration of Efficient Liquefaction of Hydrogen (IDEALHY), 2013.

(369) *The fuel cell technologies office multi-year research, development, and demonstration plan*; US Department of Energy, 2016.

(370) Burgunder, A.; Martinez, A.; Tamhankar, S. Current Status of Hydrogen Liquefaction Costs. *DOE Hydrogen and Fuel Cells Program Record*; Department of Energy: Washington, DC, USA, 2019.

(371) Reuß, M.; Grube, T.; Robinius, M.; Preuster, P.; Wasserscheid, P.; Stolten, D. Seasonal storage and alternative carriers: A flexible hydrogen supply chain model. *Appl. Energy.* **2017**, *200*, 290−302.

(372) Heuser, P.-M.; Ryberg, D. S.; Grube, T.; Robinius, M.; Stolten, D. Techno-economic analysis of a potential energy trading link between Patagonia and Japan based on CO_2 free hydrogen. *Int. J. Hydrogen Energy.* **2019**, *44* (25), 12733−12747.

(373) Li, X. J.; Allen, J. D.; Stager, J. A.; Ku, A. Y. Paths to low-cost hydrogen energy at a scale for transportation applications in the USA and China via liquid-hydrogen distribution networks. *Clean Energy* **2020**, *4* (1), 26−47.

(374) Cihlar, J.; Lejarreta, A. V.; Wang, A.; Melgar, F.; Jens, J.; Rio, P. *Hydrogen generation in Europe: Overview of costs and key benefits*, 2021.

(375) Raab, M.; Maier, S.; Dietrich, R.-U. Comparative techno-economic assessment of a large-scale hydrogen transport via liquid transport media. *Int. J. Hydrogen Energy.* **2021**, *46* (21), 11956−11968.

(376) Kampitsch, M.; Gruber, T. Liquefied hydrogen in the supply chain for hydrogen based mobility. *Presentation at the 21st world hydrogen energy conference*, Zaragoza, Spain; 2016.

(377) Elgowainy, A.; Frank, E. Opportunities and Challenges of Liquid Hydrogen Supply Chain. *Presentation at the Liquid Hydrogen Technologies Workshop*; https://www.energy.gov/sites/default/files/2022-03/Liquid%20H2%20Workshop-ANL.pdf (Accessed May 2022).

(378) Hydrogen Delivery Technical Team Roadmap, 2013, https://www.energy.gov/eere/fuelcells/articles/hydrogen-delivery-roadmap (Accessed May 2022).

(379) The future of hydrogen: seizing today's opportunities. *Report prepared by the IEA for the G20 Japan*; OECD, 2019 DOI: 10.1787/1e0514c4-en.

(380) Hecht, E. S.; Chowdhury, B. R. Characteristic of cryogenic hydrogen flames from high-aspect ratio nozzles. *Int. J. Hydrogen Energy.* **2021**, *46* (23), 12320−12328.

(381) Chowdhury, B. R.; Hecht, E. S. Dispersion of cryogenic hydrogen through high-aspect ratio nozzles. *Int. J. Hydrogen Energy.* **2021**, *46* (23), 12311−12319.

(382) Kobayashi, H.; Muto, D.; Daimon, Y.; Umemura, Y.; Takesaki, Y.; Maru, Y.; Yagishita, T.; Nonaka, S.; Miyanabe, K. Experimental study on cryo-compressed hydrogen ignition and flame. *Int. J. Hydrogen Energy.* **2020**, *45* (7), 5098−5109.

(383) Ustolin, F.; Lamb, J. J.; Burheim, O. S.; Pollet, B. G. Energy and safety of hydrogen storage. *Hydrogen, Biomass Bioenergy*; Elsevier, 2020; pp 133−153.

(384) Abohamzeh, E.; Salehi, F.; Sheikholeslami, M.; Abbassi, R.; Khan, F. Review of hydrogen safety during storage, transmission, and applications processes. *J. Loss Prev Process Ind.* **2021**, *72*, 104569.

(385) Delvosalle, C.; Fievez, C.; Pipart, A.; Debray, B. ARAMIS project: A comprehensive methodology for the identification of reference accident scenarios in process industries. *J. Hazard. Mater.* **2006**, *130* (3), 200−219.

(386) Brown, A.; Nunes, E.; Teruya, C.; Anacleto, L.; Fedrigo, J.; Artoni, M. Quantitative Risk Analysis Of Gaseous Hydrogen Storage Unit. *International Conference on Hydrogen Safety*, Pisa, Italy; Hysafe, 2005; 220003.

(387) Correa-Jullian, C.; Groth, K. M. Data requirements for improving the Quantitative Risk Assessment of liquid hydrogen storage systems. *Int. J. Hydrogen Energy.* **2022**, *47* (6), 4222−4235.

(388) Suzuki, T.; Shiota, K.; Izato, Y.-i.; Komori, M.; Sato, K.; Takai, Y.; Ninomiya, T.; Miyake, A. Quantitative risk assessment using a Japanese hydrogen refueling station model. *Int. J. Hydrogen Energy.* **2021**, *46* (11), 8329−8343.

(389) Lowesmith, B. J.; Hankinson, G.; Chynoweth, S. Safety issues of the liquefaction, storage and transportation of liquid hydrogen: An analysis of incidents and HAZIDS. *Int. J. Hydrogen Energy.* **2014**, *39* (35), 20516−20521.

(390) Al-Shanini, A.; Ahmad, A.; Khan, F. Accident modelling and safety measure design of a hydrogen station. *Int. J. Hydrogen Energy.* **2014**, *39* (35), 20362−20370.

(391) Yoo, B.-H.; Wilailak, S.; Bae, S.-H.; Gye, H.-R.; Lee, C.-J. Comparative risk assessment of liquefied and gaseous hydrogen refueling stations. *Int. J. Hydrogen Energy.* **2021**, *46* (71), 35511−35524.

(392) Yang, Y.; Wang, G.; Zhang, S.; Zhang, L.; Lin, L. Review of hydrogen standards for China. *E3S Web of Conferences*; EDP Sciences, 2019; Vol. *118*, p 03032.

(393) International Organization for Standardization (ISO), https://www.iso.org (Accessed Jan 2023).

(394) American National Standards Institute (ANSI), www.ansi.org (Accessed Jan 2023).

(395) Compressed Gas Association (CGA), https://www.cganet.com (Accessed Sep 2022).

(396) National Fire Protection Association (NFPA), https://www.nfpa.org (Accessed Sep 2022).

(397) The American Society of Mechanical Engineers (ASME), https://www.asme.org (Accessed Sep 2022).

(398) European Committee for Standardization (CEN), https://standards.cen.eu/ (Accessed Sep 2022).

(399) Standardization Administration of the P.R.C. (SAC), http://www.sac.gov.cn/sacen/ (Accessed Sep 2022).

(400) Japanese Industrial Standards Committee (JISC), https://www.jisc.go.jp/eng/index.html (Accessed Sep 2022).

(401) Yang, Y.; Xu, H.; Lu, Q.; Bao, W.; Lin, L.; Ai, B.; Zhang, B. Development of Standards for Hydrogen Storage and Transportation. *E3S Web of Conferences*; EDP Sciences, 2020; Vol. *194*, p 02018.

(402) Yang, Y.; Lin, L.; Bao, W. Development of standards for liquid hydrogen in China. *IOP Conference Series: Earth and Environmental Science*; IOP Publishing, 2022; Vol. *1011*, p 012001.

(403) Klell, M. Storage of hydrogen in the pure form. *Handbook of hydrogen storage: new materials for future energy storage* **2010**, 1.

(404) Olabi, A.G.; bahri, A. s.; Abdelghafar, A. A.; Baroutaji, A.; Sayed, E. T.; Alami, A. H.; Rezk, H.; Abdelkareem, M. A. Large-vscale hydrogen production and storage technologies: Current status and future directions. *Int. J. Hydrogen Energy* **2021**, *46* (45), 23498−23528.

(405) Drnevich, R. Hydrogen delivery: liquefaction and compression. *Strategic initiatives for hydrogen delivery workshop*, May 7, 2003; DOE, 2003.

(406) Teplow, W.; Marsh, B.; Hulen, J.; Spielman, P.; Kaleikini, M.; Fitch, D.; Rickard, W. Dacite melt at the Puna geothermal venture wellfield, Big Island of Hawaii. *GRC Trans.* **2009**, *33*, 989−994.

(407) Foumier, R. O. The transition from hydrostatic to greater than hydrostatic fluid pressure in presently active continental hydrothermal systems in crystalline rock. *Geophys. Res. Lett.* **1991**, *18* (5), 955−958.

(408) Espinosa-Paredes, G.; Garcia-Gutierrez, A. Estimation of static formation temperatures in geothermal wells. *Energy Convers Manag.* **2003**, *44* (8), 1343−1355.

(409) Garcia, J.; Hartline, C.; Walters, M.; Wright, M.; Rutqvist, J.; Dobson, P. F.; Jeanne, P. The Northwest Geysers EGS demonstration project, California: Part 1: characterization and reservoir response to injection. *Geothermics.* **2016**, *63*, 97−119.

(410) Kaspereit, D.; Mann, M.; Sanyal, S.; Rickard, B.; Osborn, W.; Hulen, J. Updated conceptual model and reserve estimate for the Salton Sea geothermal field, Imperial Valley, California. *GRC Trans.* **2016**, *40*, 57−66.

(411) Al-Hamed, K. H.; Dincer, I. Analysis and economic evaluation of a unique carbon capturing system with ammonia for producing ammonium bicarbonate. *Energy Convers Manag.* **2022**, *252*, 115062.

(412) Al-Hamed, K. H. Modeling and experimental investigation of renewable energy and ammonia-based systems for carbon capturing and useful outputs. Thesis; University of Ontario Institute of Technology, 2022.

(413) Rezaie, H.; Ziabasharhagh, M.; Mafi, M. A review of hydrogen liquefaction, current situation and its future. *International Conference on Engineering Applied Sciences*; IEEE, 2016.

(414) Howe, G.; Skinner, G.; Finn, A. Advanced precooling for optimized hydrogen liquefaction. *Adv. Hydrogen Technol. (H2Tech)* **2021**, *1*, 18−22; https://www.costain.com/media/599622/h2tech-hydrogen-liquefaction.pdf (Accessed Jan 2023).

(415) Johnson, V.; Wilson, W. Performance of NBS hydrogen liquefier plant. *Advances in Cryogenic Engineering*; Springer, 1960; pp 329−335.

(416) *Liquid Hydrogen Technologies Workshop, Hydrogen and Fuel Cell Technologies Office*, https://www.energy.gov/eere/fuelcells/liquid-hydrogen-technologies-workshop. *Accessed on: Jan 2023.*

(417) Fesmire, J. E.; Swanger, A. Overview of the New LH$_2$ Sphere at NASA Kennedy Space Center. *DOE/NASA Advances in Liquid Hydrogen Storage Workshop*; DOE/NASA, 2021; https://www.energy.gov/sites/default/files/2021-10/new-lh2-sphere.pdf (Accessed Jan 2023).

(418) Fesmire, J.; Swanger, A.; Jacobson, J.; Notardonato, W. Energy efficient large-scale storage of liquid hydrogen. *IOP Conference Series: Materials Science and Engineering*; IOP Publishing, 2022; Vol. *1240*, 012088.